INSTITUTO POLITÉCNICO NACIONAL

ESCUELA SUPERIOR DE FÍSICA Y MATEMÁTICAS

ABSORBED DOSE CALCULATION FOR WHOLE BRAIN RADIOTHERAPY USING A DETERMINISTIC APPROACH

BY

LIC. ENRIQUE ALBERTO BETANCOURT GARCIA

THESIS SUBMITTED TO THE COLLEGE OF PROFESSORS IN PARTIAL FULFILLMENT OF THE REQUIREMENTS FOR THE DEGREE OF MASTER OF SCIENCE IN MATHEMATICAL PHYSICS
AT THE
INSTITUTO POLITÉCNICO NACIONAL

THESIS ADVISORS:
DR. EDMUNDO DEL VALLE GALLEGOS (IPN)
DR. ARTURO DELFÍN LOYA (ININ)

MEXICO CITY, MEXICO, JANUARY 2018

Abstract

Cancer in Mexico is one of the main causes of hospital morbidity, responsible for near seventy thousand deaths per year. In addition to the physical impact of cancer, there are several socio-economic consequences, mainly in disadvantaged communities where access to health services are limited. In Mexico, the average cost of medical care per patient varies from Mex$110,459.00 to Mex$544,274.00. The high cost of cancer treatment affects our economy and the citizens of our society, many of whom lack access to high-quality cancer care. Treatment planning systems are directly associated with a high cost due to computational power with a price range of US$50,000.00 to US$230,000, without considering the maintenance cost. In addition, the devaluation of the Mexican peso against the American dollar raises the cost of delivering a radiotherapy treatment, making it less and less accessible to Mexican people.The development of a national treatment planning system and linear accelerators intended for cancer treatment could help to reduce costs, patient waiting list, and to raise the number of patients treated in each center. The advantages are not only clinical, this process of innovation leads to an environment of knowledge and national competition. The main objective of this work is to establish the bases for the application of anational Analytical Anisotropic Algorithms in the calculation of absorbed dose in radiotherapy treatments.

Keywords: Treatment Planning System, Analytical Anisotropic Algorithm, radiotherapy

Resumen

El cáncer en México es una de las principales causas de morbilidad hospitalaria, responsable de cerca de setenta mil muertes por año. Además del impacto físico producido por el cáncer, existen varias afectaciones socio-económicas, principalmente en comunidades desfavorecidas donde el acceso a los servicios de salud es limitado. En México, el costo promedio de la atención médica por paciente en México varía de Mex $ 110,459.00 a Mex $ 544,274.00. El alto costo del tratamiento del cáncer afecta nuestra economía y a los ciudadanos de nuestra sociedad, muchos de los cuales carecen de acceso a atención oncológica de alta calidad. El alto precio de los sistemas de planeación en radioterapia está directamente asociado con su poder computacional, con un rango de precios de US $ 50,000.00 a US $ 230,000, sin considerar el costo de mantenimiento. Además, la devaluación del peso mexicano frente al dólar estadounidense aumenta el costo de brindar un tratamiento de radioterapia, haciéndolo cada vez menos accesible para los mexicanos. El desarrollo de un sistema de planeación nacional en radioterapia y de aceleradores lineales destinados al tratamiento del cáncer podría ayudar a reducir los costos del tratamiento, la lista de espera de pacientes y para aumentar el número de pacientes tratados en cada centro hospitalario. Las ventajas no son solo clínicas, este proceso de innovación produce un ambiente de conocimiento y competencia nacional en el área de radioterapia. El objetivo principal de este trabajo es establecer las bases para la aplicación del *Analytical Anisotropic Algorithms* en el cálculo de la dosis absorbida en tratamientos de radioterapia.

Palabras Clave: Sistema de planeación, Analytical Anisotropic Algorithm, radioterapia

Contents

List of Figures

List of Abbreviations

2D,3D . . . . . Two or three dimensional

AAA . . . . . Analytical Anisotropic Algorithm

ASTRO . . . . American Society for Radiation Oncology

CEPXS . . . . Coupled Electron-Photon X Sections

CS . . . . . Coherent Scattering

CSD . . . . . Continuous Slowing Down

CT . . . . . Computer Tomography

DICOM . . . . Digital Imaging and Communication in Medicine

DOM . . . . . Discrete Ordinates Method

DTA . . . . . Distance To Agreement

DVH . . . . . Dose Volume Histogram

EGSnrc . . . . Electron Gamma Shower from the National Research Council Canada

GBBS . . . . . Grid Based Boltzmann Solvers

GEANT . . . . GEometry ANd Tracking

GPU . . . . . Graphics Processor Unit

HU . . . . . Hounsfield Units

IC . . . . . Incoherent Scattering

ICRU . . . . . International Commission on Radiation Units and Measurements

IMRT . . . . . Intensity Modulated Radiation Therapy

KERMA . . . Kinetic Energy Released per unit Mass

LBTE . . . . . Linear Boltzmann Transport Equation

linac . . . . . Linear accelerator

MCNP . . . . Monte Carlo N-Particle transport code

MGM . . . . . Multi-Group Method

MRI . . . . . Magnetic Resonance Imaging

NIST . . . . . National Institute of Standards and Technology

NDOCPE . . . Nodal Discrete-Ordinates Coupled Photon-Electron

NTCP . . . . . Normal Tissue Complication Probability

PDD . . . . . Percent Depth Dose

PE . . . . . Photon Energy

PEA . . . . . Photo Electric Absorption

PEF . . . . . Pair Production in Electron Field

PENELOPE . Penetration and ENErgy LOss of Positrons and Electrons

PET . . . . . Positron Emission Imaging

PIL . . . . . Python Image Library

PNF . . . . . Pair Production in Nuclear Field

QA . . . . . Quality Assurance

ROI . . . . . Region Of Interest

RNT-0 . . . . Raviart-Thomas-Nédelec of index 0

SPECT . . . . Single Photon Emission Computer Tomography

STP . . . . . Standard Temperature and Pressure

TAOCS . . . . Total Attenuation withOut Coherent Scattering

TAWCS . . . . Total Attenuation With Coherent Scattering

TCP . . . . . Tumour Control Probability

TPS . . . . . Treatment Planning System

UPS . . . . . Uninterruptible Power Supply

VMAT . . . . Volumetric Modulated Arc Therapy

VTK . . . . . Visualization ToolKit

WBRT . . . . Whole Brain Radiotherapy

National prosperity is created, not inherited.

— Michael E. Porter *de Harvard Bussiness Review*

1 Introduction

Contents

1.1 Radiotherapy

One of the primary modalities used in the treatment of cancer is the radiation therapy or radiotherapy. Radiotherapy aims to control the tumoral malignancy while reducing the damage to healthy tissue. A safe and accurate delivery of radiation therapy demands a meticulous documentation of every phase of the process. Because of the many steps involved, from the diagnosis to the delivery of the treatment, the International Commission on Radiation Units and Measurements (ICRU) has recommended that the difference between the prescribed and the delivery dose must be performed within $\pm 5\%$.

The delivery of the prescribed radiation treatment is imparted by a linear

accelerator (linac). The prescribed radiation treatment is calculated in a treatment planning system (TPS). TPS calculates the beam shape and dose distributions of each treatment adjusting the radiation fields to fit the dimensions of the tumoral tissue while reducing the irradiation of healthy tissue. However, the dose response of tumoral and normal tissue is determined by the tumor control probability (TCP) and normal tissue complication probability (NTCP). To accomplish a 95% of TCP a lethal dose tumor dose must be prescribed by the radiation oncologist. The dose prescribed relies upon the type and localization of a tumor, the stage of the disease, the radiation type delivered, the surrounding tissues, etc. For delivering an accurate dose that considers each aspect mention above, the treatment planning system must consist of various algorithms that encompass:

- Patient data information: type of malignancy, stage of the disease, name of the patient, etc.
- The mechanical movements: collimators, treatment table, gantry, anti-collision system, beam modifiers, etc.
- Console system tests: operational specifications and safety applications.
- Beam parameters: Beam output, monitor characteristic as linearity, dose rate accuracy, flatness, the stability of the output with gantry position, penumbra, etc.

As a result of the complexity of the treatment planning system, medical physicists requires a solid knowledge of physics, physical information about radiation beams, commissioning, calibration, quality assurance of the therapy equipment, etc. For the slightest miscalculation could lead to an overdose or underdose treatment delivery compared to the prescribed dose. Consequently, a strict quality assurance (QA) for the TPS is a compelled necessity.

1.2 Radiotherapy in Mexico

Cancer in Mexico is one of the main causes of hospital morbidity, responsible for near seventy thousand deaths per year [**CANCER2013**]. In addition to the physical impact of cancer, there are several socio-economic consequences, mainly in disadvantaged communities where access to health services are limited. The average cost of medical care per patient in Mexico varies from Mex$110,459.00 to Mex$544,274.00. The cost depends on the type of treatment, the stage of the disease, medical care, etc. The cheapest radiotherapy treatment offered in Mexico, by public healthcare, has a cost of Mex$1,091.00 per session [**DOF2016**], this means that the whole radiotherapy treatment would cost, approximately, Mex$32,730.00. The whole cancer treatment must include the cost of the detection, chemotherapy, radiotherapy, surgical procedures, medicines, and medical follow-up of the disease. With a much lower median income, the proportion of expenditures directly paid by the patient is much higher, in many cases approaching the entire cost. The high cost of cancer treatment affects our economy and the citizens of our society, many of whom lack access to high-quality cancer care.

Efforts from all medical fields have been made all around the world in order to reduce the cost of the cancer medical treatment. Nevertheless, accurate and fast calculations of the prescribed dose in the TPS are directly associated with a high cost due to computational power. The radiotherapy planning system, for example, has a price range of US$50,000.00 to US$230,000 [**WHOMFacts**], without considering the maintenance cost. In addition, the devaluation of the Mexican peso against the American dollar raises the cost of delivering a radiotherapy treatment, making it less and less accessible to Mexican people.

The development of a national TPS and linear accelerators intended for cancer treatment could help to reduce costs, patient waiting list, and to raise the number of patients treated in each center. The advantages are not only clinical, this process of innovation leads to an environment of knowledge and national competition.

1.3 Objectives and outline

The main objective of this work is to establish the bases for the application of a national Analytical Anisotropic Algorithms in the calculation of absorbed dose in radiotherapy treatments. The photon and the electron beam spectra were modeled by the Linear Boltzmann Transport Equation and the Fokker-Plank transport equation in a homogeneous media. The dose calculation was validated by a qualitative analysis of the percentage depth dose and profile beam that resulted from the simulation of a 6 MeV monoenergetic beam into a water phantom. The simulation was then implemented into a brain CT images for the simplest radiation therapy treatment, the Whole Brain Radiotherapy.

Future work will focus on a clinical and Monte Carlo validation of the simulated beam in a water phantom and in different media, an implementation that allows the user to contour organs at risk, the implementation of a user-friendly interface, etc.

2

Physics of Dose Calculation Algorithms

Contents

2.1 Treatment planning systems

Radiation treatment planning represents a major part of the treatment of radiotherapy. The treatment planning systems (TPS) used in an external beam radiation therapy generate beam shapes and dose distributions aiming to maximize the tumor

control while minimizing the irradiation to the organs at risk. The TPS computes the expected dose distribution in the patient organs utilizing images obtained by computerized tomography. The TPS computes the expected distribution within the patient calculating beam arrangements, beam modifiers, the source to surface distance, etc. The high complexity of radiotherapy equipment requires a highly trained staff in order to minimize potential accidents. Every aspect of the radiation therapy is crucial in order to provide an accurate and precise treatment. All the steps involved in the workflow of the radiation therapy must be performed as accurately as possible, taking into account that a high uncertainty in one step could severely affect the accuracy of the treatment outcome and in consequence the patient's health. The steps involved in the treatment planning process are enlisted as follows

- Image acquisition
- Image and patient registration
- Delimitation and delineation of regions of interest
- Planning and follow up of the treatment, introducing the number, position, and weight of the beams
- Dose calculation and beam optimization
- Physicist and physicians plan review
- Dosimetric evaluation of the treatment
- Delivery of the treatment

The image acquisition usually utilizes CT images to visualize the patient geometry where the structures of interest are outlined and targeted as tumor volume or organ at risk for their posterior follow up in the treatment planning.

Regarding the numerous steps involved in the treatment radiation process, the International Commission on Radiation Units and Measurements has recommended

a dosimetric accuracy to be within ± 5% of the prescribed dose for the entire treatment chain. Giving the importance of accomplishing the dosimetric accuracy, every phase of the procedure requires the effort from specially trained staff with a solid knowledge of radiation physics [**RTP62**].

The majority of the commercially available TPS is based on analytical approximations in the calculation of the prescribed dose. TPS has evolved from a simple 2D-matrix of numbers representing a dose distribution in a plane to more complex algorithms such as AAA, Convolution-superposition, Clarkson [**Lu2013**], etc. To ensure an accurate treatment delivery, it is necessary a Quality Assurance (QA) program that encompasses acceptance testing, commissioning of special procedures, and the safe maintenance and operation of equipment [**RTP47**].

2.1.1 Patient image acquisition data

Modern treatment planning systems heavily rely on accurate patient data information. TPS incorporates this information from CT images and more recently from nuclear magnetic resonance imaging (MRI) and single photon and positron emission tomography (SPECT and PET). The primary considerations that need to be taken into account for an accurate image acquisition data are the patient dimensions, the type of treatment, and landmarks (as fiducial marks) necessary to match the patient position on the patient and the treatment plan.

The contrast provided by the CT images allows exporting the information required for the TPS as skin contour, the region of interest (ROI) and tumor localization. Nowadays, advanced TPS can display the patient anatomy along with the tumor target and dose distribution in a 3D model. To have a contrast suitable for delimiting all the information necessary the CT scanner should be properly calibrated. The calibration derives a relationship between the CT numbers (or Hounsfield Units) and the electron density of the tissues. By definition, the Hounsfield Units (HU) assigns a number of common substances according to their linear attenuation

coefficient measured under standard temperature and pressure (STP) conditions. The HU is then defined by:

$$HU = 1000 \times \frac{\mu - \mu_{water}}{\mu_{water} - \mu_{air}} \tag{2.1}$$

where μ_{water} and μ_{air} are the linear attenuation coefficients of water and air respectively. Hence, the HU related to water and air is 0 and -1000, correspondingly.

Although the correlation between the electron density and the HU is used to calibrate the CT scanner, it is possible to convert electron density to mass density with the equation:

$$\rho = \rho_w \frac{n/n_w}{\rho_e/\rho_{ew}} \tag{2.2}$$

where $\rho_e/\rho_{ew} = 1 + HU/1000$, n is the number of atomic units per electron for the specific material and $n_w = 1.802$.

Although initially the calibration that uses the electron density is commonly used, due to the well-known correlation between the heterogeneity correction factors and the electron density, the equation is shown above demonstrates that CT scanners can be calibrated in both terms.

2.1.2 Dose calculations for treatment planning systems

From the earliest handmade treatment planning systems, numerous advances have taken place thanks to technological developments. The computer codes based on different algorithms are heavily tested upon their release. Various commercial algorithms used by TPS are:

- Pencil Beam
- Clarkson

- Convolution-Superposition
- Analytical Anisotropic Algorithm (AAA)
- Monte Carlo simulation

Except for Monte Carlo method, every algorithm mentioned above is an analytical method. Monte Carlo has been recognized as the gold standard for dose calculation; however, a significant disadvantage is the long computation time required to achieve satisfactory uncertainties as well as minimal statistical noise. Analytical methods used for the calculation of the absorbed dose are based on the solution of the transport equation for photons and electrons through the interaction cross sections that are well known.

In the Pencil Beam algorithm the shape of the beams, after passing the collimation device of the accelerator, from a group of forward-directed "pencils." Pencil beams model the collection of beams in a Gaussian distribution. Clarkson algorithm divides the radiation into primary and scattered components. The calculation of the dose sums the contribution of both components. Likewise, Convolution-Superposition algorithm separates the radiation beam into a primary and a scattered component. The scattering produced varies due to changes in the beam shape and intensity as well as the patient geometry and tissue inhomogeneities. The Analytical Anisotropic Algorithm (AAA) combines the pencil beam and convolution-superposition algorithms. AAA separates the models for primary and scattered photons and electron scattered from the beam. AAA takes into account the tissue heterogeneities by the use of 13 lateral photon scattered kernels [**Sievinen2005**].

2.1.3 Hadware components of a treatment planning system

Due to the specific necessities of radiation therapy planning, it is essential to consider some basic hardware components of a TPS. The considerations that must be taken into account are:

- Central processing unit
- Graphics display
- Digitizing devices
- Output devices
- Network and communication devices

One of the most important aspects of the central processing unit is the memory and processor speed, required for the TPS to run the software efficiently. The graphics display must be capable of displaying high-resolution images in a short period, along with a sub-millimeter resolution that does not distort the input. The digitizing devices refer to the acquisition of the patient information introduced in the TPS manually, meaning that the shapes of the transverse contours of the regions of interest should be traced manually. The output devices include printers, plotters, and UPS (uninterruptible power supplies). Lastly, the network and communication devices specify that the TPS must be able to network on remote computers, servers and the linac, including its record-and-verify system.

2.1.4 Image display and dose volume histograms

The analysis of displays of the dose distribution calculated by the TPS is one of the main ways that physicians make decisions about how the treatment plan should be optimized. The information required to analyze the proper calculation of the simulated treatment is the dose volume histograms (DVH) of the regions of interest (ROI), the dose distribution of the evaluated treatment, and the point of maximum dose.

The DVH is a plot of the cumulative dose-volume frequency distribution that shows the simulated radiation distribution in a volume of interest. The DVH is a requisite for analyzing the dose received by the volume of interest and the

organs at risk. The DVHs are displayed according to the evaluated treatment; they are computed to evaluate the fulfilling of all the requirements demanded by the treatment plan. To provide a higher accuracy TPS allows to modify the weight of the DVHs to satisfy the user criteria. The use of cumulative DVH is a common practice to compare different structures collectively, an example of this is shown in Figure 2.1. The dose volume recommendations vary according to the type of treatment and they are based on normal tissue tolerance to the irradiation that can be found in the ICRU 83 [**Hodapp2012**] and the ASTRO reports [**AMS**] However in some scenarios, if the delivered dose to the organs at risk do not fulfill the dosimetric goals, the radiation oncologist must take a clinical decision that evaluates the risk of reducing the tumor coverage against the potential damage to the healthy tissues (Figure 2.1). Organs such as optic chiasm, optic nerves, and brainstem are the most critical organs to avoid due to the severe consequences of radiation-induced injury.

The use of dose distributions allows the users to compare the resulting distribution qualitatively, and to evaluate conformal dose gradients enveloping healthy organs. The display of 3D dose distributions permits to visualize the result of different beam orientations, energies of the beam, intensities, and type of treatments (conformal, IMRT, VMAT). Occasionally, treatment may require a high accuracy in the calculated dose, this kind of treatment demands at least a measurement-based verification of the calculated dose distribution in a plane, preferably in the isocenter plane. The dose distribution needs to be compared to another dose distribution by quantitative and qualitative methods. In addition to the qualitative visual evaluation, the quantitative evaluation is performed by the gamma test γ. The gamma test combines the calculation of the dose difference and distance to agreement (DTA) criteria as $\gamma(\%, mm)$. The gamma test evaluates point by point the dose distribution to determine if each point of the dose distribution passes or fails the test, according to the user criteria. The dose distribution is compared against a validated dose distribution like a Monte Carlo simulation or an accurate measurement at reference conditions.

The point of maximum dose must be located inside the organ of interest, and according to the treatment, it should reach a percentage limit of the prescribed dose to a tumor.

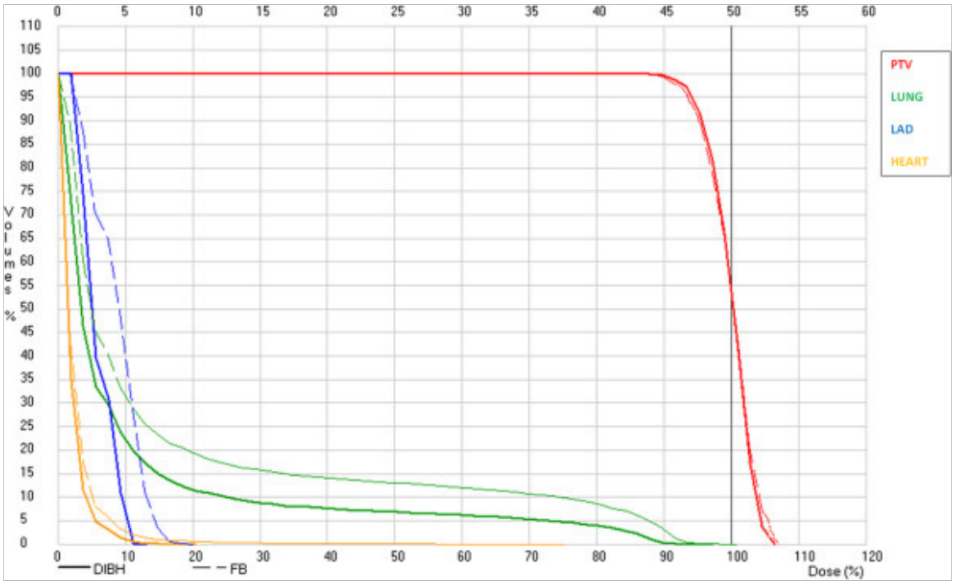

Figure 2.1: Cummulative DVH

2.2 Physics of treatment planning systems

Linear accelerators based external beam radiotherapy produce electrons, used for superficial treatments, and photons, used for deep located ROI. Still, the most common modality is the linac photon treatment. Linac produces photons with maximum energies of 6, 10, 15, 18, and 20 MeV, being the energy of 6 MeV the most used by general treatments.

2.2.1 Interaction of uncharged particles with matter

The energy given by radiation therapy aims to transform the cells in the tumoral tissue to prevent their replication by damaging the molecules of DNA. The dose delivered into the medium, means the average energy deposited by unit mass, produces a biological damage to the cells. This damage is produced by the charged

particles that result from the interaction of photons with the material. The dominant processes of the photon interaction with matter are the photoelectric effect, the Compton effect, and the coherent scattering. The probability of each process interaction depends on the photon energy and the medium.

The coherent scattering is produced when a photon interacts with an electron in a bound orbital. A photon is scattered with almost the same incident energy and is emitted in another direction at a minimal angle. The energy imparted to the medium is negligible. The probability of this effect is higher for larger Z and low photon energies.

The photoelectric effect takes place when a photon interacts with an atom by ejecting a bound orbital electron, denoted as photoelectron. This interaction leaves a vacancy in the shell of the atom. After that, an electron from a higher electronic shell fills up the vacancy, and a characteristic photon is emitted. Alternatively, an Auger electron is produced. The probability of interaction depends upon Z^3 [**Podogrsak2005**].

For radiotherapy energies and medium, the most probable effect is the Compton effect. Compton effect is the result of a photon interaction with a free or unbound electron. The photon is then deflected with a scattering angle. The photon then transfers a part of its kinetic energy to the electron. The relationship between the dominant effect by atomic number is shown in Figure 2.2.

2.2.2 The Boltzman and Fokker-Planck transport equations

The dose calculation into the patient, in deterministic algorithms, is obtained by solving the Linear Boltzmann Transport Equation (LBTE). The LBTE describes the macroscopic behavior of ionizing particles as they interact with matter. LBTE takes into account any particles: neutrons, gamma-rays, electrons, etc. The exact dose within the volume is obtained by solving the LBTE. The methods to solve the

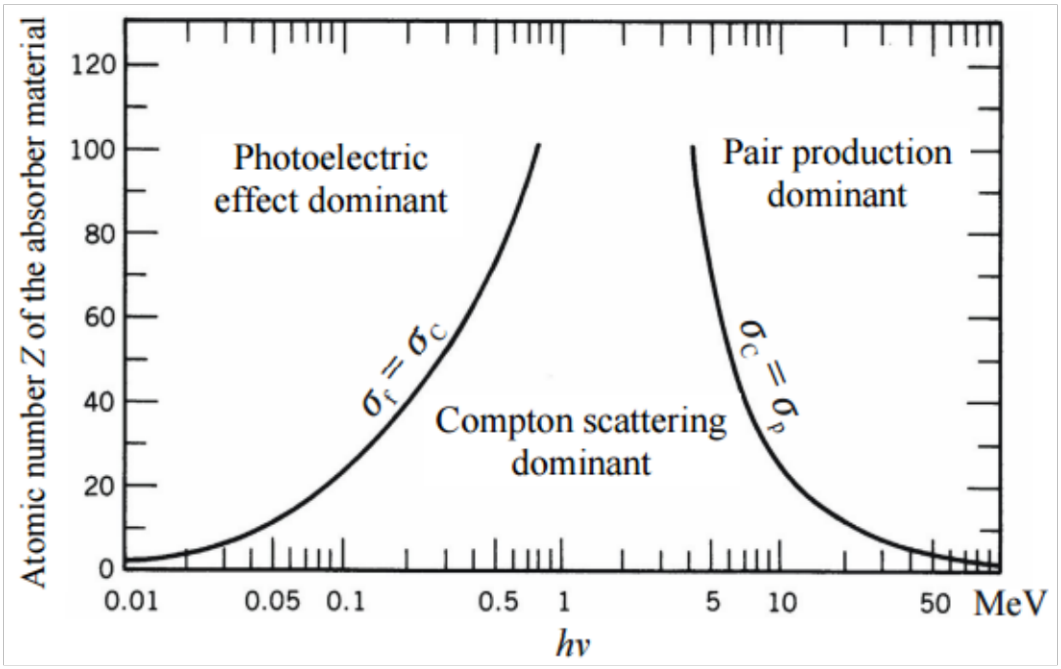

Figure 2.2: Dominant effects by atomic number and energy

LBTE deterministically are called grid-based solvers (GBBS). GBBS discretize the space, angle, and energy to explicitly solve the LBTE by different techniques as spherical harmonics, characteristic methods, and discrete ordinates.

The LBTE is an equation balance, where each of its terms is related to the particles moving or interacting. Hence, the time-independent three-dimensional Transport equations for photon and electrons inside a volume V are:

$$\hat{\Omega} \cdot \vec{\nabla}\psi^{\gamma} + \Sigma^{\gamma}\psi^{\gamma} = q^{\gamma\gamma} + q^{\gamma} \tag{2.3}$$

$$\hat{\Omega} \cdot \vec{\nabla}\psi^{e} + \Sigma^{e}\psi^{e} - \frac{\partial}{\partial E}(S_R\psi^{e}) = q^{ee} + q^{\gamma e} + q^{e} \tag{2.4}$$

where, ψ^{γ} is the particle flux, $\hat{\Omega}$ the unitary direction of the particles, $\Sigma^{\gamma/e}$ is the probability of interaction inside the volume, *total cross sections*, S_R is the restricted collisional plus radiative Stopping Power [**Vassiliev**].

On the left side of the equation $\hat{\Omega} \cdot \vec{\nabla}\psi^{\gamma/e}$ represents the streaming operator ,*i.e.* the number of particles moving into the volume, $\Sigma^{\gamma/e}\psi^{\gamma/e}$ represents the number of particles interacting with a total probability of interaction $\Sigma^{\gamma/e}$. In case

of the electron transport equation de Continuous Slowing Down operator (CSD) is $\frac{\partial}{\partial E}(S_R\psi^e)$ which relates the number of electrons streamed trough the volume and its continuous loss of energy due to this stream. The terms on the right side of the equations (2.4,2.5) are the sources, which represent the total number of particles entering the volume by external sources (q^γ, q^e), by photon sources resulted from photon interactions $(q^{\gamma\gamma})$, by electron sources resulted from electron-electron interactions $(q^{ee})$and by electron source resulted from photon-electron interactions $(q^{\gamma e})$ [**Vassiliev**].

These equations are restricted to their boundary and initial conditions.

2.2.3 KERMA, absorbed dose, and monitor units

The absorbed dose calculation, produced by photon beams, is based on the interaction of particles within a medium measured at reference conditions. The energy transfer from a photon to medium occurs in two manners:

- By the interaction of the photon field with the atoms in the medium.
- By the transfer of energy from charged particles to the medium (excitation and secondary ionization).

The energy transferred dE_{tr} from a photon to the primary electron in a medium dm is defined by the KERMA or Kinetic Energy Released per unit Mass.

$$K = \frac{dE_{tr}}{dm} \tag{2.5}$$

The absorbed dose D is calculated by the mean energy imparted $d\overline{E}$ to a mass dm by ionizing radiation in a finite volume. The units of the absorbed dose are J/kg or Gray (Gy).

$$D = \frac{d\overline{E}}{dm} \tag{2.6}$$

2.3 Calibration process

The TPS takes the information from the linac calibration to calculate the dose delivered to a patient. The measurements of the calibration are taken under reference conditions. As a minimum, the measurements consists of percent depth dose curves (PDD), and cross beam profiles (OARs). The measurements are performed first for single beams at different energies and beam size configurations.

2.3.1 Percentage depth dose

A photon beam traveling through a patient is affected by the inverse square law, attenuation and the scattering of the photon. The combination of this three effects produces a dose distribution within the patient. When the photon beam enters the patient delivers a dose that increases rapidly until it reaches a value of maximum dose at z_{max}, then it decreases until it exits the patient. The point of maximum dose at z_{max} depends on the energy of the delivered beam, for example, $z_{max} = 1.5\ [cm]$ for 6 $[MeV]$ photon beams. The dose region between the surface and z_{max} is defined as build-up region. The build-up region is produced when secondary electrons deposit their energy in the medium by indirect ionization, the larger the energy, the larger z_{max}.

The percentage depth dose (PDD) is measured by the central axis dose distribution of the beam size. The measurements are taken for reference conditions and normalized to $D_{max} = 100\%$ at z_{max}. In clinical practice, the PDD comparisons are performed for point differences in various square fields and different energies of the linac. An example of different PDD curves is shown in Figure 2.3.

2.3.2 Beam profiles

The beam profiles are measured perpendicular to the central beam axis at a given depth, usually at 10 $[cm]$. An example of different beam profiles is shown in

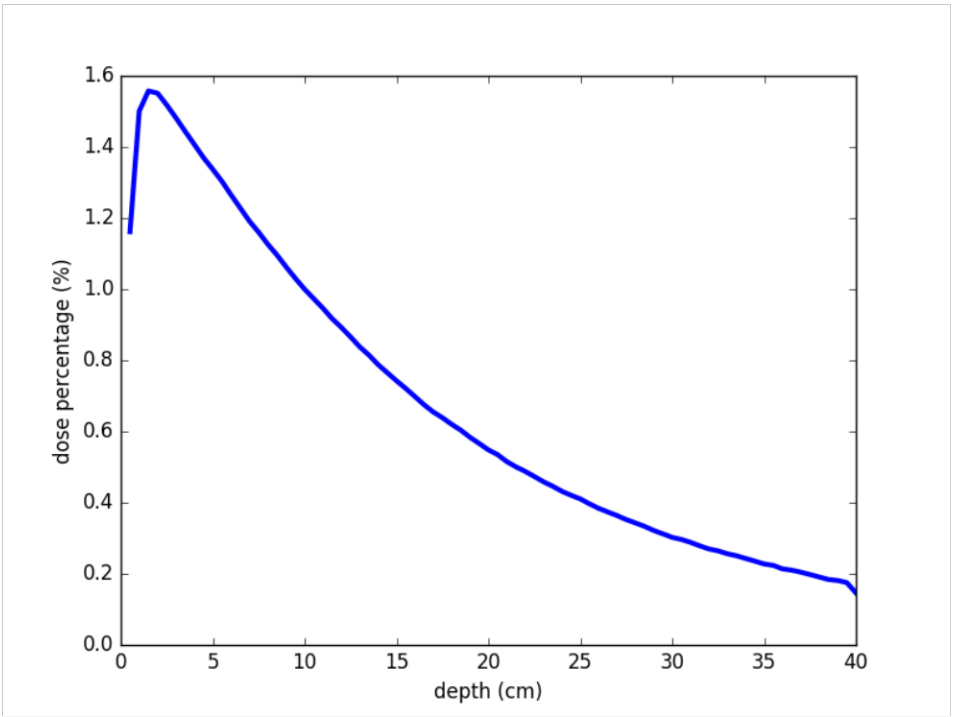

Figure 2.3: Percentage of Dose in Depth

Figure 2.4. The comparison of beam profiles is performed by the measurements of the beam flatness and symmetry. The beam flatness F evaluates the difference between the point of minimum and maximum dose (D_{min}, D_{max}), this difference must be less than 3%, meaning that

$$F = 100 \times (D_{max} - D_{min} \div D_{max} + D_{min}) \tag{2.7}$$

The beam symmetry S is a measure that evaluates the beam uniformity parameter. The beam symmetry comparisons must not exceed the 2% difference.

2.4 Whole Brain Radiotherapy

One of the most simple radiotherapy treatments is the called Whole Brain Radiotherapy (WBRT). WBRT consists of two parallel opposed fields, the pair of fields is directed along the same axis from opposite sides. Because of the simplicity and

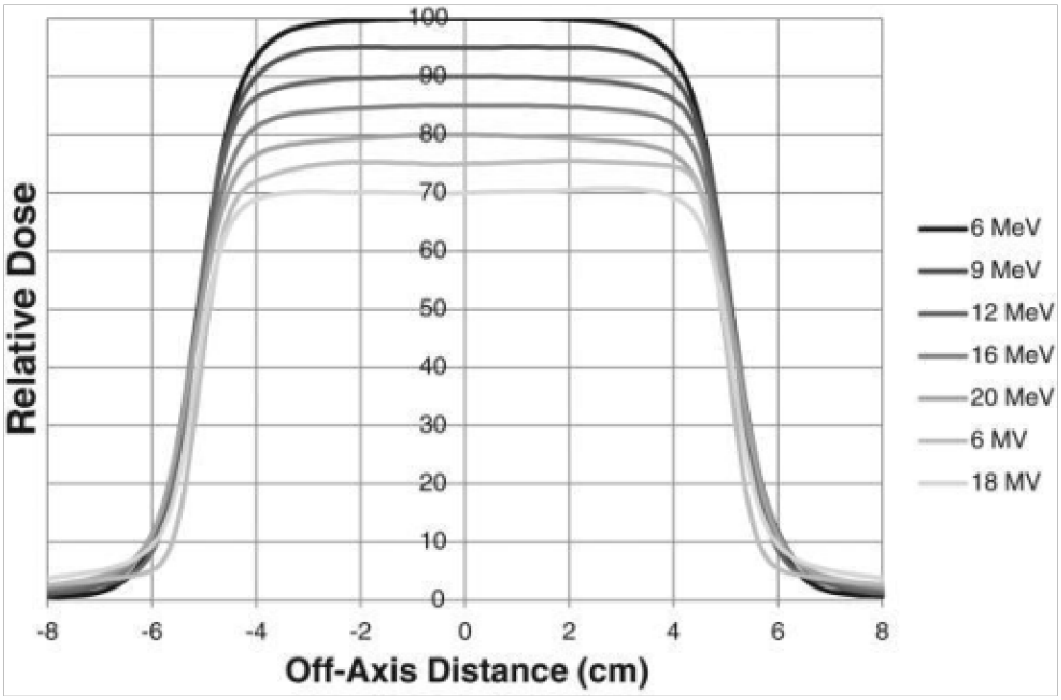

Figure 2.4: Beam profile in the XZ plane for a 6 MeV photon beam.

easy reproducibility of the set-up, along with the homogeneous irradiated medium, WBRT is the ideal choice for a first verification treatment. The dose distribution of the parallel fields is obtained by just adding both depth dose contributions, a clinical example of the procedure is shown in Figure 2.5. The critical structures to evaluate are the brain, the eyes, and the optical chiasma.

The Whole Brain Radiotherapy is the treatment choice for patients who have brain metastases that affect critical areas or are too large to be treated with surgery. The most common WBRT prescription is 30 $[Gy]$ in ten 3 $[Gy]$ fractions. Although WBRT trials show an increment of median survival ranges from 2.4 to 4.8 months, it also produces neurocognitive toxicity associated with the treatment. The treatment may primarily affect the short-term memory recall and as late toxicity severe dementia.

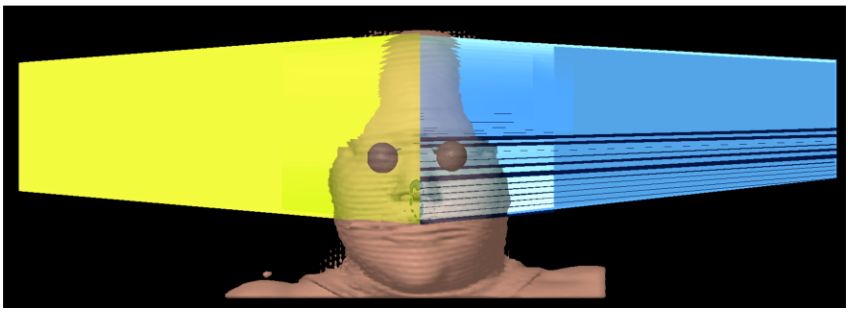

Figure 2.5: WBRT treatment plannning of two opposed parallel fields

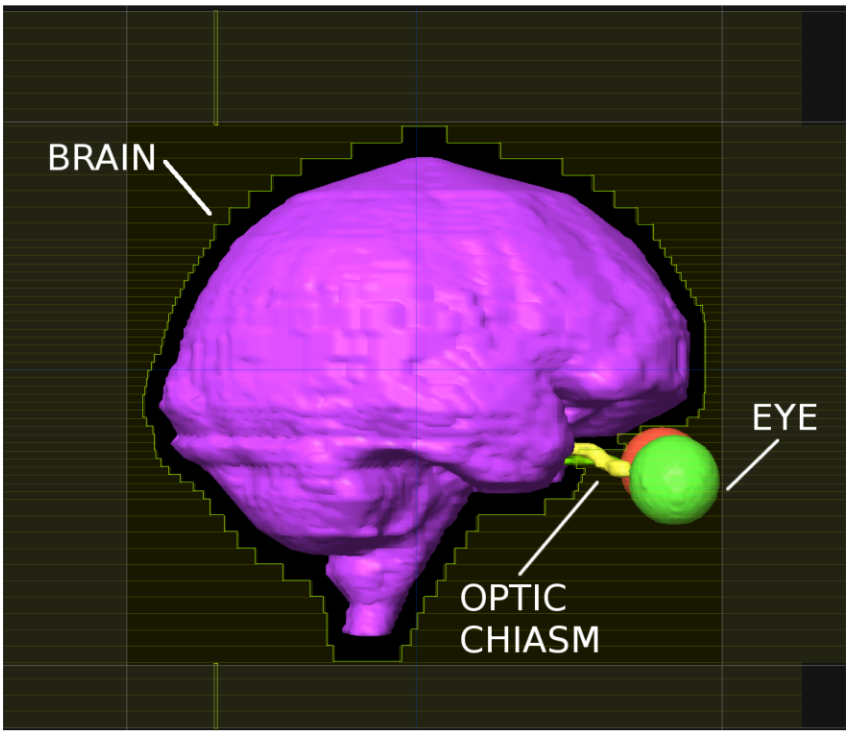

Figure 2.6: Critical structures in WBRT

3

The Analytical Anisotropic Algorithm

Contents

3.1 General description

The Analytical Anisotropic Algorithm (AAA) is a pencil beam superposition algorithm. AAA divides the modeling of primary photons and scattered particles like photons or electrons. As an analytical method used in radiotherapy, one of its major advantages is the short computational times compared to Monte Carlo.

The AAA calculation model is simulated in two parts, namely: a) the configuration algorithm and b) the dose calculation algorithm. The configuration algorithm considers the characterization of the clinical beam that is determined by the type of particle including its fluence and energy. The simulated clinical beam leads to a multiple source model. The total source consists of a primary photon source and the electron source. The dose calculation algorithm is designed to interact with the medium. The medium, being the images of the patient body taken from the CT data set, is divided into a grid built up by voxels with particular electron and mass densities. Finally, the dose distribution within the material is calculated by the superposition of the dose provided by the beam.

3.2 Physics of the Analytical Anisotropic Algorithm

The Analytical Anisotropic Algorithm uses fundamental physical parameters for the simulation of photon and electron angular fluence taking into account the spatial position vector, the energy of the particles, restricted collision plus radiative stopping power, etc. These parameters are taken from the beam calibration and consider the type of treatment, energy, and the photon linear attenuation coefficients and electron cross sections of the medium. Now on, linear attenuation coefficients will be also referred as photon cross sections of the medium.

AAA employs three basic assumptions:

- the secondary particles from pair production are assumed to be electrons, instead of one electron and one positron,
- partial coupling technique is considered, meaning that photons produce electrons, but electrons do not produce photons, and
- the energy of photons that are generated by the electrons is assumed to be delivered locally.

The assumptions mentioned here above have a minor effect in the energy deposition field and are similar to those utilized by some computer codes based on Monte Carlo method.

3.3 Solution method

To solve the coupled Linear Boltzmann Transport Equations (LBTE) it is important to have in mind the six independent variables involved which are: 3, x, y, and z, for the position vector, 2, θ and φ, for the solid angle, and 1 for the energy. The order to discretize these independent variables will be as follows:

- Energy. The energy interval going from a minimum energy, E_{min}, to a maximum energy, E_{max}, will be discretized in a set of G sub-intervals $[E_{g-1}, E_g]$, for $g = 1, ..., G$ and a balance of particles will be obtained on each one following the so-called multi-group energy method as it will be described lately.[REF]

- Angle. The angular dependence of the fluence and also of the angular flux will be represented by a set of discrete angular directions $\hat{\Omega}_n$ over the unit sphere such that with a corresponding set of weights ω_n, with $n = 1, ...N(N + 2)$, N being the order of the angular approximation usually refrred as S_N, they integrate with an acceptable accuracy integrals over the unit sphere. This approximation is well known as the Discrete-Ordinates Method (DOM).[REF]

- Space. Here, the spatial domains will be cuboids which will be decomposed by a grid of $I \times J \times K$ voxels, where each one is bounded in the x direction by $[x_{i+1}, x_i]$, in the y direction by $[y_{j+1}, y_j]$, and in the z direction by $[z_{k+1}, z_k]$, for $i = 1, ..., I$, $j = 1, ..., J$, and $k = 1, ..., K$.[REF]

Once that the previous steps have been performed, then, as it will be shown, a polynomial nodal method known as $RTN - 0$ (Raviart-Thomas-Nédelec of index

0)[REF], will be applied to get finally a low-order system of algebraic equations which is exactly solved for each voxel (i, j, k), angular direction $(\hat{\Omega}_n)$, and energy-group g.

For a photon point source, $q^{\gamma}(\hat{\Omega}, E)$[Units], located at $\vec{r_p}$, the coupled photon-electron $(\gamma - e)$ LBTEs can be written as

$$\hat{\Omega} \cdot \vec{\bigtriangledown}\psi^{\gamma}(\vec{r}, \hat{\Omega}, E) + \Sigma^{\gamma}(\vec{r}, E)\psi^{\gamma}(\vec{r}, \hat{\Omega}, E) = q^{\gamma\gamma}(\vec{r}, \hat{\Omega}, E) + q^{\gamma}(\hat{\Omega}, E)\delta(\vec{r} - \vec{r_p}) \quad (3.1)$$

$$\begin{aligned} \hat{\Omega} \cdot \vec{\bigtriangledown}\psi^{e}(\vec{r}, \hat{\Omega}, E) + \Sigma^{e}(\vec{r}, E)\psi^{e}(\vec{r}, \hat{\Omega}, E) = \\ \frac{\partial}{\partial E}(S_R\psi^{e}(\vec{r}, \hat{\Omega}, E)) + q^{ee}(\vec{r}, \hat{\Omega}, E) + q^{\gamma e}(\vec{r}, \hat{\Omega}, E) + q^{e}(\vec{r}, \hat{\Omega}, E) \end{aligned} \quad (3.2)$$

where $\psi^{\gamma}(\vec{r}, \hat{\Omega}, E)$ can be written as the sum of $\psi^{\gamma}_{unc}(\vec{r}, \hat{\Omega}, E)$ and $\psi^{\gamma}_{coll}(\vec{r}, \hat{\Omega}, E)$, the uncollided and collided photon angular fluences, respectively. The collided angular fluence refers to photons which have not interacted within the medium, and the collided angular fluence relates to the ones that did interact. Hence, equations (3.1) and (3.2) become

$$\hat{\Omega} \cdot \vec{\bigtriangledown}\psi^{\gamma}_{unc}(\vec{r}, \hat{\Omega}, E) + \Sigma^{\gamma}(\vec{r}, E)\psi^{\gamma}_{unc}(\vec{r}, \hat{\Omega}, E) = q^{\gamma}(\hat{\Omega}, E)\delta(\vec{r} - \vec{r_p}) \quad (3.3)$$

$$\hat{\Omega} \cdot \vec{\bigtriangledown}\psi^{\gamma}_{coll}(\vec{r}, \hat{\Omega}, E) + \Sigma^{\gamma}(\vec{r}, E)\psi^{\gamma}_{coll}(\vec{r}, \hat{\Omega}, E) = q^{\gamma\gamma}_{coll}(\vec{r}, \hat{\Omega}, E) + q^{\gamma\gamma}_{unc}(\vec{r}, \hat{\Omega}, E) \quad (3.4)$$

$$\begin{aligned} \hat{\Omega} \cdot \vec{\bigtriangledown}\psi^{e}(\vec{r}, \hat{\Omega}, E) + \Sigma^{e}(\vec{r}, E)\psi^{e}(\vec{r}, E) = \\ \frac{\partial}{\partial E}(S_R\psi^{e}(\vec{r}, \hat{\Omega}, E)) + q^{ee}(\vec{r}, \hat{\Omega}, E) + q^{\gamma e}_{coll}(\vec{r}, \hat{\Omega}, E) + q^{\gamma e}_{unc}(\vec{r}, \hat{\Omega}, E) + q^{e}(\vec{r}, \hat{\Omega}, E) \end{aligned} \quad (3.5)$$

This substitution leads to a decoupled system that can be solved in a forward way. Here, $q^{\gamma\gamma}_{unc}(\vec{r}, \hat{\Omega}, E)$ and $q^{\gamma e}_{unc}(\vec{r}, \hat{\Omega}, E)$ are called first scattered photon and electron sources. Therefore, the solution of equation (3.3) returns an uncollided photon angular fluence from a point source as [REF]

$$\psi^{\gamma}_{unc}(\vec{r}, \hat{\Omega}, E) = \delta(\hat{\Omega} - \hat{\Omega}_{\vec{r},\vec{r_p}})\frac{q^{\gamma}(\hat{\Omega}, E)}{4\pi}\frac{e^{-\tau(\vec{r},\vec{r_p})}}{|\vec{r} - \vec{r_p}|^2} \quad (3.6)$$

where,

$$\hat{\Omega}_{\vec{r},\vec{r_p}} = \frac{\vec{r} - \vec{r_p}}{|\vec{r} - \vec{r_p}|} \quad (3.7)$$

and

$$\tau(\vec{r},\vec{r}_p) = \int_{\vec{r}_p}^{\vec{r}} \Sigma^{\gamma}(\vec{(}r),\hat{\Omega},E)dxdydz \tag{3.8}$$

3.3.1 The Multi-Group Method

The first step, as described in Section 3.1, is the discretization of the independent variable E, the energy of the particle. To do so, the Multi-Group Method (MGM) was applied [REF]. This method consists in performing a balance of particles in each one of the G energy sub-intervals that $[E_{min}, E_{max}]$ is divided into. This action leads to the definition of group-averaged cross sections and angular group fluxes [REF] so that equation (3.3), the one related to the uncollided photon flux, may be written as a set of G equations given by

$$\hat{\Omega}\cdot\vec{\bigtriangledown}\psi^{\gamma}_{unc,g}(\vec{r},\hat{\Omega}) + \Sigma^{\gamma}_{g}(\vec{r})\psi^{\gamma}_{unc,g}(\vec{r},\hat{\Omega}) = q^{\gamma}_{g}(\hat{\Omega})\delta(\vec{r}-\vec{r_p}); g \;=\; 1,...,G. \tag{3.9}$$

In addition, the equation corresponding to the collided photon flux, *i.e.*, equation (3.4) becomes

$$\begin{aligned}\hat{\Omega}\cdot\vec{\bigtriangledown}\psi^{\gamma}_{coll,g}(\vec{r},\hat{\Omega}) + \Sigma^{\gamma}_{g}(\vec{r},\hat{\Omega})\psi^{\gamma}_{coll,g}(\vec{r},\hat{\Omega}) = \\ q^{\gamma\gamma}_{coll,g}(\vec{r},\hat{\Omega}) + q^{\gamma\gamma}_{unc,g}(\vec{r},\hat{\Omega});\; g \;=\; 1,...,G.\end{aligned} \tag{3.10}$$

Finally, the coupled photon-electron equation (3.5) writes now as

$$\begin{aligned}\hat{\Omega}\cdot\vec{\bigtriangledown}\psi^{e}_{g}(\vec{r},\hat{\Omega}) + \Sigma^{e}\psi^{e}_{g}(\vec{r},\hat{\Omega}) = \\ q^{ee}_{CSD,g}(\vec{r},\hat{\Omega}) + q^{ee}_{g}(\vec{r},\hat{\Omega}) + \\ q^{\gamma e}_{coll,g}(\vec{r},\hat{\Omega}) + q^{\gamma e}_{unc,g}(\vec{r},\hat{\Omega}) + q^{e}_{g}(\vec{r},\hat{\Omega});\; g \;=\; 1,...,G,\end{aligned} \tag{3.11}$$

where the first term in the right hand side of equation (3.11) represents the Continuos Slowing Down that can be written in terms of an electron scattering cross section that does not have upscattering contributions according to Morel [REF] . The group-averaged uncollided flux is given by

$$\psi^{\gamma}_{unc,g}(\vec{r},\hat{\Omega}) = \delta(\hat{\Omega}-\hat{\Omega}_{\vec{r},\vec{r_p}})\frac{q^{\gamma}_{g}(\hat{\Omega})}{4\pi}\frac{e^{-\tau(\vec{r},\vec{r_p})}}{|\vec{r}-\vec{r_p}|^2};\; g \;=\; 1,...,G. \tag{3.12}$$

As it can be seen, equations (3.4) and (3.5) can be written with a scattering term plus a source term $q^{\gamma/e}_{ex,g}(\vec{r},\hat{\Omega})$, for photons or electrons, where the scattering term may couple their interactions,

$$\begin{aligned}\hat{\Omega}\cdot\vec{\bigtriangledown}\psi^{\gamma/e}_{g}(\vec{r},\hat{\Omega})+\Sigma^{\gamma/e}_{g}(\vec{r})\psi^{\gamma/e}_{g}(\vec{r},\hat{\Omega})=\\ \sum_{g'=1}^{G}\int_{4\pi}\Sigma^{\gamma/e}_{s,g'\to g}(\vec{r},\hat{\Omega}'\to\hat{\Omega})\psi^{\gamma/e}_{g'}(\vec{r},\hat{\Omega}')d\hat{\Omega}'+q^{\gamma/e}_{ex,g}(\vec{r},\hat{\Omega});\end{aligned} \tag{3.13}$$

3.3.2 The Discrete-Ordinates Method (DOM)

Discrete-Ordinates Methods (DOM) are based on the discretization of the angular directions, where in each octant the total number of discrete-ordinates is $N(N+2)$ as indicated in Figure 3.2. The Boltzmann Transport Equation for the discrete-ordinate $\hat{\Omega}_n$ is

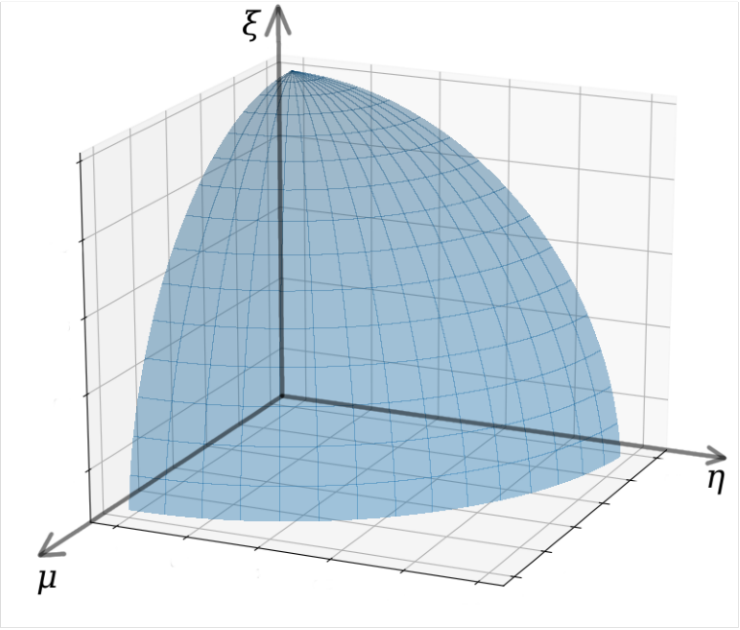

Figure 3.1: Symmetric discrete ordinates set

$$\mu_n\frac{\partial}{\partial x}\psi^{\gamma/e}_{gn}(\vec{r})+\eta_n\frac{\partial}{\partial y}\psi^{\gamma/e}_{gn}(\vec{r})+\xi_n\frac{\partial}{\partial z}\psi^{\gamma/e}_{gn}(\vec{r})+\Sigma^{\gamma/e}(\vec{r})\psi^{\gamma/e}_{gn}(\vec{r})=q^{\gamma/e}_{gn}(\vec{r}) \tag{3.14}$$

$$\begin{aligned} \mu_n &= \cos\theta_n \\ \eta_n &= \sin\theta_n \sin\varphi_n \\ \xi_n &= \sin\theta_n \cos\varphi_n \end{aligned} \tag{3.15}$$

and $\vec{r} = \vec{r}(x, y, z)$ and $\hat{\Omega}_n = \hat{\Omega}(\mu_n, \eta_n, \xi_n)$, and $\psi^{\gamma}_{gn}(\vec{r}) = \psi^{\gamma}_{g}(\vec{r}, \hat{\Omega}_n)$. Meanwhile the discrete-ordinates approximation of the source over the $N(N+2)$ ordinates per octant is

$$q^{\gamma/e}_{gn}(\vec{r}) = \sum_{g'=1}^{G} \sum_{m=1}^{N(N+2)} w_m \Sigma^{\gamma/e}_{s,g'\to g}(\vec{r}, \hat{\Omega}_n \cdot \hat{\Omega}_m) \psi^{\gamma/e}_{g'm}(\vec{r}) + q^{\gamma/e}_{ex,g}(\vec{r}, \hat{\Omega}_n). \tag{3.16}$$

3.3.3 Solution of the LBTEs for a Volume Discretization

For the purposes of this work just cuboid volumes were considered. Lets define a cuboid volume $V = [a, b] \times [c, d] \times [e, f] \subset \mathbb{R}^3$ and divide it into voxels of dimensions $\Delta x_i, \Delta y_j, \Delta z_k$ so this voxels are bounded by $x_1, x_2, ..., x_{I+1}; y_1, y_2, ..., y_{J+1}$ and $z_1, z_2, ..., z_{K+1}$ (Figure 3.1). It is important to consider that photon- and electron-cross sections remain constant inside each voxel, namely that they are space independent.

The solution of LBTE equation is performed by the discretization of energy, direction, and space as mentioned. Now, considering a mono-energetic and mono-directional particles, from equation (3.14) it is obtained

$$\mu \frac{\partial \psi^{\gamma/e}}{\partial x} + \eta \frac{\partial \psi^{\gamma/e}}{\partial y} + \xi \frac{\partial \psi^{\gamma/e}}{\partial z} + \Sigma^{\gamma/e}_{t} \psi^{\gamma/e} = q^{\gamma/e} \tag{3.17}$$

that changing to the normalized coordinates x_r, y_r, and z_r in $[-1, +1]$ for x, y, and z respectively, *i.e.*

$$x_r = \frac{2x - (x_R + x_L)}{\Delta x_i}, y_r = \frac{2y - (y_F + y_N)}{\Delta y_j}, z_r = \frac{2z - (z_T + z_B)}{\Delta z_k} \tag{3.18}$$

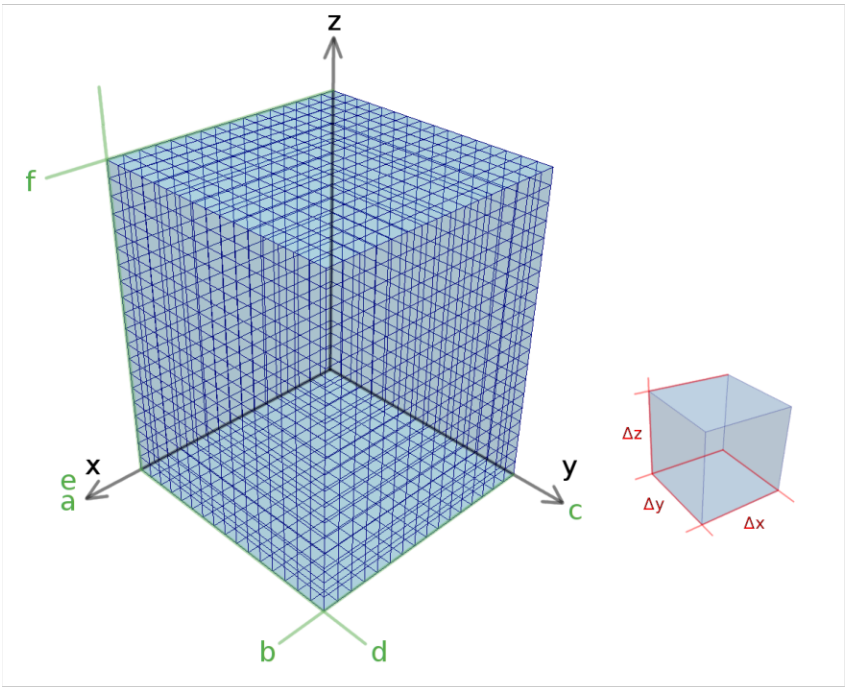

Figure 3.2: Voxelized volume grid

where for the sake of simplicity, x_{i+1} and x_i have been denoted by x_R and x_L, y_{j+1} and y_j have been denoted by y_F and y_N, and z_{k+1} and z_k have been denoted by z_T and z_B, respectively. Doing this, equation (3.17) results into,

$$\frac{2\mu}{\Delta x_i}\frac{\partial \psi^{\gamma/e}}{\partial x_r} + \frac{2\eta}{\Delta y_j}\frac{\partial \psi^{\gamma/e}}{\partial y_r} + \frac{2\xi}{\Delta z_k}\frac{\partial \psi^{\gamma/e}}{\partial z_r} + \Sigma_t^{\gamma/e}\psi^{\gamma/e} = q^{\gamma/e} \tag{3.19}$$

Now, using an approximation ψ_h for ψ the corresponding residual for equation (3.19) results as follows,

$$R[\psi_h] = \frac{2\mu}{\Delta x_i}\frac{\partial \psi_h^{\gamma/e}}{\partial x_r} + \frac{2\eta}{\Delta y_j}\frac{\partial \psi_h^{\gamma/e}}{\partial y_r} + \frac{2\xi}{\Delta z_k}\frac{\partial \psi_h^{\gamma/e}}{\partial z_r} + \Sigma_t^{\gamma/e}\psi_h^{\gamma/e} - q^{\gamma/e} \tag{3.20}$$

Here, ψ_h is a polynomial function interpolating ψ_L^{00}, ψ_R^{00}, ψ_N^{00}, ψ_F^{00}, ψ_B^{00}, ψ_T^{00}, and ψ_C^{000}, which are the averaged angular fluxes at *L*eft, *R*ight, *N*ear, *F*ar, *B*ottom, and *T*op edges of a voxel and the averaged angular flux in the voxel. This interpolation corresponds to the RTN-0 polynomial nodal method which basis functions are the following [REF]

$$u_L^{00} = \frac{1}{2}(P_{100} - P_{200}),\ u_R^{00} = \frac{1}{2}(P_{100} + P_{200}) \tag{3.21}$$

$$u_N^{00} = \frac{1}{2}(P_{010} - P_{020}),\ u_F^{00} = \frac{1}{2}(P_{010} + P_{020}) \tag{3.22}$$

$$u_B^{00} = \frac{1}{2}(P_{001} - P_{002}),\ u_T^{00} = \frac{1}{2}(P_{001} + P_{002}) \tag{3.23}$$

$$u_C^{000} = P_{000} - P_{200} - P_{020} - P_{002} \tag{3.24}$$

where, $P_{\ell mn}(x_r, y_r, z_r) = P_\ell(x_r)P_m(y_r)P_n(z_r)$, $P_\ell(x_r)$ being the Legendre polynomial of degree ℓ in x_r over the interval $[-1, +1]$. Then, the approximation by the RTN-0 for the fluence can be written as

$$\psi_n(x, y, z) = \sum_S \psi_S^{00} u_S^{00}(x, y, z) + \psi_C^{000} u_C^{000}(x, y, z) \tag{3.25}$$

where S can be L, R, N, F, B, and T. The next step is to ask that the residual given by equation (3.20) be orthogonal to the following basis functions: $P_{000}(x_r, y_r, z_r), P_{100}(x_r, y_r, z_r), P_{010}$ and $P_{001}(x_r, y_r, z_r)$ to obtain the following set of four equations,

$$\frac{\mu}{\Delta x_i}[\psi_R^{00} - \psi_L^{00}] + \frac{\eta}{\Delta y_j}[\psi_F^{00} - \psi_N^{00}] + \frac{\xi}{\Delta z_k}[\psi_T^{00} - \psi_B^{00}] + \Sigma_t \psi_C^{000} = q_C^{000}. \tag{3.26}$$

$$\frac{3\mu}{\Delta x_i}[\psi_R^{00} + \psi_L^{00} - 2\psi_C^{000}] + \frac{\eta}{\Delta y_j}[\psi_F^{10} - \psi_N^{10}] + \frac{\xi}{\Delta z_k}[\psi_T^{10} - \psi_B^{10}] + \Sigma_t \psi_C^{100} = q_C^{100}. \tag{3.27}$$

$$\frac{\mu}{\Delta x_i}[\psi_R^{10} - \psi_L^{10}] + \frac{3\eta}{\Delta y_j}[\psi_F^{00} + \psi_N^{00} - 2\psi_C^{000}] + \frac{\xi}{\Delta z_k}[\psi_T^{10} - \psi_B^{10}] + \Sigma_t \psi_C^{010} = q_C^{010}, \tag{3.28}$$

$$\frac{\mu}{\Delta x_i}[\psi_R^{10} - \psi_L^{10}] + \frac{\eta}{\Delta y_j}[\psi_F^{10} - \psi_N^{10}] + \frac{3\xi}{\Delta z_k}[\psi_T^{00} + \psi_B^{00} - 2\psi_C^{000}] + \Sigma_t \psi_C^{001} = q_C^{001}, \tag{3.29}$$

where ψ_R^{00}, ψ_L^{00} are the averaged fluences or angular fluxes on the right and left side of the voxel, ψ_B^{00}, ψ_T^{00} are the averaged fluences or angular fluxes of the bottom

and top side of the voxel and ψ_F^{00}, ψ_N^{00} are the averaged fluxes or angular fluxes on the farthest and nearest side of the voxel.

It is important to consider that the Legendre moments $100, 010$, and 001 of fluences or angular fluxes on each direction are defined as

$$\psi_C^{100} = \frac{1}{2}(\psi_R^{00} - \psi_L^{00}) \tag{3.30}$$

$$\psi_C^{010} = \frac{1}{2}(\psi_F^{00} - \psi_N^{00}) \tag{3.31}$$

$$\psi_C^{001} = \frac{1}{2}(\psi_T^{00} - \psi_B^{00}). \tag{3.32}$$

Now defining α, β, and γ as follows,

$$\alpha = \frac{\mu}{\Delta x_i}, \beta = \frac{\eta}{\Delta y_j}, \gamma = \frac{\xi}{\Delta z_k}, \tag{3.33}$$

then equations (3.26) to (3.29) lead to the next system of equations,

$$\begin{bmatrix} \alpha & \beta & \gamma & \Sigma_t \\ 3\alpha+\beta+\gamma+\Sigma_t & 0 & 0 & -6\alpha \\ 0 & \alpha+3\beta+\gamma+\Sigma_t & 0 & -6\beta \\ 0 & 0 & \alpha+\beta+3\gamma+\Sigma_t & -6\gamma \end{bmatrix} \begin{bmatrix} \psi_C^{000} \\ \psi_R^{00} \\ \psi_F^{00} \\ \psi_T^{00} \end{bmatrix} = \begin{bmatrix} q^{000} + \alpha\psi_L^{00} + \beta\psi_N^{00} + \gamma\psi_B^{00} \\ q^{100} + (-3\alpha + \frac{\Sigma_t}{2})\psi_L^{00} \\ q^{010} + (-3\beta + \frac{\Sigma_t}{2})\psi_N^{00} \\ q^{001} + (-3\gamma + \frac{\Sigma_t}{2})\psi_B^{00} \end{bmatrix}. \tag{3.34}$$

which is solved analytically by a each specific voxel (i, j, k), angular direction $\hat{\Omega}_n$ and energy group g following a natural strategy based in the signs of the direction cosines μ, η, and ξ . This means that the solution algorithm depends on which of the eight octants $\hat{\Omega}_n$ is in. One of the next eight sweeping directions through the voxelized grid are possible:

$\mu_n > 0, \eta_n > 0, \xi_n > 0$ left to right; bottom to top; near to far

$\mu_n > 0, \eta_n > 0, \xi_n < 0$ left to right; bottom to top; far to near

$\mu_n > 0, \eta_n < 0, \xi_n > 0$ left to right; top to bottom; near to far

$\mu_n > 0, \eta_n < 0, \xi_n < 0$ left to right; top to bottom; far to near

$\mu_n < 0, \eta_n > 0, \xi_n > 0$ right to left; bottom to top; near to far

$\mu_n < 0, \eta_n > 0, \xi_n < 0$ right to left; bottom to top; far to near

$\mu_n < 0, \eta_n < 0, \xi_n > 0$ right to left; top to bottom; near to far

$\mu_n < 0, \eta_n < 0, \xi_n < 0$ right to left; top to bottom; far to near.

3.3.4 Absorbed dose calculation

Finally, the calculation of the absorbed dose can be calculated by the following equation

$$D^e = \frac{1}{\rho} \sum_{g=1}^{G-1} \psi_g^e(\vec{r}) \beta(E_g) + \psi_G^e(\vec{r}) \Sigma_a^e E_G \tag{3.35}$$

where $\Sigma_a^e = \frac{\beta(E_G)}{E_G - E_f}$ and E_G is the highest energy considered, E_f is the medium point energy between two energy groups, and ψ_g^e is the electron scalar flux corresponding to energy-group g.

3.4 Photon cross sections

Unlike electrons, photons are neutral particles and do not loss continuously energy as they travel in a medium. Photon interactions within a given medium are governed statistically by probabilities of interaction[**Tuner**]. The calculation of this probabilities usually is done by experimental or theoretical work and there exist database that provide this information with tables where photon cross sections are given for a set of energies. For instance XCOM is a computer program developed on 1987 by M. J. Berger and J. H. Hubbell on the National Institute of Standards

and Technology (NIST) for calculating photon cross sections at energies from 1 keV to 100 GeV in any element, compound or mixture [**XCOM**]. The results of this database were used for materials commonly founded in a WBRT [REF] treatment such as water, brain tissue, and dense bone. In Appendices A to G part of such a tables are reproduced and used in this work. They are truncated for energies greater than $6MeV$. These cross sections are available on-line and were useful to perform the calculations corresponding to photons distribution in a medium represented by a 3D domain re-built with the associated computarized axial tomography images.

To get the photon cross-sections for each one of the compounds within the 3D domain, it was necessary to provide the source energy, the energy interval, and the mass and atomic densities. [REF]

3.5 Coupled Photon-Electron cross sections

As electrons travels through a medium, they are subject to Coulomb forces by atomic electrons. In these interactions electrons loss energy continuously.

Energetic ions interact via elastic and inelastic collisions with atomic nuclei and atomic electrons. Inelastic collisions with electrons can be accurately approximated by the so-called Continuous Slowing Down approach.

Elastic interactions with nuclei may result in large energy transfers and angular deflections, and therefore they are represented by a differential scattering cross section. The transport of ions can then be described by the linear transport equations for the angular flux, and well established numerical solution methods can be used in principle.

Coupled photon-electron cross sections may be generated with the code CEPXS (Coupled Electron-Photon X Sections) [REF]. Unfortunately, due to the lack of this code electron cross sections generated with the domestic code TEOD [REF] were used instead in combination with a source contribution due to uncollided

photons. TEOD [**Reyes**] is based in the method described by Morel [**Morel**]. Particularly for this work, initial photon fluence is considered to be outside of the patient simultaneously electron initial fluence is zero.

3.6 The NDOCPE Code

Based on the methods used to discretize and to get an approximation for photon and electron angular fluxes and fluences, as well as the absorbed dose for a radiotherapy simulation the code NDOCPE (Nodal Discrete-Ordinates Coupled Photon-Electron) was developed. It was written in Julia computational language version 0.5 where inherent parallelism of energy and angular loops has been taken into account. The source code is as long as 3,250 lines and its performance depends on the number of CPUs available to accomplish a task and that the user wants to use.

The code requires photon cross sections previosuly prepared by the user for a given set of materials and energy groups that may be obtained from the XCOM website [REF]. It also requires the coupled photon-electron cross sections that may be generated with the code CEPXS (Coupled Electron-Photon X Sections) [REF]. Unfortunately, due to the lack of this code electron cross sections generated with TEOD [REF] were used instead in combination with a source contribution due to uncollided photons. To generate the electron cross sections the user must know the mass and electron densities of each one of the materials involved in a given domain. Photon and electron cross sections must be generated for the same number of energy groups.

Once that the user has acquired the 3D domain with its materials distribution the photon source intensity and spectra must be provided in an input file.

The output file of the NDOCPE Code provides enough information to visualize PDD (z profile) and RF (xz and yz radial profiles).

3.7 Benchmarking

It has been demonstrated that the gold standard for dose calculation in radiotherapy is the Monte Carlo simulation; its long computational times make it clinically impractical for the every-day radiation treatment calculations. Nonetheless, the Monte Carlo method has been widely used for benchmarking analytical codes, especially within heterogeneous media.

The benchmarking simulations compare simple measurements against the code to be implemented. The necessary measurements must consist of Percentage Depth Dose (PDD) and beam profiles simulated at reference conditions. The terms of the simulated comparisons need to be the same.

3.7.1 GEANT4

GEANT4 (GEometry ANd Tracking 4) is a Monte Carlo toolkit that simulates the particle trajectory throug matter. Because of its flexibility, it is possible to simulate a broad variety of physics components. The Geant4 data libraries for electron ans gammma processes are EPDL97, EEDL, and EADL. Geant4 have been extensively validated for medical physics applications, comparing the output results against other Monte Carlo coses used in medical physics: MCNP, EGSnrc, PENELOPE.

4

Materials and Methods

Contents

4.1 Python

Nowadays, Python is one of the most popular programming languages used by scientists thanks to its extensive community and the diverse collection of packages available. Python version 2.7 was used mainly for the development of visualization tools. The next subsections comprise a brief description of the libraries and the scripts developed with them.

4.1.1 Python Libraries

- **pyDicom**. Python package for working with DICOM files such as medical images, reports, and radiotherapy objects.
  This library was used to retrieve the CT calibration information, pixel spacing, and pixel array from DICOM images.

- **numpy**. Fundamental package for scientific computing with Python. Among the wide capabilities of this library, is a tool for managing array objects. It was used to discretize the patient volume and create the cross sections arrays.

- **vtk**. The Visualization Toolkit (VTK) is an open-source, freely available software system for 3D computer graphics, image processing, and visualization. It is written in C++ but works with Python via wrappers. Hereafter will be referred as vtk. This set of tools was used to build the patient 3D model from a set of CT images and to visualize it using a GPU.

- **tvtk**. A complementary vtk library created for Python, it contents a diverse set of tools that wrap around all vtk classes.
  Used to build 3D volumes from a numpy array.

- **pillow**. A fork from the Python Image Library (PIL). This library was created to easily process images. In this work pillow was used to convert images from DICOM protocol and array data to PNG and JPEG format.

- **matplotlib**. It is a Python 2D plotting library which produces publication quality figures in a variety of hardcopy formats and interactive environments across platforms. This library was used to generate 3D surface angular flux plots, PDD, and beam profile plots.

4.1.2 Developed scripts in Python

The scripts developed in Python were focused in majority to the creation of evaluation and visualization tools. Below are listed a description of the developed codes.

- **patientVolume.py**. This script converts a set of DICOM images into numpy arrays of mass and electron densities then discretizes the array to ICRU90 patient materials that are saved as numpy objects.
- **photon_cs.py**. This script uses as input an array of materials and a list of energies to create scattering and coherent cross sections arrays that are saved as numpy objects.
- **electron_cs.py**. This script uses as input an array of materials and a list of energies to create scattering, absorbed and transferred cross sections arrays based on a stopping power data set. The resulting arrays are saved as numpy objects.
- **pdd.py**. This script uses as input a numpy array object with dose or scalar flux distribution and plots a normalized PDD.
- **profile.py**. This script uses as an input a numpy array object with dose or scalar flux distribution and plots the beam profiles in planes XZ or YZ.
- **array2vtk.py**. This script converts a numpy array object into a structured grid vtk file so it can be visualized by Paraview or by Vis3D.py
- **arrayplot.py**. This script uses the matplotlib library to visualize 3D surface plots of the dose or scalar flux.
- **array2img.py**. Using pillow library, this script plots a single slice or the total number of slices of a 3D array saved as a numpy object.
- **DICOM2Vol.py**. Creates a vtk format volume from a set of CT DICOM images. It allows to apply a different range of thresholds.
- **Vis3D.py**. Renders a vtk file using GPUs, allowing to visualize objects with scalar and gradient opacity.
- **DoseDist.py**. Reads a GEANT4 output and creates a numpy array object and a vtk object file.

- **exec.py**. It executes and parses arguments to the Python and Julia programming language scripts in order to run a full simulation and visualization of the results.

4.2 Julia

The Boltzmann Transport Equation solver was developed in Julia programming language version 0.5.0. The scripts have the capability to run in parallel improving the accuracy and reducing the execution time.

The libraries used to develop these scripts are listed bellow

4.2.1 Julia Libraries

- **NPZ**. It converts an array into a numpy array. The dose distribution is exported into a numpy array object for further analysis in Python.
- **WriteVTK**. It converts an array into a vtk object. In this work, this script converts the dose distribution or scalar flux distribution array into a vtk object for visualization purposes.

4.2.2 Developed scripts in Julia

The focus of these scripts was to use the tools and capabilities of Julia language to create a high performance Boltzmann Transport Equation solver for photons and electrons. Parallelization was implemented for this codes.

- **photon_solver.jl**. Photon Boltzmann Transport Equation Solver. It takes as inputs: the mass density numpy array, the text file containing the energy groups, and the coherent and scattering photon cross sections numpy arrays.

The script returns the angular flux numpy arrays on X, Y, and Z axis along with the voxel angular flux.

- **electron_solver.jl**. Electron Transport Equation Solver. It takes as inputs: the mass density numpy array, the text file containing the energy groups, absorption, transferred and scattering electron cross sections numpy arrays, angular photon flux arrays on X, Y, and Z axis along with the voxel angular flux. It returns the scalar flux and dose arrays along with a vtk format file.

4.3 Visualization tools

For the construction of the next visual representations, a common workflow was followed. DICOM images were read using the pydicom library, and the corresponding data array were stored into a numpy array, a 3-D array is created parsing each 2-D image.

4.3.1 Sagittal, Coronal, and Axial images

CT images usually are obtained from an axial image; this means that each image is a slice on the XY plane from the patient. The construction of sagittal and coronal images was made breaking down the 3D array into 2D arrays and storing each 2D array into an image by the developed script arr2img.py. For sagittal images, the 3D array was made by breaking it down into the YZ plane, looping on the x axis. Therefore, the coronal images were created by the XZ plane looping on the y axis.

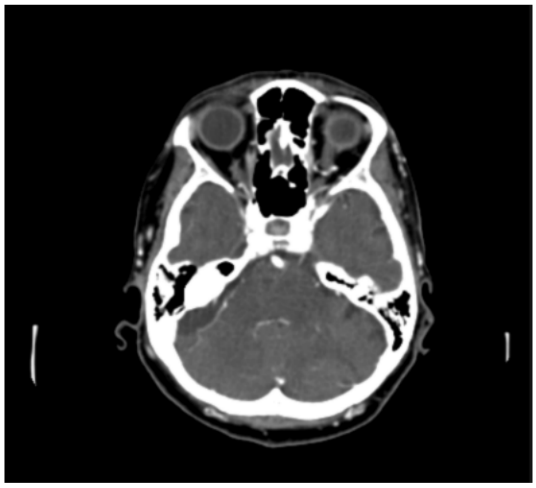

Figure 4.1: Axial slice

Figure 4.2: Coronal slice

Figure 4.3: Sagittal slice

4.3.2 3D Visualization

Volume rendering consists in generating a 2D view of an object that is integrated into a 3D volume. This method incorporates a function of the image along parallel rays to create a single 2D representation of the image. In this approach, each beam maps information of each voxel like transparency level and intensity. Some volumes that are composed of an enormous quantity of elements will require a Graphics Processor Unit (GPU) for visualization.

The proper display is needed in TPS to create the best treatment plan possible for each patient. The lack of quality in CT images can severely affect the quality on the treatment of the patient. Using the Python scripts DICOM2volume.py and Vis3D.py and a GPU NVIDIA GTX 960M 2GB GDDR5 for the construction and visualization of the patient was possible with different opacity and color settings.

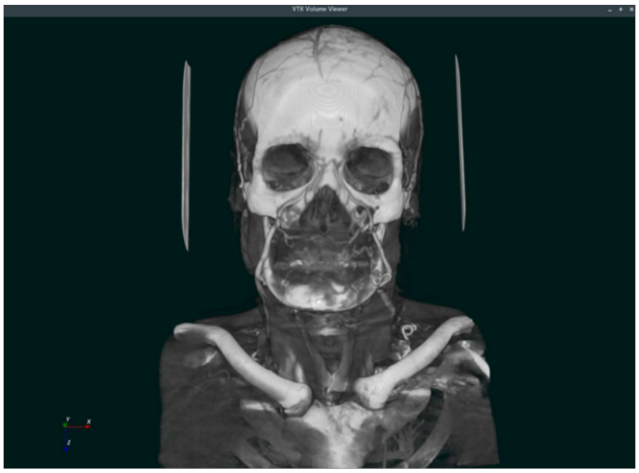

Figure 4.4: GPU render of the patient. Front view

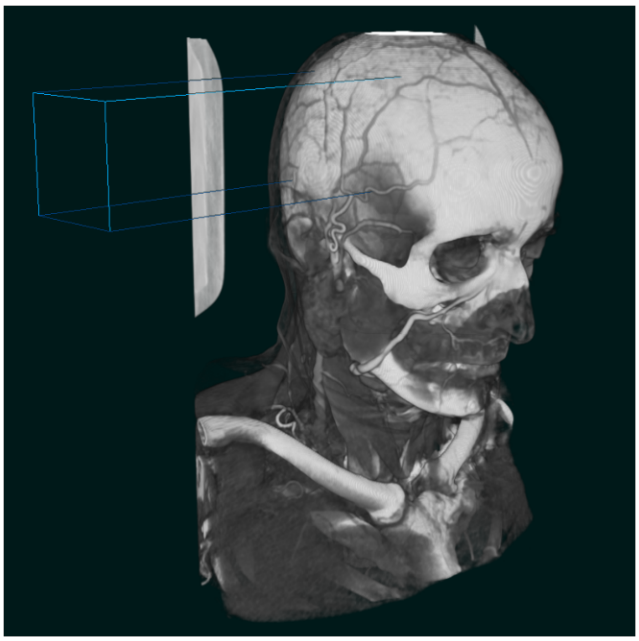

Figure 4.5: GPU render of the patient with simulated beam. Left View

4.4 Volume discretization and cross sections

The volume discretization was perfomed in three steps: the Hounsfield Units discretization, the electron and mass density calculations, and the determination of the cross sections according to the electron or mass density of the material.

The cross sections are the fundamental quantities that any LBTE solver needs to calculate the fluence and the scalar flux on the patient's volume. To obtain the cross sections the first step was to convert CT images data into Hounsfield units, Hounsfield units are strongly related to the composition and density of each voxel. There are a wide variety of protocols to discretize an image into Hounsfield units, for the convenience of this work the discretization method that has been adopted from the ICRU90 protocol [**ICRU90**]. This protocol stablishes a material discretization according with the mass density of the voxels analized.

The calculation of the electron and mass densities were computed using the Hounsfield Units as described in subsection 2.1.1. Having the mass density of the

Min (mg/cm^3)	Max (mg/cm^3)	Material
0.000	0.207	Air
0.207	0.919	Lungs
0.919	0.979	Adipose
0.979	1.004	Breast
1.004	1.043	Water
1.043	1.109	Liver
1.109	1.113	Muscle
1.113	1.496	Trabecular Bone
1.496	1.654	Dense Bone

Table 4.1: Density and Material discretization used by GEANT4

CT images, the discretization is made selecting a material range that coincides with the most relatable approximation of the mass density; the discretization is shown in the table below[**ICRU90**].

Posterior to the mass and electron density the designation of the photon cross sections are computed by the tables shown in Appendix A. Electron cross sections were generated according to the stopping power for different energies using NIST stopping power data base.

4.5 Simulated treatment

For a realistic treatment evaluation, the AAA algorithm was verified for a real radiotherapy treatment with patient-specific CT images. The selected simulated treatment was whole brain radiotherapy. Due to the anatomy homogeneity of the selected treatment and the easy radiotherapy technique, it is considered a suitable treatment for the earliest algorithm evaluation.

The patient-specific information was obtained from public domain CT images. The slice thickness of all the images was $0.7\,mm$ with an $512x512$ resolution. Whole Brain Radiotherapy consists of a prescribed dose of 30 Gy in 10 fractions. The treatment plan is imparted by two opposed fields of $40 \times 40 cm^2$ separately. The

recommended energy for this treatment is 6 MeV.

The simulated treatment process was delevoped into the next steps,

1. The patient CT image is introduced as input information; the patient volume is then discretized. The discretization process was described in the previous section. The result of this technique is a cross section 3D grid.

2. Given initial conditions for the geometric grid, the photon flux distribution is calculated per energy group using the julia script photon_solver.jl. A file containing the angular flux over all the voxels, is created.

3. The electron_solver.jl script reads the photon angular flux file to calculate the angular electron flux distribution per energy group. Once the angular electron flux distribution is obtained, the absorbed dose is calculated by the same script. As results two files are obtained: an absorbed dose distribution numpy array and a visualization absorbed dose distribution file.

5

Results and discussion

Contents

5.1 Solver benchmark results

Different types of sources were tested in order to determine the quality of the results. The sources used to observe the scalar flux distribution in an homogeneous volume were: a) Box source at the half of the volume, b) cross source at the middle of the volume, c) two opposite finite-element size sources close on the top and bottom of the volume (Figures 5.1 to 5.3). These images demonstrate an expected ray effect caused by the cross sections of the volume and the discrete ordinates discretization scheme. These results were obtained with the developed scripts photon_solver.jl, electron_solver.jl, photon_cs.py, electron_cs.py and visualized using arr2plot.py and Paraview.

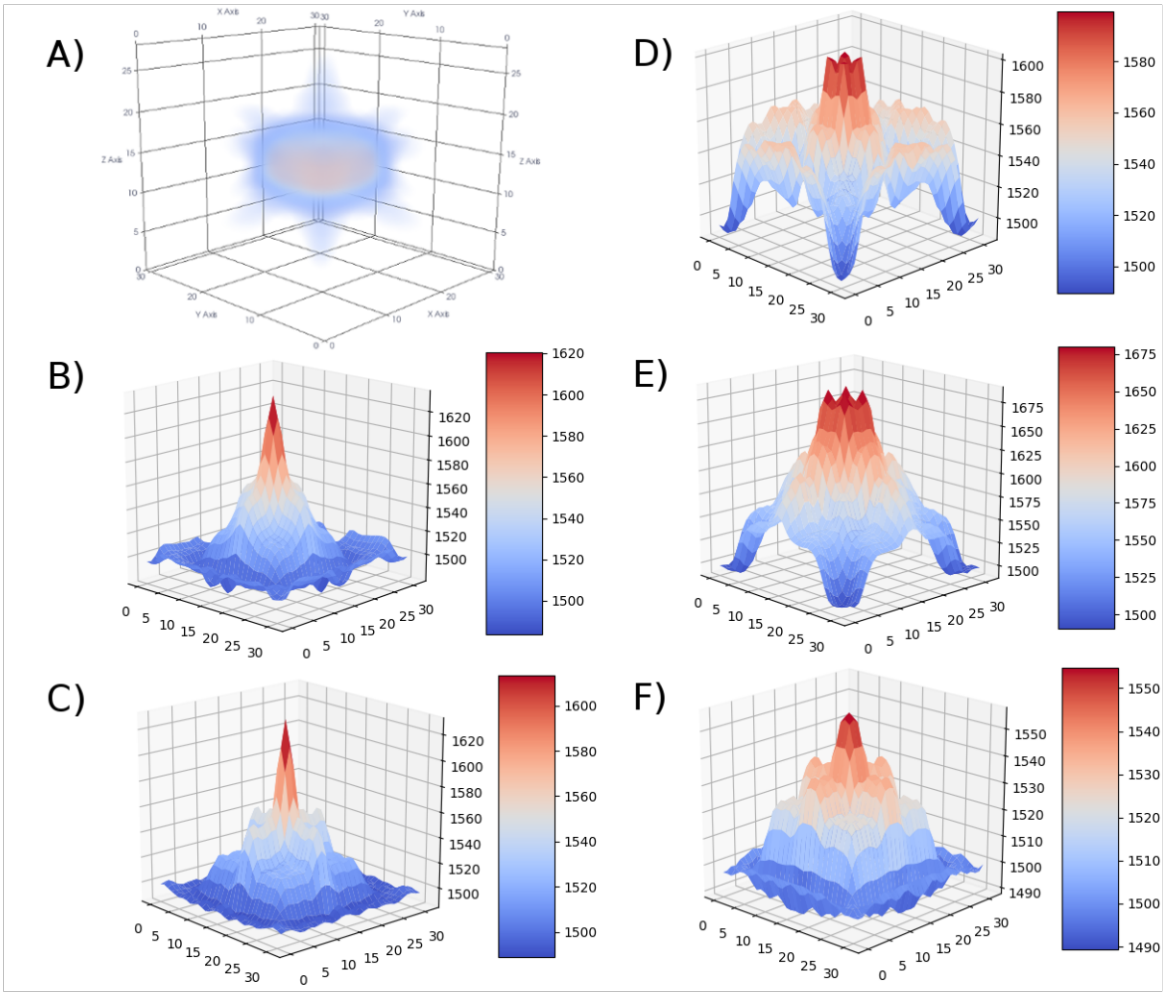

Figure 5.1: 6MeV Monoenergetic beam for a cubic shaped source in a water phantom A) 3D Scalar photon flux distribution. B) - F) Scalar photon flux from z = 0 to z = 30

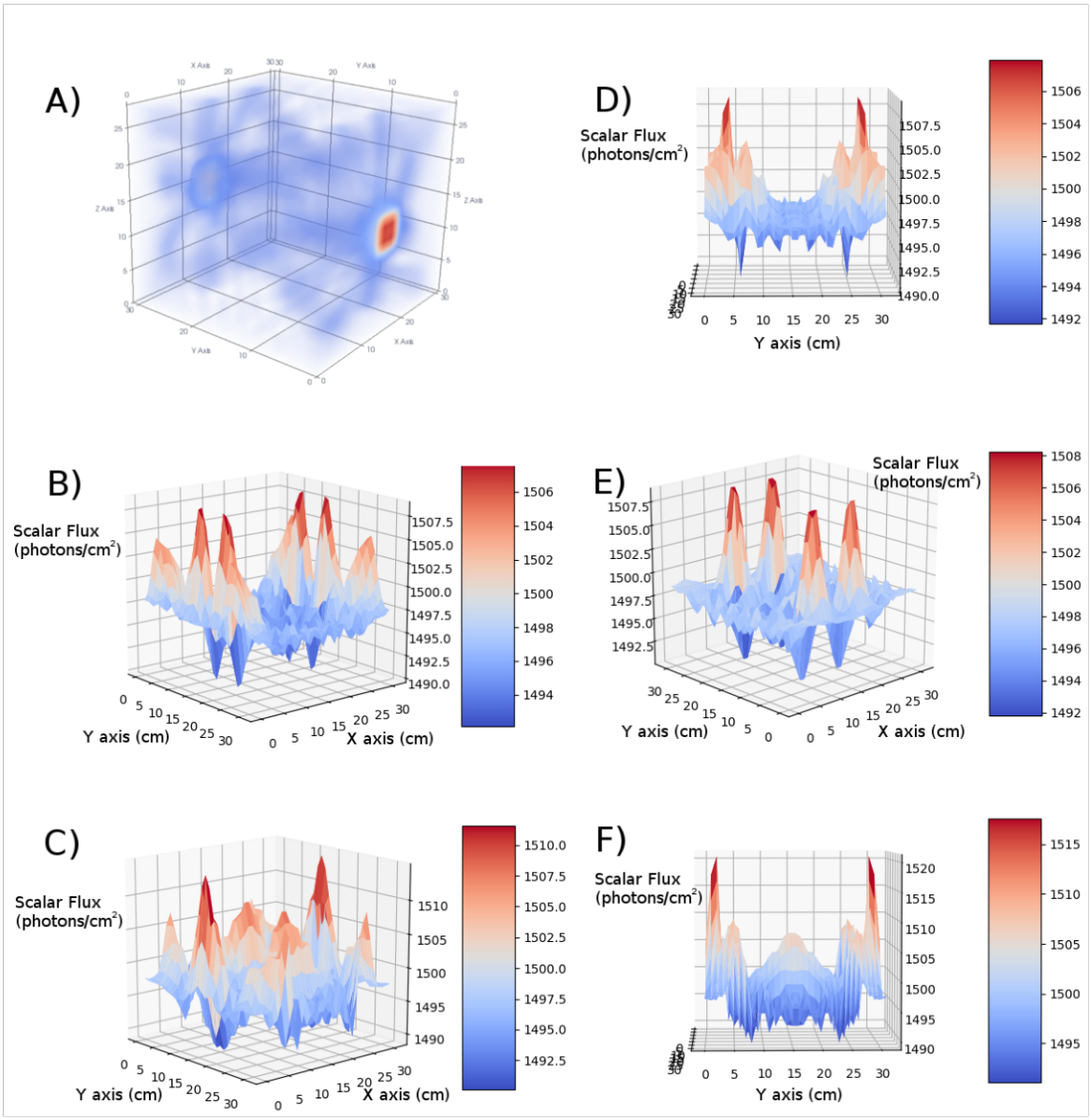
A)
B)
Scalar Flux
(photons/cm²)
Y axis (cm)
X axis (cm)
C)
Scalar Flux
(photons/cm²)
Y axis (cm)
X axis (cm)
D)
Scalar Flux
(photons/cm²)
Y axis (cm)
E)
Scalar Flux
(photons/cm²)
Y axis (cm)
X axis (cm)
F)
Scalar Flux
(photons/cm²)
Y axis (cm)

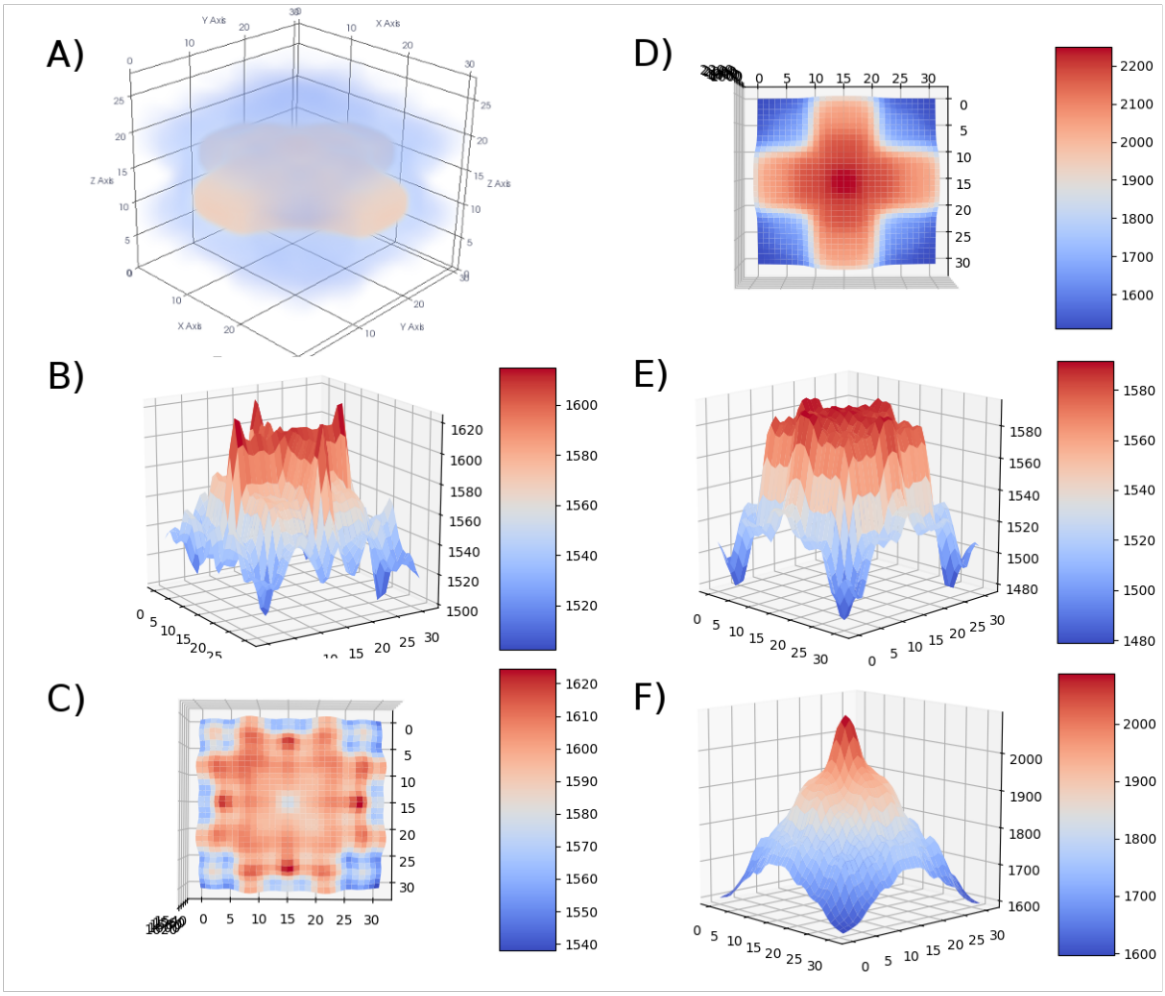

Figure 5.2: 6MeV Monoenergetic beam for a cross shaped source in a water phantom A) 3D Scalar photon flux distribution. B)-F) Scalar photon flux from z=0 to z=30

5.2 Visualization Results

The DICOM images set denominated as MANIX was taken from Osirix DICOM Medical Image Database. Reconstruction of the patient volume and visualization was performed with the developed python scripts: **patientVolume.py** and **Vis3D.py**. Since visualization process is based on ray casting technique is possible to visualize a wide range of materials and tissues as shown in Figures 5.4 to 5.6. The visualization script has the capability to perform the rendering using scalar and gradient opacity.

Figure 5.3: Pacient volume reconstruction and rendering at a range of 0 to 255 gray pixel value. Soft tissue and skin is visible within this range

Sagittal, axial, and coronal plane slices were obtained from the 3D Volume array (Fig 5.7 - 5.9) using the python script **array2img.py**.

Figure 5.4: Pacient volume reconstruction and rendering at a range of 10 to 255 gray pixel values.

5.3 Water phantom

PDD, beam profiles, and 3D absorbed dose distribution were obtained for a $32 \times 32 \times 29$ voxel water phantom with a 6 MeV monoenergetic beam. The field size was of 10×10 voxels performed with NDOCPE.

For the PDD the point of maximum dose is reached within 1.5 cm of depth. The charasterstic PDD curve is clearly reached. The beam profiles are symmetric and flat correspondingly with an homogeneous energy beam. The deposited dose is within the range of the beam field, depositing most of the dose in the 10×10 field.

5.4 Simulated treatment results

The beam simulation computed in the water phantom was transported into the CT brain images for the Whole Brain Radiotheapy simulation. The energy used

Figure 5.5: Pacient volume reconstruction and rendering at a range of 30 to 120 gray pixel values.

was $6\,MeV$ with a 10×10 beam field. The simulation of the 40×40 opposing fields was carried out in one single process. The dose distribution generated by the simulation of the monoenergetic beam was normalized to the point of maximum dose. Patient discretization was realized according ICRU recommendations (Figure 5.14). The final result was obtained by overlapping the dose distribution with the voxelized images of the patient brain (Figure 5.16). As expected the dose distribution was homogeneous in most parts of the brain, the critical structures however showed a dose level that could compromise their functioning as the contour of the regions at interest was not reached at this point. The point of maximum dose is computed in the delimited region of the brain.

The DVH showed a 90% of the volume of the brain reached 90% of the maximum dose.

Figure 5.6: Coronal volume slice.

Figure 5.7: Sagittal volume slice.

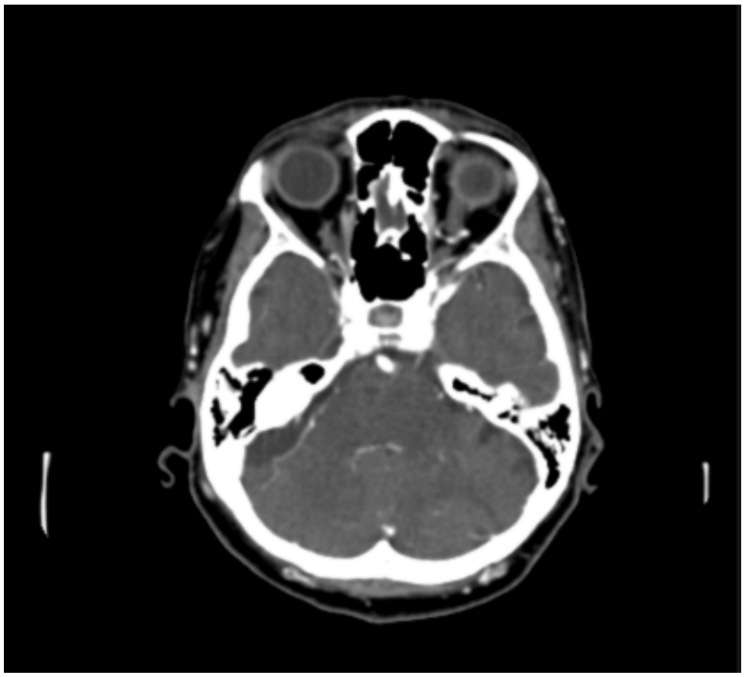

Figure 5.8: Axial volume slice.

Figure 5.9: GEANT4 dose distribution for a 6MeV monoenergetic photon beam

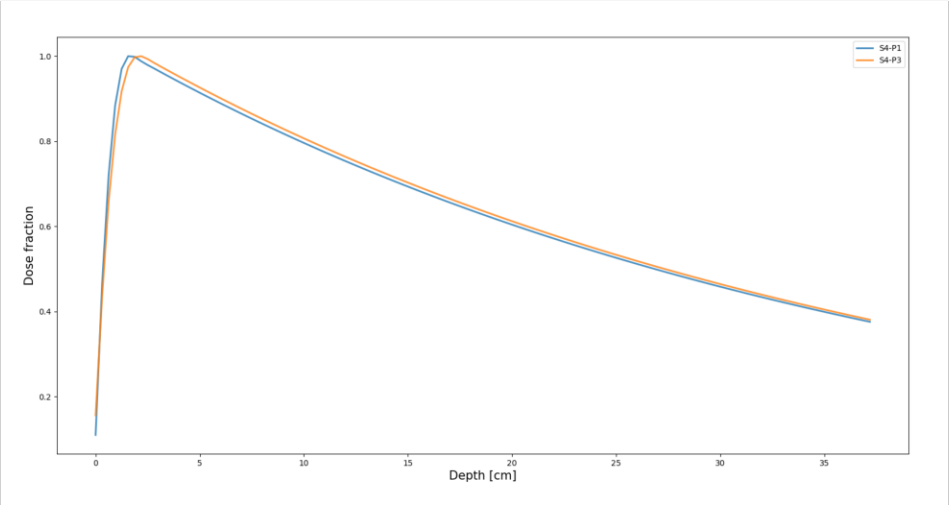

Figure 5.10: Percentage Depth Dose for S4 MOD

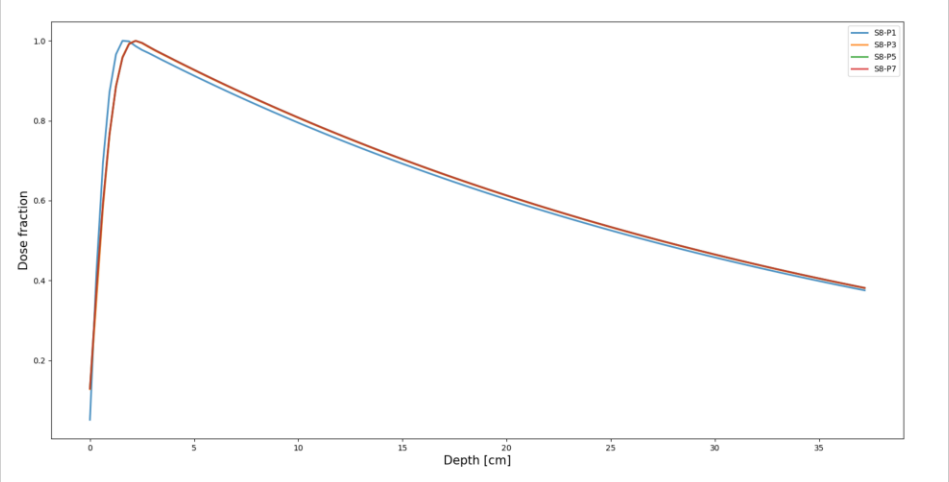

Figure 5.11: Percentage Depth Dose for S8 MOD

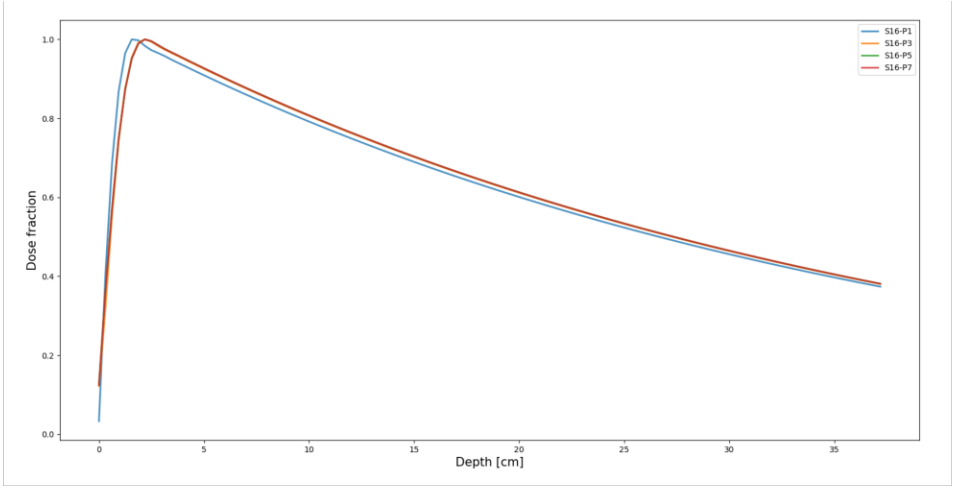

Figure 5.12: Percentage Depth Dose for S16 MOD

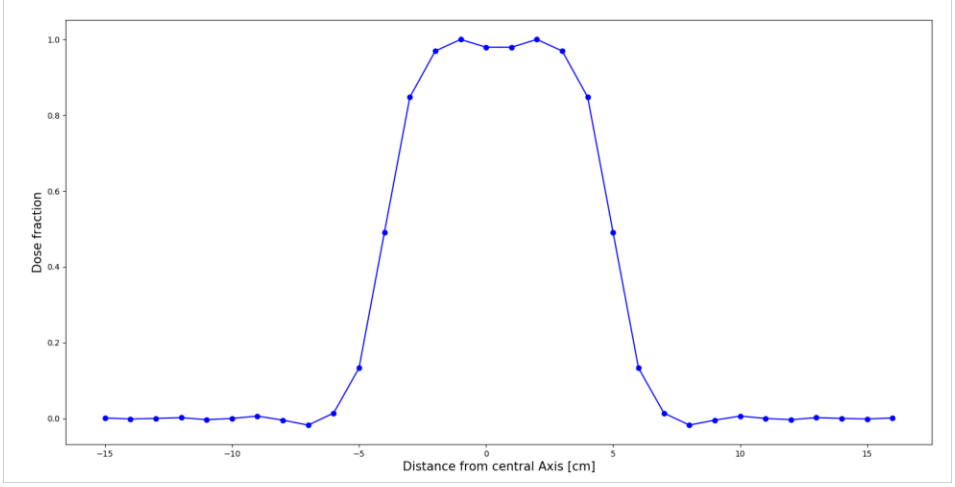

Figure 5.13: YZ beam profile

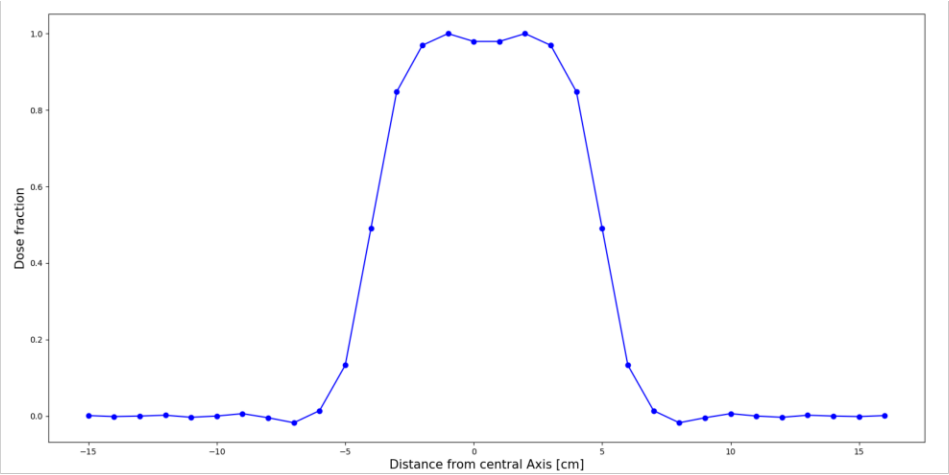

Figure 5.14: XZ beam profile

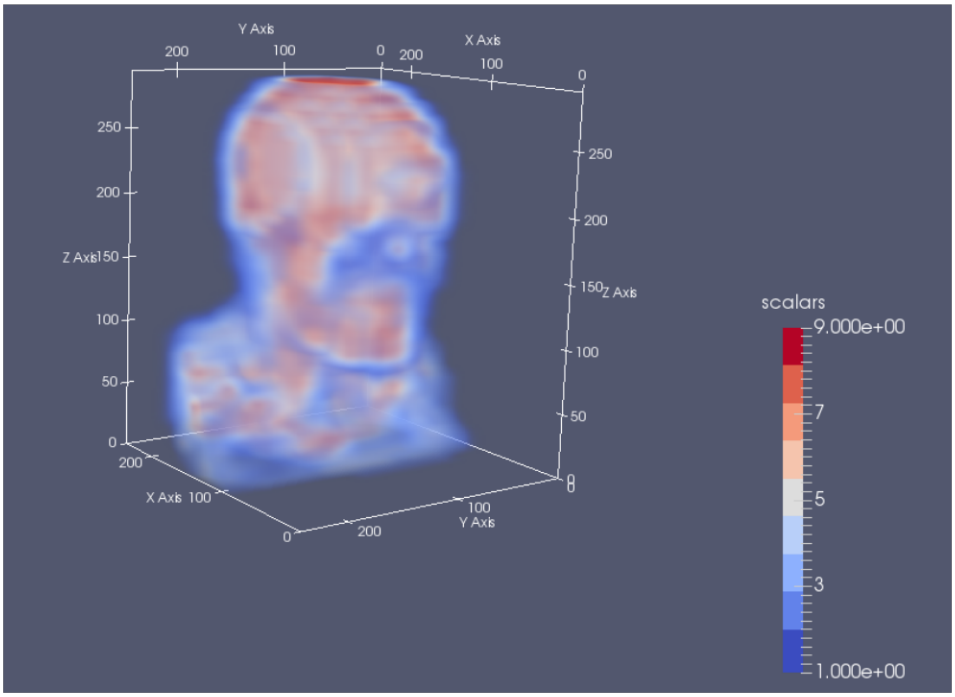

Figure 5.15: Patient discretization in 9 materials

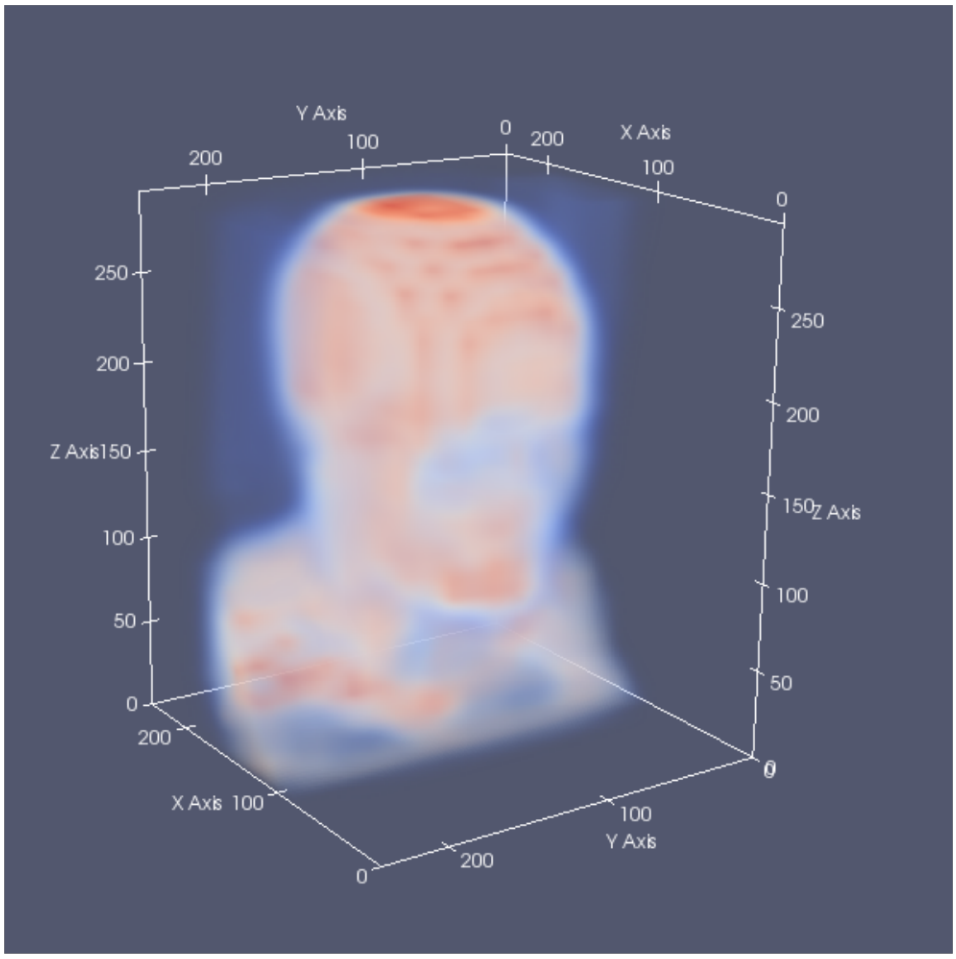

Figure 5.16: Patient dose distribution

6

Conclusions

One of the primary modalities used in the treatment of cancer is the radiation therapy or radiotherapy. Radiotherapy aims to control the tumoral malignancy while reducing the damage to healthy tissue. Radiation treatment planning represents a major part of the treatment of radiotherapy. The treatment planning systems (TPS) used in external beam radiation therapy generate beam shapes and dose distributions aiming to maximize the tumor control while minimizing the irradiation to the organs at risk.

Accurate and fast calculations of the prescribed dose in the TPS are directly associated with a high cost due to computational power. In Mexico, the average cost of a radiotherapy planning system varies from 50,000.00 to 230,000 (USD), without considering the maintenance cost. In addition, the devaluation of the peso against the dollar raises the cost of delivering a radiotherapy treatment, making it less and less accessible to Mexicans.

The development of a national TPS and linear accelerators intended for cancer treatment could help to reduce costs, patient waiting list, and to raise the number of patients treated in each center. The advantages are not only clinical, this process

of innovation leads to an environment of knowledge and national competition.

The present work aims to begin the development of a national treatment planning system. The first approach started with the simulation of the dose calculation by solving the Boltzmann equation transport for photons and electrons in a homogeneous media. The dose calculation was validated by a qualitative analysis of the percentage depth dose and profile beams that resulted from the simulation of a 6 MeV monoenergetic beam into a water phantom. The simulation was then implemented into a brain CT images for the simplest radiation therapy treatment, the whole brain radiotherapy.

The simulation of the particle transport and the solution of the Bolztmann equation, for dose calculation purposes, was performed in several Python and Julia codes. The characteristics of the simulation were followed according WBRT protocol. The initial parameters informations were a set of CT images of the patient. The mean time simulation was of 384 seconds for 8 processor core. Because it is possible to run the codes using parallelization, for an average high-performance computer the time is reduced to 48 seconds for 8 processor cores for each measurement.

The verifications measurements as Percentage Depth Dose and beam profiles were simulated for both codes. The geometry construction consisted of a water tank of $320 \times 320 \times 280\, mm^3$. For all the measurements the source-surface-distance was $100\, cm$.

The qualitative results of the PDD and beam profiles showed the characteristic shape of the measurements. The maximum dose for the PDD is reached at $1.57\, cm$ for a $S_1 6$ MOD.

The simulation on the brain CT images showed a homogeneous dose distribution within the brain as expected. The contour of the regions at interest is however not reached at this point. The point of maximum dose is reached within the brain and had a value of $3.1 Gy$. The DVH showed a 90% of the volume of the

brain reached 90% of the maximum dose.

The dose calculation algorithm proposed by solving the Boltzmann transport equation represents a first approach for the development of a national treatment planning system. However, a considerable amount of work is needed towards a fist realistic national treatment planning system.

Further work seems necessary for the validation of the simulated beam clinical and with the use of Monte Carlo simulation, the delimitation of the critical structures that could not comprise their functioning, the simulation of beam modifiers, and the implementation of a user-friendly interface.

Appendices

A

Photon Cross Sections

The electron and photon cross sections were obtained for the adipose tissue, air, breast, dense bone, liver, lung, muscle, trabecular bone, and water. The information materials were downloaded from the open source XCOM.

For the information material the following particle information is provided,

- Photon Energy (PE), in $[MeV]$
- Scattering Coherent (SC), in $\frac{cm^2}{g}$
- Scattering Incoherent (SI), in $\frac{cm^2}{g}$
- Photo-Electric Absortion (PEA), in $\frac{cm^2}{g}$
- Pair Production in Nuclear Field (PNF), in $\frac{cm^2}{g}$
- Pair Production in Electron Field (PEF), in $\frac{cm^2}{g}$
- Total Attenuation with Coherent Scattering (TAWCS), in $\frac{cm^2}{g}$
- Total Attenuation without Coherent Scattering (TAOCS), in $\frac{cm^2}{g}$

A.1 Adipose Tissue

PE	SC	SI	PEA	PNF	PEF	TAWCS	TAOCS
$1 \cdot 10^{-3}$	1.12	$1.58 \cdot 10^{-2}$	2,627	0	0	2,628	2,627
$1.04 \cdot 10^{-3}$	1.11	$1.68 \cdot 10^{-2}$	2,388	0	0	2,389	2,388
$1.07 \cdot 10^{-3}$	1.1	$1.78 \cdot 10^{-2}$	2,171	0	0	2,172	2,171
$1.07 \cdot 10^{-3}$	1.1	$1.78 \cdot 10^{-2}$	2,177	0	0	2,178	2,177
$1.5 \cdot 10^{-3}$	1.01	$3.14 \cdot 10^{-2}$	861.2	0	0	862.2	861.2
$2 \cdot 10^{-3}$	0.89	$4.82 \cdot 10^{-2}$	379	0	0	380	379.1
$2.47 \cdot 10^{-3}$	0.78	$6.35 \cdot 10^{-2}$	204.5	0	0	205.4	204.6
$2.47 \cdot 10^{-3}$	0.78	$6.35 \cdot 10^{-2}$	206.4	0	0	207.2	206.4
$2.64 \cdot 10^{-3}$	0.75	$6.87 \cdot 10^{-2}$	169.9	0	0	170.7	170
$2.82 \cdot 10^{-3}$	0.71	$7.4 \cdot 10^{-2}$	139.8	0	0	140.6	139.9
$2.82 \cdot 10^{-3}$	0.71	$7.4 \cdot 10^{-2}$	141.2	0	0	142	141.3
$3 \cdot 10^{-3}$	0.67	$7.9 \cdot 10^{-2}$	118	0	0	118.8	118.1
$4 \cdot 10^{-3}$	0.51	0.1	49.92	0	0	50.54	50.02
$5 \cdot 10^{-3}$	0.4	0.12	25.35	0	0	25.87	25.47
$6 \cdot 10^{-3}$	0.33	0.13	14.48	0	0	14.94	14.61
$8 \cdot 10^{-3}$	0.23	0.15	5.92	0	0	6.3	6.07
$1 \cdot 10^{-2}$	0.17	0.16	2.94	0	0	3.27	3.09
$1.5 \cdot 10^{-2}$	0.1	0.17	0.81	0	0	1.08	0.98
$2 \cdot 10^{-2}$	$6.83 \cdot 10^{-2}$	0.18	0.32	0	0	0.57	0.5
$3 \cdot 10^{-2}$	$3.57 \cdot 10^{-2}$	0.19	$8.49 \cdot 10^{-2}$	0	0	0.31	0.27
$4 \cdot 10^{-2}$	$2.18 \cdot 10^{-2}$	0.18	$3.3 \cdot 10^{-2}$	0	0	0.24	0.22
$5 \cdot 10^{-2}$	$1.46 \cdot 10^{-2}$	0.18	$1.58 \cdot 10^{-2}$	0	0	0.21	0.2
$6 \cdot 10^{-2}$	$1.05 \cdot 10^{-2}$	0.18	$8.64 \cdot 10^{-3}$	0	0	0.2	0.19
$8 \cdot 10^{-2}$	$6.13 \cdot 10^{-3}$	0.17	$3.33 \cdot 10^{-3}$	0	0	0.18	0.17
0.1	$4 \cdot 10^{-3}$	0.16	$1.59 \cdot 10^{-3}$	0	0	0.17	0.16
0.15	$1.82 \cdot 10^{-3}$	0.15	$4.21 \cdot 10^{-4}$	0	0	0.15	0.15
0.2	$1.03 \cdot 10^{-3}$	0.14	$1.66 \cdot 10^{-4}$	0	0	0.14	0.14
0.3	$4.62 \cdot 10^{-4}$	0.12	$4.69 \cdot 10^{-5}$	0	0	0.12	0.12
0.4	$2.6 \cdot 10^{-4}$	0.11	$2.01 \cdot 10^{-5}$	0	0	0.11	0.11
0.5	$1.67 \cdot 10^{-4}$	$9.68 \cdot 10^{-2}$	$1.08 \cdot 10^{-5}$	0	0	$9.7 \cdot 10^{-2}$	$9.68 \cdot 10^{-2}$
0.6	$1.16 \cdot 10^{-4}$	$8.95 \cdot 10^{-2}$	$6.74 \cdot 10^{-6}$	0	0	$8.97 \cdot 10^{-2}$	$8.95 \cdot 10^{-2}$
0.8	$6.52 \cdot 10^{-5}$	$7.87 \cdot 10^{-2}$	$3.4 \cdot 10^{-6}$	0	0	$7.87 \cdot 10^{-2}$	$7.87 \cdot 10^{-2}$
1	$4.18 \cdot 10^{-5}$	$7.07 \cdot 10^{-2}$	$2.12 \cdot 10^{-6}$	0	0	$7.08 \cdot 10^{-2}$	$7.07 \cdot 10^{-2}$
1.02	$4 \cdot 10^{-5}$	$7 \cdot 10^{-2}$	$1.97 \cdot 10^{-6}$	0	0	$7.01 \cdot 10^{-2}$	$7 \cdot 10^{-2}$
1.25	$2.67 \cdot 10^{-5}$	$6.33 \cdot 10^{-2}$	$1.33 \cdot 10^{-6}$	$1.48 \cdot 10^{-5}$	0	$6.33 \cdot 10^{-2}$	$6.33 \cdot 10^{-2}$
1.5	$1.86 \cdot 10^{-5}$	$5.75 \cdot 10^{-2}$	$9.68 \cdot 10^{-7}$	$8.19 \cdot 10^{-5}$	0	$5.76 \cdot 10^{-2}$	$5.76 \cdot 10^{-2}$
2	$1.04 \cdot 10^{-5}$	$4.91 \cdot 10^{-2}$	$6.09 \cdot 10^{-7}$	$3.26 \cdot 10^{-4}$	0	$4.94 \cdot 10^{-2}$	$4.94 \cdot 10^{-2}$
2.04	$1 \cdot 10^{-5}$	$4.85 \cdot 10^{-2}$	$5.89 \cdot 10^{-7}$	$3.52 \cdot 10^{-4}$	0	$4.88 \cdot 10^{-2}$	$4.88 \cdot 10^{-2}$
3	$4.64 \cdot 10^{-6}$	$3.86 \cdot 10^{-2}$	$3.41 \cdot 10^{-7}$	$9.33 \cdot 10^{-4}$	$1.35 \cdot 10^{-5}$	$3.96 \cdot 10^{-2}$	$3.96 \cdot 10^{-2}$
4	$2.61 \cdot 10^{-6}$	$3.22 \cdot 10^{-2}$	$2.34 \cdot 10^{-7}$	$1.52 \cdot 10^{-3}$	$5.51 \cdot 10^{-5}$	$3.38 \cdot 10^{-2}$	$3.38 \cdot 10^{-2}$
5	$1.67 \cdot 10^{-6}$	$2.78 \cdot 10^{-2}$	$1.77 \cdot 10^{-7}$	$2.03 \cdot 10^{-3}$	$1.1 \cdot 10^{-4}$	$3 \cdot 10^{-2}$	$3 \cdot 10^{-2}$
6	$1.16 \cdot 10^{-6}$	$2.46 \cdot 10^{-2}$	$1.43 \cdot 10^{-7}$	$2.5 \cdot 10^{-3}$	$1.69 \cdot 10^{-4}$	$2.73 \cdot 10^{-2}$	$2.72 \cdot 10^{-2}$
7	$8.52 \cdot 10^{-7}$	$2.21 \cdot 10^{-2}$	$1.19 \cdot 10^{-7}$	$2.91 \cdot 10^{-3}$	$2.28 \cdot 10^{-4}$	$2.52 \cdot 10^{-2}$	$2.52 \cdot 10^{-2}$
8	$6.53 \cdot 10^{-7}$	$2.01 \cdot 10^{-2}$	$1.02 \cdot 10^{-7}$	$3.29 \cdot 10^{-3}$	$2.85 \cdot 10^{-4}$	$2.37 \cdot 10^{-2}$	$2.37 \cdot 10^{-2}$
9	$5.16 \cdot 10^{-7}$	$1.85 \cdot 10^{-2}$	$8.95 \cdot 10^{-8}$	$3.63 \cdot 10^{-3}$	$3.39 \cdot 10^{-4}$	$2.25 \cdot 10^{-2}$	$2.25 \cdot 10^{-2}$
10	$4.18 \cdot 10^{-7}$	$1.71 \cdot 10^{-2}$	$7.96 \cdot 10^{-8}$	$3.94 \cdot 10^{-3}$	$3.92 \cdot 10^{-4}$	$2.15 \cdot 10^{-2}$	$2.15 \cdot 10^{-2}$
11	$3.45 \cdot 10^{-7}$	$1.6 \cdot 10^{-2}$	$7.17 \cdot 10^{-8}$	$4.22 \cdot 10^{-3}$	$4.41 \cdot 10^{-4}$	$2.06 \cdot 10^{-2}$	$2.06 \cdot 10^{-2}$
12	$2.9 \cdot 10^{-7}$	$1.5 \cdot 10^{-2}$	$6.51 \cdot 10^{-8}$	$4.47 \cdot 10^{-3}$	$4.88 \cdot 10^{-4}$	$1.99 \cdot 10^{-2}$	$1.99 \cdot 10^{-2}$
13	$2.47 \cdot 10^{-7}$	$1.41 \cdot 10^{-2}$	$5.97 \cdot 10^{-8}$	$4.71 \cdot 10^{-3}$	$5.32 \cdot 10^{-4}$	$1.94 \cdot 10^{-2}$	$1.94 \cdot 10^{-2}$
14	$2.13 \cdot 10^{-7}$	$1.34 \cdot 10^{-2}$	$5.51 \cdot 10^{-8}$	$4.94 \cdot 10^{-3}$	$5.75 \cdot 10^{-4}$	$1.89 \cdot 10^{-2}$	$1.89 \cdot 10^{-2}$
15	$1.86 \cdot 10^{-7}$	$1.27 \cdot 10^{-2}$	$5.12 \cdot 10^{-8}$	$5.14 \cdot 10^{-3}$	$6.15 \cdot 10^{-4}$	$1.84 \cdot 10^{-2}$	$1.84 \cdot 10^{-2}$
16	$1.63 \cdot 10^{-7}$	$1.21 \cdot 10^{-2}$	$4.77 \cdot 10^{-8}$	$5.34 \cdot 10^{-3}$	$6.53 \cdot 10^{-4}$	$1.81 \cdot 10^{-2}$	$1.81 \cdot 10^{-2}$
18	$1.29 \cdot 10^{-7}$	$1.1 \cdot 10^{-2}$	$4.21 \cdot 10^{-8}$	$5.7 \cdot 10^{-3}$	$7.24 \cdot 10^{-4}$	$1.75 \cdot 10^{-2}$	$1.75 \cdot 10^{-2}$
20	$1.04 \cdot 10^{-7}$	$1.02 \cdot 10^{-2}$	$3.77 \cdot 10^{-8}$	$6.02 \cdot 10^{-3}$	$7.89 \cdot 10^{-4}$	$1.7 \cdot 10^{-2}$	$1.7 \cdot 10^{-2}$
22	$8.63 \cdot 10^{-8}$	$9.45 \cdot 10^{-3}$	$3.41 \cdot 10^{-8}$	$6.32 \cdot 10^{-3}$	$8.49 \cdot 10^{-4}$	$1.66 \cdot 10^{-2}$	$1.66 \cdot 10^{-2}$
24	$7.25 \cdot 10^{-8}$	$8.83 \cdot 10^{-3}$	$3.11 \cdot 10^{-8}$	$6.59 \cdot 10^{-3}$	$9.05 \cdot 10^{-4}$	$1.63 \cdot 10^{-2}$	$1.63 \cdot 10^{-2}$
26	$6.18 \cdot 10^{-8}$	$8.29 \cdot 10^{-3}$	$2.86 \cdot 10^{-8}$	$6.83 \cdot 10^{-3}$	$9.57 \cdot 10^{-4}$	$1.61 \cdot 10^{-2}$	$1.61 \cdot 10^{-2}$
28	$5.33 \cdot 10^{-8}$	$7.82 \cdot 10^{-3}$	$2.65 \cdot 10^{-8}$	$7.06 \cdot 10^{-3}$	$1.01 \cdot 10^{-3}$	$1.59 \cdot 10^{-2}$	$1.59 \cdot 10^{-2}$
30	$4.64 \cdot 10^{-8}$	$7.4 \cdot 10^{-3}$	$2.46 \cdot 10^{-8}$	$7.27 \cdot 10^{-3}$	$1.05 \cdot 10^{-3}$	$1.57 \cdot 10^{-2}$	$1.57 \cdot 10^{-2}$
40	$2.61 \cdot 10^{-8}$	$5.88 \cdot 10^{-3}$	$1.83 \cdot 10^{-8}$	$8.12 \cdot 10^{-3}$	$1.24 \cdot 10^{-3}$	$1.53 \cdot 10^{-2}$	$1.53 \cdot 10^{-2}$
50	$1.67 \cdot 10^{-8}$	$4.91 \cdot 10^{-3}$	$1.46 \cdot 10^{-8}$	$8.77 \cdot 10^{-3}$	$1.39 \cdot 10^{-3}$	$1.51 \cdot 10^{-2}$	$1.51 \cdot 10^{-2}$
60	$1.16 \cdot 10^{-8}$	$4.23 \cdot 10^{-3}$	$1.21 \cdot 10^{-8}$	$9.29 \cdot 10^{-3}$	$1.51 \cdot 10^{-3}$	$1.5 \cdot 10^{-2}$	$1.5 \cdot 10^{-2}$
80	$6.53 \cdot 10^{-9}$	$3.34 \cdot 10^{-3}$	$9.03 \cdot 10^{-9}$	$1.01 \cdot 10^{-2}$	$1.7 \cdot 10^{-3}$	$1.51 \cdot 10^{-2}$	$1.51 \cdot 10^{-2}$
100	$4.18 \cdot 10^{-9}$	$2.77 \cdot 10^{-3}$	$7.2 \cdot 10^{-9}$	$1.06 \cdot 10^{-2}$	$1.84 \cdot 10^{-3}$	$1.53 \cdot 10^{-2}$	$1.53 \cdot 10^{-2}$
150	$1.86 \cdot 10^{-9}$	$1.97 \cdot 10^{-3}$	$4.78 \cdot 10^{-9}$	$1.16 \cdot 10^{-2}$	$2.09 \cdot 10^{-3}$	$1.57 \cdot 10^{-2}$	$1.57 \cdot 10^{-2}$

200	$1.04 \cdot 10^{-9}$	$1.55 \cdot 10^{-3}$	$3.58 \cdot 10^{-9}$	$1.22 \cdot 10^{-2}$	$2.26 \cdot 10^{-3}$	$1.6 \cdot 10^{-2}$	$1.6 \cdot 10^{-2}$
300	$4.64 \cdot 10^{-10}$	$1.1 \cdot 10^{-3}$	$2.38 \cdot 10^{-9}$	$1.29 \cdot 10^{-2}$	$2.47 \cdot 10^{-3}$	$1.65 \cdot 10^{-2}$	$1.65 \cdot 10^{-2}$
400	$2.61 \cdot 10^{-10}$	$8.59 \cdot 10^{-4}$	$1.78 \cdot 10^{-9}$	$1.34 \cdot 10^{-2}$	$2.61 \cdot 10^{-3}$	$1.68 \cdot 10^{-2}$	$1.68 \cdot 10^{-2}$
500	$1.67 \cdot 10^{-10}$	$7.11 \cdot 10^{-4}$	$1.43 \cdot 10^{-9}$	$1.37 \cdot 10^{-2}$	$2.7 \cdot 10^{-3}$	$1.71 \cdot 10^{-2}$	$1.71 \cdot 10^{-2}$
600	$1.16 \cdot 10^{-10}$	$6.09 \cdot 10^{-4}$	$1.19 \cdot 10^{-9}$	$1.39 \cdot 10^{-2}$	$2.77 \cdot 10^{-3}$	$1.72 \cdot 10^{-2}$	$1.72 \cdot 10^{-2}$
800	$6.53 \cdot 10^{-11}$	$4.75 \cdot 10^{-4}$	$8.91 \cdot 10^{-10}$	$1.41 \cdot 10^{-2}$	$2.87 \cdot 10^{-3}$	$1.75 \cdot 10^{-2}$	$1.75 \cdot 10^{-2}$
1,000	$4.18 \cdot 10^{-11}$	$3.91 \cdot 10^{-4}$	$7.12 \cdot 10^{-10}$	$1.43 \cdot 10^{-2}$	$2.94 \cdot 10^{-3}$	$1.77 \cdot 10^{-2}$	$1.77 \cdot 10^{-2}$
1,500	$1.86 \cdot 10^{-11}$	$2.73 \cdot 10^{-4}$	$4.75 \cdot 10^{-10}$	$1.46 \cdot 10^{-2}$	$3.04 \cdot 10^{-3}$	$1.79 \cdot 10^{-2}$	$1.79 \cdot 10^{-2}$
2,000	$1.04 \cdot 10^{-11}$	$2.11 \cdot 10^{-4}$	$3.56 \cdot 10^{-10}$	$1.48 \cdot 10^{-2}$	$3.1 \cdot 10^{-3}$	$1.81 \cdot 10^{-2}$	$1.81 \cdot 10^{-2}$
3,000	$4.64 \cdot 10^{-12}$	$1.47 \cdot 10^{-4}$	$2.37 \cdot 10^{-10}$	$1.49 \cdot 10^{-2}$	$3.17 \cdot 10^{-3}$	$1.82 \cdot 10^{-2}$	$1.82 \cdot 10^{-2}$
4,000	$2.61 \cdot 10^{-12}$	$1.13 \cdot 10^{-4}$	$1.78 \cdot 10^{-10}$	$1.5 \cdot 10^{-2}$	$3.2 \cdot 10^{-3}$	$1.83 \cdot 10^{-2}$	$1.83 \cdot 10^{-2}$
5,000	$1.67 \cdot 10^{-12}$	$9.28 \cdot 10^{-5}$	$1.42 \cdot 10^{-10}$	$1.51 \cdot 10^{-2}$	$3.23 \cdot 10^{-3}$	$1.84 \cdot 10^{-2}$	$1.84 \cdot 10^{-2}$
6,000	$1.16 \cdot 10^{-12}$	$7.87 \cdot 10^{-5}$	$1.19 \cdot 10^{-10}$	$1.51 \cdot 10^{-2}$	$3.24 \cdot 10^{-3}$	$1.84 \cdot 10^{-2}$	$1.84 \cdot 10^{-2}$
8,000	$6.53 \cdot 10^{-13}$	$6.06 \cdot 10^{-5}$	$8.9 \cdot 10^{-11}$	$1.51 \cdot 10^{-2}$	$3.27 \cdot 10^{-3}$	$1.85 \cdot 10^{-2}$	$1.85 \cdot 10^{-2}$
10,000	$4.18 \cdot 10^{-13}$	$4.95 \cdot 10^{-5}$	$7.12 \cdot 10^{-11}$	$1.52 \cdot 10^{-2}$	$3.28 \cdot 10^{-3}$	$1.85 \cdot 10^{-2}$	$1.85 \cdot 10^{-2}$
15,000	$1.86 \cdot 10^{-13}$	$3.42 \cdot 10^{-5}$	$4.74 \cdot 10^{-11}$	$1.52 \cdot 10^{-2}$	$3.3 \cdot 10^{-3}$	$1.86 \cdot 10^{-2}$	$1.86 \cdot 10^{-2}$
20,000	$1.04 \cdot 10^{-13}$	$2.63 \cdot 10^{-5}$	$3.56 \cdot 10^{-11}$	$1.52 \cdot 10^{-2}$	$3.31 \cdot 10^{-3}$	$1.86 \cdot 10^{-2}$	$1.86 \cdot 10^{-2}$
30,000	$4.64 \cdot 10^{-14}$	$1.81 \cdot 10^{-5}$	$2.37 \cdot 10^{-11}$	$1.53 \cdot 10^{-2}$	$3.32 \cdot 10^{-3}$	$1.86 \cdot 10^{-2}$	$1.86 \cdot 10^{-2}$
40,000	$2.61 \cdot 10^{-14}$	$1.39 \cdot 10^{-5}$	$1.78 \cdot 10^{-11}$	$1.53 \cdot 10^{-2}$	$3.33 \cdot 10^{-3}$	$1.86 \cdot 10^{-2}$	$1.86 \cdot 10^{-2}$
50,000	$1.67 \cdot 10^{-14}$	$1.13 \cdot 10^{-5}$	$1.42 \cdot 10^{-11}$	$1.53 \cdot 10^{-2}$	$3.33 \cdot 10^{-3}$	$1.86 \cdot 10^{-2}$	$1.86 \cdot 10^{-2}$
60,000	$1.16 \cdot 10^{-14}$	$9.58 \cdot 10^{-6}$	$1.19 \cdot 10^{-11}$	$1.53 \cdot 10^{-2}$	$3.33 \cdot 10^{-3}$	$1.86 \cdot 10^{-2}$	$1.86 \cdot 10^{-2}$
80,000	$6.53 \cdot 10^{-15}$	$7.35 \cdot 10^{-6}$	$8.9 \cdot 10^{-12}$	$1.53 \cdot 10^{-2}$	$3.34 \cdot 10^{-3}$	$1.86 \cdot 10^{-2}$	$1.86 \cdot 10^{-2}$
$1 \cdot 10^5$	$4.18 \cdot 10^{-15}$	$5.97 \cdot 10^{-6}$	$7.12 \cdot 10^{-12}$	$1.53 \cdot 10^{-2}$	$3.34 \cdot 10^{-3}$	$1.87 \cdot 10^{-2}$	$1.87 \cdot 10^{-2}$

A.2 Air

PE	SC	SI	PEA	PNF	PEF	TAWCS	TAOCS
$1 \cdot 10^{-3}$	1.35	$1.05 \cdot 10^{-2}$	3,577	0	0	3,578	3,577
$1.5 \cdot 10^{-3}$	1.24	$2.13 \cdot 10^{-2}$	1,179	0	0	1,180	1,179
$2 \cdot 10^{-3}$	1.11	$3.36 \cdot 10^{-2}$	521.9	0	0	523.1	522
$3 \cdot 10^{-3}$	0.85	$5.78 \cdot 10^{-2}$	159.9	0	0	160.8	160
$3.2 \cdot 10^{-3}$	0.81	$6.23 \cdot 10^{-2}$	131.7	0	0	132.6	131.8
$3.2 \cdot 10^{-3}$	0.81	$6.23 \cdot 10^{-2}$	142.3	0	0	143.1	142.3
$4 \cdot 10^{-3}$	0.66	$7.8 \cdot 10^{-2}$	74.02	0	0	74.76	74.1
$5 \cdot 10^{-3}$	0.52	$9.36 \cdot 10^{-2}$	37.94	0	0	38.55	38.03
$6 \cdot 10^{-3}$	0.42	0.11	21.83	0	0	22.35	21.94
$8 \cdot 10^{-3}$	0.29	0.12	9.03	0	0	9.44	9.15
$1 \cdot 10^{-2}$	0.22	0.13	4.52	0	0	4.87	4.65
$1.5 \cdot 10^{-2}$	0.13	0.15	1.26	0	0	1.54	1.41
$2 \cdot 10^{-2}$	$8.63 \cdot 10^{-2}$	0.16	0.5	0	0	0.74	0.66
$3 \cdot 10^{-2}$	$4.56 \cdot 10^{-2}$	0.16	0.14	0	0	0.34	0.3
$4 \cdot 10^{-2}$	$2.79 \cdot 10^{-2}$	0.16	$5.32 \cdot 10^{-2}$	0	0	0.24	0.22
$5 \cdot 10^{-2}$	$1.88 \cdot 10^{-2}$	0.16	$2.56 \cdot 10^{-2}$	0	0	0.21	0.19
$6 \cdot 10^{-2}$	$1.35 \cdot 10^{-2}$	0.16	$1.41 \cdot 10^{-2}$	0	0	0.19	0.17
$8 \cdot 10^{-2}$	$7.91 \cdot 10^{-3}$	0.15	$5.48 \cdot 10^{-3}$	0	0	0.17	0.16
0.1	$5.17 \cdot 10^{-3}$	0.15	$2.63 \cdot 10^{-3}$	0	0	0.15	0.15
0.15	$2.36 \cdot 10^{-3}$	0.13	$7.01 \cdot 10^{-4}$	0	0	0.14	0.13
0.2	$1.34 \cdot 10^{-3}$	0.12	$2.79 \cdot 10^{-4}$	0	0	0.12	0.12
0.3	$6 \cdot 10^{-4}$	0.11	$7.9 \cdot 10^{-5}$	0	0	0.11	0.11
0.4	$3.38 \cdot 10^{-4}$	$9.51 \cdot 10^{-2}$	$3.39 \cdot 10^{-5}$	0	0	$9.55 \cdot 10^{-2}$	$9.52 \cdot 10^{-2}$
0.5	$2.17 \cdot 10^{-4}$	$8.69 \cdot 10^{-2}$	$1.83 \cdot 10^{-5}$	0	0	$8.71 \cdot 10^{-2}$	$8.69 \cdot 10^{-2}$
0.6	$1.51 \cdot 10^{-4}$	$8.04 \cdot 10^{-2}$	$1.14 \cdot 10^{-5}$	0	0	$8.06 \cdot 10^{-2}$	$8.04 \cdot 10^{-2}$
0.8	$8.47 \cdot 10^{-5}$	$7.07 \cdot 10^{-2}$	$5.77 \cdot 10^{-6}$	0	0	$7.08 \cdot 10^{-2}$	$7.07 \cdot 10^{-2}$
1	$5.43 \cdot 10^{-5}$	$6.35 \cdot 10^{-2}$	$3.59 \cdot 10^{-6}$	0	0	$6.36 \cdot 10^{-2}$	$6.36 \cdot 10^{-2}$
1.02	$5.2 \cdot 10^{-5}$	$6.29 \cdot 10^{-2}$	$3.35 \cdot 10^{-6}$	0	0	$6.3 \cdot 10^{-2}$	$6.29 \cdot 10^{-2}$
1.25	$3.47 \cdot 10^{-5}$	$5.68 \cdot 10^{-2}$	$2.27 \cdot 10^{-6}$	$1.77 \cdot 10^{-5}$	0	$5.69 \cdot 10^{-2}$	$5.69 \cdot 10^{-2}$
1.5	$2.41 \cdot 10^{-5}$	$5.16 \cdot 10^{-2}$	$1.65 \cdot 10^{-6}$	$9.77 \cdot 10^{-5}$	0	$5.18 \cdot 10^{-2}$	$5.17 \cdot 10^{-2}$
2	$1.36 \cdot 10^{-5}$	$4.41 \cdot 10^{-2}$	$1.03 \cdot 10^{-6}$	$3.89 \cdot 10^{-4}$	0	$4.45 \cdot 10^{-2}$	$4.45 \cdot 10^{-2}$
2.04	$1.3 \cdot 10^{-5}$	$4.35 \cdot 10^{-2}$	$1 \cdot 10^{-6}$	$4.19 \cdot 10^{-4}$	0	$4.4 \cdot 10^{-2}$	$4.39 \cdot 10^{-2}$
3	$6.03 \cdot 10^{-6}$	$3.47 \cdot 10^{-2}$	$5.76 \cdot 10^{-7}$	$1.11 \cdot 10^{-3}$	$1.21 \cdot 10^{-5}$	$3.58 \cdot 10^{-2}$	$3.58 \cdot 10^{-2}$
4	$3.39 \cdot 10^{-6}$	$2.89 \cdot 10^{-2}$	$3.94 \cdot 10^{-7}$	$1.8 \cdot 10^{-3}$	$4.95 \cdot 10^{-5}$	$3.08 \cdot 10^{-2}$	$3.08 \cdot 10^{-2}$
5	$2.17 \cdot 10^{-6}$	$2.5 \cdot 10^{-2}$	$2.99 \cdot 10^{-7}$	$2.42 \cdot 10^{-3}$	$9.87 \cdot 10^{-5}$	$2.75 \cdot 10^{-2}$	$2.75 \cdot 10^{-2}$
6	$1.51 \cdot 10^{-6}$	$2.21 \cdot 10^{-2}$	$2.4 \cdot 10^{-7}$	$2.97 \cdot 10^{-3}$	$1.52 \cdot 10^{-4}$	$2.52 \cdot 10^{-2}$	$2.52 \cdot 10^{-2}$
7	$1.11 \cdot 10^{-6}$	$1.99 \cdot 10^{-2}$	$2 \cdot 10^{-7}$	$3.47 \cdot 10^{-3}$	$2.04 \cdot 10^{-4}$	$2.35 \cdot 10^{-2}$	$2.35 \cdot 10^{-2}$
8	$8.48 \cdot 10^{-7}$	$1.81 \cdot 10^{-2}$	$1.72 \cdot 10^{-7}$	$3.91 \cdot 10^{-3}$	$2.56 \cdot 10^{-4}$	$2.22 \cdot 10^{-2}$	$2.22 \cdot 10^{-2}$
9	$6.7 \cdot 10^{-7}$	$1.66 \cdot 10^{-2}$	$1.5 \cdot 10^{-7}$	$4.32 \cdot 10^{-3}$	$3.05 \cdot 10^{-4}$	$2.12 \cdot 10^{-2}$	$2.12 \cdot 10^{-2}$
10	$5.43 \cdot 10^{-7}$	$1.54 \cdot 10^{-2}$	$1.34 \cdot 10^{-7}$	$4.68 \cdot 10^{-3}$	$3.52 \cdot 10^{-4}$	$2.04 \cdot 10^{-2}$	$2.04 \cdot 10^{-2}$
11	$4.49 \cdot 10^{-7}$	$1.44 \cdot 10^{-2}$	$1.2 \cdot 10^{-7}$	$5.02 \cdot 10^{-3}$	$3.96 \cdot 10^{-4}$	$1.98 \cdot 10^{-2}$	$1.98 \cdot 10^{-2}$
12	$3.77 \cdot 10^{-7}$	$1.35 \cdot 10^{-2}$	$1.09 \cdot 10^{-7}$	$5.32 \cdot 10^{-3}$	$4.38 \cdot 10^{-4}$	$1.92 \cdot 10^{-2}$	$1.92 \cdot 10^{-2}$
13	$3.21 \cdot 10^{-7}$	$1.27 \cdot 10^{-2}$	$1 \cdot 10^{-7}$	$5.61 \cdot 10^{-3}$	$4.78 \cdot 10^{-4}$	$1.88 \cdot 10^{-2}$	$1.88 \cdot 10^{-2}$
14	$2.77 \cdot 10^{-7}$	$1.2 \cdot 10^{-2}$	$9.24 \cdot 10^{-8}$	$5.87 \cdot 10^{-3}$	$5.16 \cdot 10^{-4}$	$1.84 \cdot 10^{-2}$	$1.84 \cdot 10^{-2}$
15	$2.41 \cdot 10^{-7}$	$1.14 \cdot 10^{-2}$	$8.58 \cdot 10^{-8}$	$6.12 \cdot 10^{-3}$	$5.52 \cdot 10^{-4}$	$1.81 \cdot 10^{-2}$	$1.81 \cdot 10^{-2}$
16	$2.12 \cdot 10^{-7}$	$1.08 \cdot 10^{-2}$	$8 \cdot 10^{-8}$	$6.35 \cdot 10^{-3}$	$5.86 \cdot 10^{-4}$	$1.78 \cdot 10^{-2}$	$1.78 \cdot 10^{-2}$
18	$1.68 \cdot 10^{-7}$	$9.91 \cdot 10^{-3}$	$7.06 \cdot 10^{-8}$	$6.78 \cdot 10^{-3}$	$6.5 \cdot 10^{-4}$	$1.73 \cdot 10^{-2}$	$1.73 \cdot 10^{-2}$
20	$1.36 \cdot 10^{-7}$	$9.14 \cdot 10^{-3}$	$6.31 \cdot 10^{-8}$	$7.16 \cdot 10^{-3}$	$7.09 \cdot 10^{-4}$	$1.7 \cdot 10^{-2}$	$1.7 \cdot 10^{-2}$
22	$1.12 \cdot 10^{-7}$	$8.49 \cdot 10^{-3}$	$5.71 \cdot 10^{-8}$	$7.51 \cdot 10^{-3}$	$7.63 \cdot 10^{-4}$	$1.68 \cdot 10^{-2}$	$1.68 \cdot 10^{-2}$
24	$9.43 \cdot 10^{-8}$	$7.93 \cdot 10^{-3}$	$5.21 \cdot 10^{-8}$	$7.82 \cdot 10^{-3}$	$8.13 \cdot 10^{-4}$	$1.66 \cdot 10^{-2}$	$1.66 \cdot 10^{-2}$
26	$8.03 \cdot 10^{-8}$	$7.45 \cdot 10^{-3}$	$4.79 \cdot 10^{-8}$	$8.11 \cdot 10^{-3}$	$8.59 \cdot 10^{-4}$	$1.64 \cdot 10^{-2}$	$1.64 \cdot 10^{-2}$
28	$6.92 \cdot 10^{-8}$	$7.03 \cdot 10^{-3}$	$4.43 \cdot 10^{-8}$	$8.38 \cdot 10^{-3}$	$9.02 \cdot 10^{-4}$	$1.63 \cdot 10^{-2}$	$1.63 \cdot 10^{-2}$
30	$6.03 \cdot 10^{-8}$	$6.65 \cdot 10^{-3}$	$4.13 \cdot 10^{-8}$	$8.62 \cdot 10^{-3}$	$9.43 \cdot 10^{-4}$	$1.62 \cdot 10^{-2}$	$1.62 \cdot 10^{-2}$
40	$3.39 \cdot 10^{-8}$	$5.29 \cdot 10^{-3}$	$3.06 \cdot 10^{-8}$	$9.64 \cdot 10^{-3}$	$1.11 \cdot 10^{-3}$	$1.6 \cdot 10^{-2}$	$1.6 \cdot 10^{-2}$
50	$2.17 \cdot 10^{-8}$	$4.41 \cdot 10^{-3}$	$2.44 \cdot 10^{-8}$	$1.04 \cdot 10^{-2}$	$1.25 \cdot 10^{-3}$	$1.61 \cdot 10^{-2}$	$1.61 \cdot 10^{-2}$
60	$1.51 \cdot 10^{-8}$	$3.8 \cdot 10^{-3}$	$2.02 \cdot 10^{-8}$	$1.1 \cdot 10^{-2}$	$1.35 \cdot 10^{-3}$	$1.62 \cdot 10^{-2}$	$1.62 \cdot 10^{-2}$
80	$8.48 \cdot 10^{-9}$	$3 \cdot 10^{-3}$	$1.51 \cdot 10^{-8}$	$1.19 \cdot 10^{-2}$	$1.52 \cdot 10^{-3}$	$1.65 \cdot 10^{-2}$	$1.65 \cdot 10^{-2}$
100	$5.43 \cdot 10^{-9}$	$2.49 \cdot 10^{-3}$	$1.2 \cdot 10^{-8}$	$1.26 \cdot 10^{-2}$	$1.65 \cdot 10^{-3}$	$1.68 \cdot 10^{-2}$	$1.68 \cdot 10^{-2}$
150	$2.41 \cdot 10^{-9}$	$1.77 \cdot 10^{-3}$	$8 \cdot 10^{-9}$	$1.37 \cdot 10^{-2}$	$1.86 \cdot 10^{-3}$	$1.74 \cdot 10^{-2}$	$1.74 \cdot 10^{-2}$
200	$1.36 \cdot 10^{-9}$	$1.39 \cdot 10^{-3}$	$5.99 \cdot 10^{-9}$	$1.44 \cdot 10^{-2}$	$2.01 \cdot 10^{-3}$	$1.78 \cdot 10^{-2}$	$1.78 \cdot 10^{-2}$
300	$6.03 \cdot 10^{-10}$	$9.85 \cdot 10^{-4}$	$3.98 \cdot 10^{-9}$	$1.53 \cdot 10^{-2}$	$2.19 \cdot 10^{-3}$	$1.85 \cdot 10^{-2}$	$1.85 \cdot 10^{-2}$
400	$3.39 \cdot 10^{-10}$	$7.72 \cdot 10^{-4}$	$2.98 \cdot 10^{-9}$	$1.58 \cdot 10^{-2}$	$2.3 \cdot 10^{-3}$	$1.88 \cdot 10^{-2}$	$1.88 \cdot 10^{-2}$
500	$2.17 \cdot 10^{-10}$	$6.38 \cdot 10^{-4}$	$2.39 \cdot 10^{-9}$	$1.61 \cdot 10^{-2}$	$2.38 \cdot 10^{-3}$	$1.91 \cdot 10^{-2}$	$1.91 \cdot 10^{-2}$
600	$1.51 \cdot 10^{-10}$	$5.47 \cdot 10^{-4}$	$1.99 \cdot 10^{-9}$	$1.63 \cdot 10^{-2}$	$2.44 \cdot 10^{-3}$	$1.93 \cdot 10^{-2}$	$1.93 \cdot 10^{-2}$
800	$8.48 \cdot 10^{-11}$	$4.27 \cdot 10^{-4}$	$1.49 \cdot 10^{-9}$	$1.67 \cdot 10^{-2}$	$2.52 \cdot 10^{-3}$	$1.96 \cdot 10^{-2}$	$1.96 \cdot 10^{-2}$

1,000	$5.43 \cdot 10^{-11}$	$3.51 \cdot 10^{-4}$	$1.19 \cdot 10^{-9}$	$1.69 \cdot 10^{-2}$	$2.58 \cdot 10^{-3}$	$1.98 \cdot 10^{-2}$	$1.98 \cdot 10^{-2}$
1,500	$2.41 \cdot 10^{-11}$	$2.45 \cdot 10^{-4}$	$7.94 \cdot 10^{-10}$	$1.72 \cdot 10^{-2}$	$2.66 \cdot 10^{-3}$	$2.01 \cdot 10^{-2}$	$2.01 \cdot 10^{-2}$
2,000	$1.36 \cdot 10^{-11}$	$1.9 \cdot 10^{-4}$	$5.95 \cdot 10^{-10}$	$1.73 \cdot 10^{-2}$	$2.71 \cdot 10^{-3}$	$2.02 \cdot 10^{-2}$	$2.02 \cdot 10^{-2}$
3,000	$6.03 \cdot 10^{-12}$	$1.32 \cdot 10^{-4}$	$3.97 \cdot 10^{-10}$	$1.75 \cdot 10^{-2}$	$2.76 \cdot 10^{-3}$	$2.04 \cdot 10^{-2}$	$2.04 \cdot 10^{-2}$
4,000	$3.39 \cdot 10^{-12}$	$1.02 \cdot 10^{-4}$	$2.98 \cdot 10^{-10}$	$1.76 \cdot 10^{-2}$	$2.79 \cdot 10^{-3}$	$2.05 \cdot 10^{-2}$	$2.05 \cdot 10^{-2}$
5,000	$2.17 \cdot 10^{-12}$	$8.33 \cdot 10^{-5}$	$2.38 \cdot 10^{-10}$	$1.77 \cdot 10^{-2}$	$2.81 \cdot 10^{-3}$	$2.06 \cdot 10^{-2}$	$2.06 \cdot 10^{-2}$
6,000	$1.51 \cdot 10^{-12}$	$7.07 \cdot 10^{-5}$	$1.98 \cdot 10^{-10}$	$1.77 \cdot 10^{-2}$	$2.82 \cdot 10^{-3}$	$2.06 \cdot 10^{-2}$	$2.06 \cdot 10^{-2}$
8,000	$8.48 \cdot 10^{-13}$	$5.44 \cdot 10^{-5}$	$1.49 \cdot 10^{-10}$	$1.78 \cdot 10^{-2}$	$2.84 \cdot 10^{-3}$	$2.07 \cdot 10^{-2}$	$2.07 \cdot 10^{-2}$
10,000	$5.43 \cdot 10^{-13}$	$4.45 \cdot 10^{-5}$	$1.19 \cdot 10^{-10}$	$1.78 \cdot 10^{-2}$	$2.85 \cdot 10^{-3}$	$2.07 \cdot 10^{-2}$	$2.07 \cdot 10^{-2}$
15,000	$2.41 \cdot 10^{-13}$	$3.07 \cdot 10^{-5}$	$7.93 \cdot 10^{-11}$	$1.79 \cdot 10^{-2}$	$2.86 \cdot 10^{-3}$	$2.08 \cdot 10^{-2}$	$2.08 \cdot 10^{-2}$
20,000	$1.36 \cdot 10^{-13}$	$2.36 \cdot 10^{-5}$	$5.95 \cdot 10^{-11}$	$1.79 \cdot 10^{-2}$	$2.87 \cdot 10^{-3}$	$2.08 \cdot 10^{-2}$	$2.08 \cdot 10^{-2}$
30,000	$6.03 \cdot 10^{-14}$	$1.63 \cdot 10^{-5}$	$3.97 \cdot 10^{-11}$	$1.79 \cdot 10^{-2}$	$2.88 \cdot 10^{-3}$	$2.08 \cdot 10^{-2}$	$2.08 \cdot 10^{-2}$
40,000	$3.39 \cdot 10^{-14}$	$1.25 \cdot 10^{-5}$	$2.97 \cdot 10^{-11}$	$1.8 \cdot 10^{-2}$	$2.89 \cdot 10^{-3}$	$2.08 \cdot 10^{-2}$	$2.08 \cdot 10^{-2}$
50,000	$2.17 \cdot 10^{-14}$	$1.02 \cdot 10^{-5}$	$2.38 \cdot 10^{-11}$	$1.8 \cdot 10^{-2}$	$2.89 \cdot 10^{-3}$	$2.09 \cdot 10^{-2}$	$2.09 \cdot 10^{-2}$
60,000	$1.51 \cdot 10^{-14}$	$8.61 \cdot 10^{-6}$	$1.98 \cdot 10^{-11}$	$1.8 \cdot 10^{-2}$	$2.89 \cdot 10^{-3}$	$2.09 \cdot 10^{-2}$	$2.09 \cdot 10^{-2}$
80,000	$8.48 \cdot 10^{-15}$	$6.6 \cdot 10^{-6}$	$1.49 \cdot 10^{-11}$	$1.8 \cdot 10^{-2}$	$2.89 \cdot 10^{-3}$	$2.09 \cdot 10^{-2}$	$2.09 \cdot 10^{-2}$
$1 \cdot 10^5$	$5.43 \cdot 10^{-15}$	$5.37 \cdot 10^{-6}$	$1.19 \cdot 10^{-11}$	$1.8 \cdot 10^{-2}$	$2.89 \cdot 10^{-3}$	$2.09 \cdot 10^{-2}$	$2.09 \cdot 10^{-2}$

A.3 Breast

PE	SC	SI	PEA	PNF	PEF	TAWCS	TAOCS
$1 \cdot 10^{-3}$	1.16	$1.52 \cdot 10^{-2}$	2,845	0	0	2,847	2,845
$1.04 \cdot 10^{-3}$	1.15	$1.62 \cdot 10^{-2}$	2,588	0	0	2,590	2,588
$1.07 \cdot 10^{-3}$	1.15	$1.72 \cdot 10^{-2}$	2,355	0	0	2,356	2,355
$1.5 \cdot 10^{-3}$	1.05	$3.04 \cdot 10^{-2}$	938.6	0	0	939.7	938.6
$2 \cdot 10^{-3}$	0.93	$4.68 \cdot 10^{-2}$	414.7	0	0	415.6	414.7
$2.15 \cdot 10^{-3}$	0.9	$5.15 \cdot 10^{-2}$	338.6	0	0	339.6	338.7
$2.15 \cdot 10^{-3}$	0.9	$5.15 \cdot 10^{-2}$	340.8	0	0	341.8	340.9
$2.3 \cdot 10^{-3}$	0.86	$5.65 \cdot 10^{-2}$	277.6	0	0	278.6	277.7
$2.47 \cdot 10^{-3}$	0.82	$6.18 \cdot 10^{-2}$	225.9	0	0	226.8	226
$2.47 \cdot 10^{-3}$	0.82	$6.18 \cdot 10^{-2}$	227.8	0	0	228.7	227.8
$2.64 \cdot 10^{-3}$	0.79	$6.69 \cdot 10^{-2}$	187.7	0	0	188.6	187.8
$2.82 \cdot 10^{-3}$	0.75	$7.22 \cdot 10^{-2}$	154.6	0	0	155.4	154.7
$3 \cdot 10^{-3}$	0.71	$7.71 \cdot 10^{-2}$	130.5	0	0	131.3	130.5
$3.61 \cdot 10^{-3}$	0.6	$9.23 \cdot 10^{-2}$	75.49	0	0	76.19	75.58
$3.61 \cdot 10^{-3}$	0.6	$9.23 \cdot 10^{-2}$	75.49	0	0	76.19	75.58
$4 \cdot 10^{-3}$	0.55	0.1	55.37	0	0	56.02	55.47
$5 \cdot 10^{-3}$	0.43	0.12	28.19	0	0	28.74	28.31
$6 \cdot 10^{-3}$	0.35	0.13	16.13	0	0	16.61	16.26
$8 \cdot 10^{-3}$	0.24	0.15	6.62	0	0	7.01	6.76
$1 \cdot 10^{-2}$	0.18	0.16	3.29	0	0	3.63	3.44
$1.5 \cdot 10^{-2}$	0.11	0.17	0.91	0	0	1.19	1.08
$2 \cdot 10^{-2}$	$7.17 \cdot 10^{-2}$	0.18	0.36	0	0	0.61	0.54
$3 \cdot 10^{-2}$	$3.76 \cdot 10^{-2}$	0.18	$9.58 \cdot 10^{-2}$	0	0	0.32	0.28
$4 \cdot 10^{-2}$	$2.3 \cdot 10^{-2}$	0.18	$3.73 \cdot 10^{-2}$	0	0	0.24	0.22
$5 \cdot 10^{-2}$	$1.54 \cdot 10^{-2}$	0.18	$1.79 \cdot 10^{-2}$	0	0	0.21	0.2
$6 \cdot 10^{-2}$	$1.11 \cdot 10^{-2}$	0.18	$9.78 \cdot 10^{-3}$	0	0	0.2	0.19
$8 \cdot 10^{-2}$	$6.48 \cdot 10^{-3}$	0.17	$3.78 \cdot 10^{-3}$	0	0	0.18	0.17
0.1	$4.23 \cdot 10^{-3}$	0.16	$1.81 \cdot 10^{-3}$	0	0	0.17	0.16
0.15	$1.93 \cdot 10^{-3}$	0.15	$4.79 \cdot 10^{-4}$	0	0	0.15	0.15
0.2	$1.09 \cdot 10^{-3}$	0.14	$1.89 \cdot 10^{-4}$	0	0	0.14	0.14
0.3	$4.89 \cdot 10^{-4}$	0.12	$5.34 \cdot 10^{-5}$	0	0	0.12	0.12
0.4	$2.76 \cdot 10^{-4}$	0.11	$2.29 \cdot 10^{-5}$	0	0	0.11	0.11
0.5	$1.77 \cdot 10^{-4}$	$9.64 \cdot 10^{-2}$	$1.23 \cdot 10^{-5}$	0	0	$9.65 \cdot 10^{-2}$	$9.64 \cdot 10^{-2}$
0.6	$1.23 \cdot 10^{-4}$	$8.91 \cdot 10^{-2}$	$7.68 \cdot 10^{-6}$	0	0	$8.93 \cdot 10^{-2}$	$8.91 \cdot 10^{-2}$
0.8	$6.91 \cdot 10^{-5}$	$7.83 \cdot 10^{-2}$	$3.88 \cdot 10^{-6}$	0	0	$7.84 \cdot 10^{-2}$	$7.83 \cdot 10^{-2}$
1	$4.42 \cdot 10^{-5}$	$7.04 \cdot 10^{-2}$	$2.41 \cdot 10^{-6}$	0	0	$7.05 \cdot 10^{-2}$	$7.04 \cdot 10^{-2}$
1.02	$4.23 \cdot 10^{-5}$	$6.97 \cdot 10^{-2}$	$2.24 \cdot 10^{-6}$	0	0	$6.97 \cdot 10^{-2}$	$6.97 \cdot 10^{-2}$
1.25	$2.83 \cdot 10^{-5}$	$6.3 \cdot 10^{-2}$	$1.52 \cdot 10^{-6}$	$1.53 \cdot 10^{-5}$	0	$6.3 \cdot 10^{-2}$	$6.3 \cdot 10^{-2}$
1.5	$1.97 \cdot 10^{-5}$	$5.73 \cdot 10^{-2}$	$1.1 \cdot 10^{-6}$	$8.46 \cdot 10^{-5}$	0	$5.74 \cdot 10^{-2}$	$5.73 \cdot 10^{-2}$
2	$1.11 \cdot 10^{-5}$	$4.89 \cdot 10^{-2}$	$6.94 \cdot 10^{-7}$	$3.37 \cdot 10^{-4}$	0	$4.92 \cdot 10^{-2}$	$4.92 \cdot 10^{-2}$
2.04	$1.06 \cdot 10^{-5}$	$4.82 \cdot 10^{-2}$	$6.72 \cdot 10^{-7}$	$3.63 \cdot 10^{-4}$	0	$4.86 \cdot 10^{-2}$	$4.86 \cdot 10^{-2}$
3	$4.92 \cdot 10^{-6}$	$3.84 \cdot 10^{-2}$	$3.88 \cdot 10^{-7}$	$9.65 \cdot 10^{-4}$	$1.35 \cdot 10^{-5}$	$3.94 \cdot 10^{-2}$	$3.94 \cdot 10^{-2}$
4	$2.77 \cdot 10^{-6}$	$3.21 \cdot 10^{-2}$	$2.66 \cdot 10^{-7}$	$1.57 \cdot 10^{-3}$	$5.49 \cdot 10^{-5}$	$3.37 \cdot 10^{-2}$	$3.37 \cdot 10^{-2}$
5	$1.77 \cdot 10^{-6}$	$2.77 \cdot 10^{-2}$	$2.02 \cdot 10^{-7}$	$2.1 \cdot 10^{-3}$	$1.09 \cdot 10^{-4}$	$2.99 \cdot 10^{-2}$	$2.99 \cdot 10^{-2}$
6	$1.23 \cdot 10^{-6}$	$2.45 \cdot 10^{-2}$	$1.62 \cdot 10^{-7}$	$2.58 \cdot 10^{-3}$	$1.68 \cdot 10^{-4}$	$2.72 \cdot 10^{-2}$	$2.72 \cdot 10^{-2}$
7	$9.03 \cdot 10^{-7}$	$2.2 \cdot 10^{-2}$	$1.36 \cdot 10^{-7}$	$3.01 \cdot 10^{-3}$	$2.27 \cdot 10^{-4}$	$2.52 \cdot 10^{-2}$	$2.52 \cdot 10^{-2}$
8	$6.91 \cdot 10^{-7}$	$2 \cdot 10^{-2}$	$1.16 \cdot 10^{-7}$	$3.4 \cdot 10^{-3}$	$2.83 \cdot 10^{-4}$	$2.37 \cdot 10^{-2}$	$2.37 \cdot 10^{-2}$
9	$5.46 \cdot 10^{-7}$	$1.84 \cdot 10^{-2}$	$1.02 \cdot 10^{-7}$	$3.75 \cdot 10^{-3}$	$3.38 \cdot 10^{-4}$	$2.25 \cdot 10^{-2}$	$2.25 \cdot 10^{-2}$
10	$4.42 \cdot 10^{-7}$	$1.71 \cdot 10^{-2}$	$9.06 \cdot 10^{-8}$	$4.07 \cdot 10^{-3}$	$3.9 \cdot 10^{-4}$	$2.15 \cdot 10^{-2}$	$2.15 \cdot 10^{-2}$
11	$3.66 \cdot 10^{-7}$	$1.59 \cdot 10^{-2}$	$8.15 \cdot 10^{-8}$	$4.36 \cdot 10^{-3}$	$4.39 \cdot 10^{-4}$	$2.07 \cdot 10^{-2}$	$2.07 \cdot 10^{-2}$
12	$3.07 \cdot 10^{-7}$	$1.49 \cdot 10^{-2}$	$7.41 \cdot 10^{-8}$	$4.62 \cdot 10^{-3}$	$4.86 \cdot 10^{-4}$	$2 \cdot 10^{-2}$	$2 \cdot 10^{-2}$
13	$2.62 \cdot 10^{-7}$	$1.41 \cdot 10^{-2}$	$6.79 \cdot 10^{-8}$	$4.87 \cdot 10^{-3}$	$5.3 \cdot 10^{-4}$	$1.95 \cdot 10^{-2}$	$1.95 \cdot 10^{-2}$
14	$2.26 \cdot 10^{-7}$	$1.33 \cdot 10^{-2}$	$6.27 \cdot 10^{-8}$	$5.1 \cdot 10^{-3}$	$5.72 \cdot 10^{-4}$	$1.9 \cdot 10^{-2}$	$1.9 \cdot 10^{-2}$
15	$1.97 \cdot 10^{-7}$	$1.26 \cdot 10^{-2}$	$5.82 \cdot 10^{-8}$	$5.32 \cdot 10^{-3}$	$6.12 \cdot 10^{-4}$	$1.85 \cdot 10^{-2}$	$1.85 \cdot 10^{-2}$
16	$1.73 \cdot 10^{-7}$	$1.2 \cdot 10^{-2}$	$5.43 \cdot 10^{-8}$	$5.52 \cdot 10^{-3}$	$6.5 \cdot 10^{-4}$	$1.82 \cdot 10^{-2}$	$1.82 \cdot 10^{-2}$
18	$1.37 \cdot 10^{-7}$	$1.1 \cdot 10^{-2}$	$4.79 \cdot 10^{-8}$	$5.89 \cdot 10^{-3}$	$7.21 \cdot 10^{-4}$	$1.76 \cdot 10^{-2}$	$1.76 \cdot 10^{-2}$
20	$1.11 \cdot 10^{-7}$	$1.01 \cdot 10^{-2}$	$4.28 \cdot 10^{-8}$	$6.22 \cdot 10^{-3}$	$7.86 \cdot 10^{-4}$	$1.71 \cdot 10^{-2}$	$1.71 \cdot 10^{-2}$
22	$9.14 \cdot 10^{-8}$	$9.41 \cdot 10^{-3}$	$3.88 \cdot 10^{-8}$	$6.53 \cdot 10^{-3}$	$8.46 \cdot 10^{-4}$	$1.68 \cdot 10^{-2}$	$1.68 \cdot 10^{-2}$
24	$7.68 \cdot 10^{-8}$	$8.79 \cdot 10^{-3}$	$3.54 \cdot 10^{-8}$	$6.8 \cdot 10^{-3}$	$9.01 \cdot 10^{-4}$	$1.65 \cdot 10^{-2}$	$1.65 \cdot 10^{-2}$
26	$6.55 \cdot 10^{-8}$	$8.25 \cdot 10^{-3}$	$3.25 \cdot 10^{-8}$	$7.05 \cdot 10^{-3}$	$9.52 \cdot 10^{-4}$	$1.63 \cdot 10^{-2}$	$1.63 \cdot 10^{-2}$
28	$5.64 \cdot 10^{-8}$	$7.79 \cdot 10^{-3}$	$3.01 \cdot 10^{-8}$	$7.29 \cdot 10^{-3}$	$1 \cdot 10^{-3}$	$1.61 \cdot 10^{-2}$	$1.61 \cdot 10^{-2}$
30	$4.92 \cdot 10^{-8}$	$7.37 \cdot 10^{-3}$	$2.8 \cdot 10^{-8}$	$7.5 \cdot 10^{-3}$	$1.05 \cdot 10^{-3}$	$1.59 \cdot 10^{-2}$	$1.59 \cdot 10^{-2}$
40	$2.77 \cdot 10^{-8}$	$5.86 \cdot 10^{-3}$	$2.08 \cdot 10^{-8}$	$8.39 \cdot 10^{-3}$	$1.24 \cdot 10^{-3}$	$1.55 \cdot 10^{-2}$	$1.55 \cdot 10^{-2}$
50	$1.77 \cdot 10^{-8}$	$4.89 \cdot 10^{-3}$	$1.66 \cdot 10^{-8}$	$9.06 \cdot 10^{-3}$	$1.38 \cdot 10^{-3}$	$1.53 \cdot 10^{-2}$	$1.53 \cdot 10^{-2}$
60	$1.23 \cdot 10^{-8}$	$4.21 \cdot 10^{-3}$	$1.38 \cdot 10^{-8}$	$9.59 \cdot 10^{-3}$	$1.5 \cdot 10^{-3}$	$1.53 \cdot 10^{-2}$	$1.53 \cdot 10^{-2}$

80	$6.91 \cdot 10^{-9}$	$3.32 \cdot 10^{-3}$	$1.03 \cdot 10^{-8}$	$1.04 \cdot 10^{-2}$	$1.69 \cdot 10^{-3}$	$1.54 \cdot 10^{-2}$	$1.54 \cdot 10^{-2}$
100	$4.42 \cdot 10^{-9}$	$2.76 \cdot 10^{-3}$	$8.19 \cdot 10^{-9}$	$1.1 \cdot 10^{-2}$	$1.83 \cdot 10^{-3}$	$1.56 \cdot 10^{-2}$	$1.56 \cdot 10^{-2}$
150	$1.97 \cdot 10^{-9}$	$1.96 \cdot 10^{-3}$	$5.44 \cdot 10^{-9}$	$1.2 \cdot 10^{-2}$	$2.08 \cdot 10^{-3}$	$1.6 \cdot 10^{-2}$	$1.6 \cdot 10^{-2}$
200	$1.11 \cdot 10^{-9}$	$1.54 \cdot 10^{-3}$	$4.07 \cdot 10^{-9}$	$1.26 \cdot 10^{-2}$	$2.25 \cdot 10^{-3}$	$1.64 \cdot 10^{-2}$	$1.64 \cdot 10^{-2}$
300	$4.92 \cdot 10^{-10}$	$1.09 \cdot 10^{-3}$	$2.71 \cdot 10^{-9}$	$1.33 \cdot 10^{-2}$	$2.46 \cdot 10^{-3}$	$1.69 \cdot 10^{-2}$	$1.69 \cdot 10^{-2}$
400	$2.77 \cdot 10^{-10}$	$8.55 \cdot 10^{-4}$	$2.03 \cdot 10^{-9}$	$1.38 \cdot 10^{-2}$	$2.59 \cdot 10^{-3}$	$1.72 \cdot 10^{-2}$	$1.72 \cdot 10^{-2}$
500	$1.77 \cdot 10^{-10}$	$7.08 \cdot 10^{-4}$	$1.62 \cdot 10^{-9}$	$1.41 \cdot 10^{-2}$	$2.69 \cdot 10^{-3}$	$1.75 \cdot 10^{-2}$	$1.75 \cdot 10^{-2}$
600	$1.23 \cdot 10^{-10}$	$6.06 \cdot 10^{-4}$	$1.35 \cdot 10^{-9}$	$1.43 \cdot 10^{-2}$	$2.76 \cdot 10^{-3}$	$1.77 \cdot 10^{-2}$	$1.77 \cdot 10^{-2}$
800	$6.91 \cdot 10^{-11}$	$4.73 \cdot 10^{-4}$	$1.01 \cdot 10^{-9}$	$1.46 \cdot 10^{-2}$	$2.85 \cdot 10^{-3}$	$1.79 \cdot 10^{-2}$	$1.79 \cdot 10^{-2}$
1,000	$4.42 \cdot 10^{-11}$	$3.89 \cdot 10^{-4}$	$8.1 \cdot 10^{-10}$	$1.48 \cdot 10^{-2}$	$2.92 \cdot 10^{-3}$	$1.81 \cdot 10^{-2}$	$1.81 \cdot 10^{-2}$
1,500	$1.97 \cdot 10^{-11}$	$2.72 \cdot 10^{-4}$	$5.4 \cdot 10^{-10}$	$1.5 \cdot 10^{-2}$	$3.02 \cdot 10^{-3}$	$1.83 \cdot 10^{-2}$	$1.83 \cdot 10^{-2}$
2,000	$1.11 \cdot 10^{-11}$	$2.1 \cdot 10^{-4}$	$4.05 \cdot 10^{-10}$	$1.52 \cdot 10^{-2}$	$3.08 \cdot 10^{-3}$	$1.85 \cdot 10^{-2}$	$1.85 \cdot 10^{-2}$
3,000	$4.92 \cdot 10^{-12}$	$1.46 \cdot 10^{-4}$	$2.7 \cdot 10^{-10}$	$1.54 \cdot 10^{-2}$	$3.14 \cdot 10^{-3}$	$1.87 \cdot 10^{-2}$	$1.87 \cdot 10^{-2}$
4,000	$2.77 \cdot 10^{-12}$	$1.13 \cdot 10^{-4}$	$2.02 \cdot 10^{-10}$	$1.55 \cdot 10^{-2}$	$3.18 \cdot 10^{-3}$	$1.87 \cdot 10^{-2}$	$1.87 \cdot 10^{-2}$
5,000	$1.77 \cdot 10^{-12}$	$9.24 \cdot 10^{-5}$	$1.62 \cdot 10^{-10}$	$1.55 \cdot 10^{-2}$	$3.2 \cdot 10^{-3}$	$1.88 \cdot 10^{-2}$	$1.88 \cdot 10^{-2}$
6,000	$1.23 \cdot 10^{-12}$	$7.83 \cdot 10^{-5}$	$1.35 \cdot 10^{-10}$	$1.56 \cdot 10^{-2}$	$3.22 \cdot 10^{-3}$	$1.88 \cdot 10^{-2}$	$1.88 \cdot 10^{-2}$
8,000	$6.91 \cdot 10^{-13}$	$6.03 \cdot 10^{-5}$	$1.01 \cdot 10^{-10}$	$1.56 \cdot 10^{-2}$	$3.24 \cdot 10^{-3}$	$1.89 \cdot 10^{-2}$	$1.89 \cdot 10^{-2}$
10,000	$4.42 \cdot 10^{-13}$	$4.93 \cdot 10^{-5}$	$8.09 \cdot 10^{-11}$	$1.56 \cdot 10^{-2}$	$3.25 \cdot 10^{-3}$	$1.89 \cdot 10^{-2}$	$1.89 \cdot 10^{-2}$
15,000	$1.97 \cdot 10^{-13}$	$3.4 \cdot 10^{-5}$	$5.4 \cdot 10^{-11}$	$1.57 \cdot 10^{-2}$	$3.27 \cdot 10^{-3}$	$1.9 \cdot 10^{-2}$	$1.9 \cdot 10^{-2}$
20,000	$1.11 \cdot 10^{-13}$	$2.62 \cdot 10^{-5}$	$4.05 \cdot 10^{-11}$	$1.57 \cdot 10^{-2}$	$3.28 \cdot 10^{-3}$	$1.9 \cdot 10^{-2}$	$1.9 \cdot 10^{-2}$
30,000	$4.92 \cdot 10^{-14}$	$1.81 \cdot 10^{-5}$	$2.7 \cdot 10^{-11}$	$1.57 \cdot 10^{-2}$	$3.29 \cdot 10^{-3}$	$1.9 \cdot 10^{-2}$	$1.9 \cdot 10^{-2}$
40,000	$2.77 \cdot 10^{-14}$	$1.39 \cdot 10^{-5}$	$2.02 \cdot 10^{-11}$	$1.57 \cdot 10^{-2}$	$3.3 \cdot 10^{-3}$	$1.91 \cdot 10^{-2}$	$1.91 \cdot 10^{-2}$
50,000	$1.77 \cdot 10^{-14}$	$1.13 \cdot 10^{-5}$	$1.62 \cdot 10^{-11}$	$1.58 \cdot 10^{-2}$	$3.3 \cdot 10^{-3}$	$1.91 \cdot 10^{-2}$	$1.91 \cdot 10^{-2}$
60,000	$1.23 \cdot 10^{-14}$	$9.54 \cdot 10^{-6}$	$1.35 \cdot 10^{-11}$	$1.58 \cdot 10^{-2}$	$3.31 \cdot 10^{-3}$	$1.91 \cdot 10^{-2}$	$1.91 \cdot 10^{-2}$
80,000	$6.91 \cdot 10^{-15}$	$7.31 \cdot 10^{-6}$	$1.01 \cdot 10^{-11}$	$1.58 \cdot 10^{-2}$	$3.31 \cdot 10^{-3}$	$1.91 \cdot 10^{-2}$	$1.91 \cdot 10^{-2}$
$1 \cdot 10^5$	$4.42 \cdot 10^{-15}$	$5.95 \cdot 10^{-6}$	$8.09 \cdot 10^{-12}$	$1.58 \cdot 10^{-2}$	$3.31 \cdot 10^{-3}$	$1.91 \cdot 10^{-2}$	$1.91 \cdot 10^{-2}$

A.4 Dense Bone

PE	SC	SI	PEA	PNF	PEF	TAWCS	TAOCS
$1.04 \cdot 10^{-3}$	1.65	$1.4 \cdot 10^{-2}$	3,329	0	0	3,331	3,329
$1.07 \cdot 10^{-3}$	1.64	$1.49 \cdot 10^{-2}$	3,034	0	0	3,035	3,034
$1.07 \cdot 10^{-3}$	1.64	$1.49 \cdot 10^{-2}$	3,040	0	0	3,042	3,040
$1.18 \cdot 10^{-3}$	1.6	$1.75 \cdot 10^{-2}$	2,339	0	0	2,340	2,339
$1.31 \cdot 10^{-3}$	1.57	$2.05 \cdot 10^{-2}$	1,797	0	0	1,798	1,797
$1.31 \cdot 10^{-3}$	1.57	$2.05 \cdot 10^{-2}$	1,802	0	0	1,804	1,802
$1.5 \cdot 10^{-3}$	1.51	$2.56 \cdot 10^{-2}$	1,237	0	0	1,238	1,237
$2 \cdot 10^{-3}$	1.36	$3.89 \cdot 10^{-2}$	556	0	0	557.4	556.1
$2.15 \cdot 10^{-3}$	1.32	$4.28 \cdot 10^{-2}$	455.9	0	0	457.2	455.9
$2.3 \cdot 10^{-3}$	1.27	$4.7 \cdot 10^{-2}$	387.4	0	0	388.7	387.4
$2.47 \cdot 10^{-3}$	1.22	$5.13 \cdot 10^{-2}$	317.1	0	0	318.3	317.1
$2.47 \cdot 10^{-3}$	1.22	$5.13 \cdot 10^{-2}$	323	0	0	324.3	323.1
$2.64 \cdot 10^{-3}$	1.18	$5.56 \cdot 10^{-2}$	267.8	0	0	269	267.9
$2.82 \cdot 10^{-3}$	1.13	$6.01 \cdot 10^{-2}$	221.9	0	0	223.1	221.9
$2.82 \cdot 10^{-3}$	1.13	$6.01 \cdot 10^{-2}$	223.4	0	0	224.6	223.5
$3 \cdot 10^{-3}$	1.08	$6.43 \cdot 10^{-2}$	187.8	0	0	189	187.9
$3.61 \cdot 10^{-3}$	0.94	$7.75 \cdot 10^{-2}$	110.3	0	0	111.3	110.4
$3.61 \cdot 10^{-3}$	0.94	$7.75 \cdot 10^{-2}$	111.4	0	0	112.5	111.5
$4 \cdot 10^{-3}$	0.86	$8.5 \cdot 10^{-2}$	82.49	0	0	83.44	82.57
$4.04 \cdot 10^{-3}$	0.85	$8.57 \cdot 10^{-2}$	80.24	0	0	81.18	80.33
$4.04 \cdot 10^{-3}$	0.85	$8.57 \cdot 10^{-2}$	221.5	0	0	222.4	221.6
$5 \cdot 10^{-3}$	0.7	0.1	126.6	0	0	127.4	126.7
$6 \cdot 10^{-3}$	0.57	0.11	76.94	0	0	77.63	77.05
$8 \cdot 10^{-3}$	0.42	0.13	34.62	0	0	35.17	34.75
$1 \cdot 10^{-2}$	0.32	0.14	18.37	0	0	18.83	18.51
$1.5 \cdot 10^{-2}$	0.2	0.16	5.65	0	0	6	5.8
$2 \cdot 10^{-2}$	0.13	0.16	2.4	0	0	2.69	2.56
$3 \cdot 10^{-2}$	$6.95 \cdot 10^{-2}$	0.17	0.7	0	0	0.94	0.87
$4 \cdot 10^{-2}$	$4.32 \cdot 10^{-2}$	0.17	0.29	0	0	0.5	0.46
$5 \cdot 10^{-2}$	$2.95 \cdot 10^{-2}$	0.17	0.14	0	0	0.34	0.31
$6 \cdot 10^{-2}$	$2.14 \cdot 10^{-2}$	0.17	$8.16 \cdot 10^{-2}$	0	0	0.27	0.25
$8 \cdot 10^{-2}$	$1.28 \cdot 10^{-2}$	0.16	$3.29 \cdot 10^{-2}$	0	0	0.21	0.19
0.1	$8.42 \cdot 10^{-3}$	0.15	$1.63 \cdot 10^{-2}$	0	0	0.18	0.17
0.15	$3.89 \cdot 10^{-3}$	0.14	$4.52 \cdot 10^{-3}$	0	0	0.15	0.14
0.2	$2.23 \cdot 10^{-3}$	0.13	$1.84 \cdot 10^{-3}$	0	0	0.13	0.13
0.3	$1.01 \cdot 10^{-3}$	0.11	$5.38 \cdot 10^{-4}$	0	0	0.11	0.11
0.4	$5.7 \cdot 10^{-4}$	0.1	$2.35 \cdot 10^{-4}$	0	0	0.1	0.1
0.5	$3.66 \cdot 10^{-4}$	$9.21 \cdot 10^{-2}$	$1.28 \cdot 10^{-4}$	0	0	$9.25 \cdot 10^{-2}$	$9.22 \cdot 10^{-2}$
0.6	$2.54 \cdot 10^{-4}$	$8.52 \cdot 10^{-2}$	$8.02 \cdot 10^{-5}$	0	0	$8.55 \cdot 10^{-2}$	$8.53 \cdot 10^{-2}$
0.8	$1.43 \cdot 10^{-4}$	$7.49 \cdot 10^{-2}$	$4.07 \cdot 10^{-5}$	0	0	$7.5 \cdot 10^{-2}$	$7.49 \cdot 10^{-2}$
1	$9.18 \cdot 10^{-5}$	$6.73 \cdot 10^{-2}$	$2.53 \cdot 10^{-5}$	0	0	$6.74 \cdot 10^{-2}$	$6.74 \cdot 10^{-2}$
1.02	$8.79 \cdot 10^{-5}$	$6.66 \cdot 10^{-2}$	$2.39 \cdot 10^{-5}$	0	0	$6.67 \cdot 10^{-2}$	$6.66 \cdot 10^{-2}$
1.25	$5.88 \cdot 10^{-5}$	$6.02 \cdot 10^{-2}$	$1.62 \cdot 10^{-5}$	$2.28 \cdot 10^{-5}$	0	$6.03 \cdot 10^{-2}$	$6.02 \cdot 10^{-2}$
1.5	$4.08 \cdot 10^{-5}$	$5.47 \cdot 10^{-2}$	$1.17 \cdot 10^{-5}$	$1.24 \cdot 10^{-4}$	0	$5.49 \cdot 10^{-2}$	$5.49 \cdot 10^{-2}$
2	$2.3 \cdot 10^{-5}$	$4.67 \cdot 10^{-2}$	$7.27 \cdot 10^{-6}$	$4.88 \cdot 10^{-4}$	0	$4.72 \cdot 10^{-2}$	$4.72 \cdot 10^{-2}$
2.04	$2.2 \cdot 10^{-5}$	$4.61 \cdot 10^{-2}$	$7.03 \cdot 10^{-6}$	$5.26 \cdot 10^{-4}$	0	$4.67 \cdot 10^{-2}$	$4.67 \cdot 10^{-2}$
3	$1.02 \cdot 10^{-5}$	$3.67 \cdot 10^{-2}$	$3.99 \cdot 10^{-6}$	$1.39 \cdot 10^{-3}$	$1.29 \cdot 10^{-5}$	$3.82 \cdot 10^{-2}$	$3.81 \cdot 10^{-2}$
4	$5.75 \cdot 10^{-6}$	$3.07 \cdot 10^{-2}$	$2.7 \cdot 10^{-6}$	$2.24 \cdot 10^{-3}$	$5.25 \cdot 10^{-5}$	$3.3 \cdot 10^{-2}$	$3.29 \cdot 10^{-2}$
5	$3.68 \cdot 10^{-6}$	$2.65 \cdot 10^{-2}$	$2.03 \cdot 10^{-6}$	$3 \cdot 10^{-3}$	$1.05 \cdot 10^{-4}$	$2.96 \cdot 10^{-2}$	$2.96 \cdot 10^{-2}$
6	$2.55 \cdot 10^{-6}$	$2.34 \cdot 10^{-2}$	$1.63 \cdot 10^{-6}$	$3.69 \cdot 10^{-3}$	$1.61 \cdot 10^{-4}$	$2.72 \cdot 10^{-2}$	$2.72 \cdot 10^{-2}$
7	$1.88 \cdot 10^{-6}$	$2.1 \cdot 10^{-2}$	$1.35 \cdot 10^{-6}$	$4.29 \cdot 10^{-3}$	$2.17 \cdot 10^{-4}$	$2.55 \cdot 10^{-2}$	$2.55 \cdot 10^{-2}$
8	$1.44 \cdot 10^{-6}$	$1.91 \cdot 10^{-2}$	$1.16 \cdot 10^{-6}$	$4.84 \cdot 10^{-3}$	$2.71 \cdot 10^{-4}$	$2.43 \cdot 10^{-2}$	$2.43 \cdot 10^{-2}$
9	$1.14 \cdot 10^{-6}$	$1.76 \cdot 10^{-2}$	$1.01 \cdot 10^{-6}$	$5.34 \cdot 10^{-3}$	$3.23 \cdot 10^{-4}$	$2.33 \cdot 10^{-2}$	$2.33 \cdot 10^{-2}$
10	$9.19 \cdot 10^{-7}$	$1.63 \cdot 10^{-2}$	$8.95 \cdot 10^{-7}$	$5.79 \cdot 10^{-3}$	$3.73 \cdot 10^{-4}$	$2.25 \cdot 10^{-2}$	$2.25 \cdot 10^{-2}$
11	$7.6 \cdot 10^{-7}$	$1.52 \cdot 10^{-2}$	$8.04 \cdot 10^{-7}$	$6.2 \cdot 10^{-3}$	$4.2 \cdot 10^{-4}$	$2.18 \cdot 10^{-2}$	$2.18 \cdot 10^{-2}$
12	$6.38 \cdot 10^{-7}$	$1.43 \cdot 10^{-2}$	$7.3 \cdot 10^{-7}$	$6.57 \cdot 10^{-3}$	$4.64 \cdot 10^{-4}$	$2.13 \cdot 10^{-2}$	$2.13 \cdot 10^{-2}$
13	$5.44 \cdot 10^{-7}$	$1.34 \cdot 10^{-2}$	$6.68 \cdot 10^{-7}$	$6.92 \cdot 10^{-3}$	$5.06 \cdot 10^{-4}$	$2.09 \cdot 10^{-2}$	$2.09 \cdot 10^{-2}$
14	$4.69 \cdot 10^{-7}$	$1.27 \cdot 10^{-2}$	$6.16 \cdot 10^{-7}$	$7.24 \cdot 10^{-3}$	$5.47 \cdot 10^{-4}$	$2.05 \cdot 10^{-2}$	$2.05 \cdot 10^{-2}$
15	$4.09 \cdot 10^{-7}$	$1.21 \cdot 10^{-2}$	$5.71 \cdot 10^{-7}$	$7.55 \cdot 10^{-3}$	$5.84 \cdot 10^{-4}$	$2.02 \cdot 10^{-2}$	$2.02 \cdot 10^{-2}$
16	$3.59 \cdot 10^{-7}$	$1.15 \cdot 10^{-2}$	$5.32 \cdot 10^{-7}$	$7.83 \cdot 10^{-3}$	$6.21 \cdot 10^{-4}$	$1.99 \cdot 10^{-2}$	$1.99 \cdot 10^{-2}$
18	$2.84 \cdot 10^{-7}$	$1.05 \cdot 10^{-2}$	$4.69 \cdot 10^{-7}$	$8.36 \cdot 10^{-3}$	$6.89 \cdot 10^{-4}$	$1.95 \cdot 10^{-2}$	$1.95 \cdot 10^{-2}$
20	$2.3 \cdot 10^{-7}$	$9.68 \cdot 10^{-3}$	$4.19 \cdot 10^{-7}$	$8.82 \cdot 10^{-3}$	$7.5 \cdot 10^{-4}$	$1.93 \cdot 10^{-2}$	$1.93 \cdot 10^{-2}$
22	$1.9 \cdot 10^{-7}$	$8.99 \cdot 10^{-3}$	$3.78 \cdot 10^{-7}$	$9.25 \cdot 10^{-3}$	$8.07 \cdot 10^{-4}$	$1.91 \cdot 10^{-2}$	$1.91 \cdot 10^{-2}$
24	$1.6 \cdot 10^{-7}$	$8.4 \cdot 10^{-3}$	$3.45 \cdot 10^{-7}$	$9.63 \cdot 10^{-3}$	$8.6 \cdot 10^{-4}$	$1.89 \cdot 10^{-2}$	$1.89 \cdot 10^{-2}$
26	$1.36 \cdot 10^{-7}$	$7.89 \cdot 10^{-3}$	$3.17 \cdot 10^{-7}$	$9.99 \cdot 10^{-3}$	$9.09 \cdot 10^{-4}$	$1.88 \cdot 10^{-2}$	$1.88 \cdot 10^{-2}$

28	$1.17 \cdot 10^{-7}$	$7.44 \cdot 10^{-3}$	$2.93 \cdot 10^{-7}$	$1.03 \cdot 10^{-2}$	$9.55 \cdot 10^{-4}$	$1.87 \cdot 10^{-2}$	$1.87 \cdot 10^{-2}$
30	$1.02 \cdot 10^{-7}$	$7.05 \cdot 10^{-3}$	$2.73 \cdot 10^{-7}$	$1.06 \cdot 10^{-2}$	$9.97 \cdot 10^{-4}$	$1.87 \cdot 10^{-2}$	$1.87 \cdot 10^{-2}$
40	$5.75 \cdot 10^{-8}$	$5.6 \cdot 10^{-3}$	$2.02 \cdot 10^{-7}$	$1.19 \cdot 10^{-2}$	$1.18 \cdot 10^{-3}$	$1.86 \cdot 10^{-2}$	$1.86 \cdot 10^{-2}$
50	$3.68 \cdot 10^{-8}$	$4.68 \cdot 10^{-3}$	$1.61 \cdot 10^{-7}$	$1.28 \cdot 10^{-2}$	$1.32 \cdot 10^{-3}$	$1.88 \cdot 10^{-2}$	$1.88 \cdot 10^{-2}$
60	$2.55 \cdot 10^{-8}$	$4.03 \cdot 10^{-3}$	$1.33 \cdot 10^{-7}$	$1.35 \cdot 10^{-2}$	$1.43 \cdot 10^{-3}$	$1.9 \cdot 10^{-2}$	$1.9 \cdot 10^{-2}$
80	$1.44 \cdot 10^{-8}$	$3.18 \cdot 10^{-3}$	$9.94 \cdot 10^{-8}$	$1.46 \cdot 10^{-2}$	$1.61 \cdot 10^{-3}$	$1.94 \cdot 10^{-2}$	$1.94 \cdot 10^{-2}$
100	$9.19 \cdot 10^{-9}$	$2.64 \cdot 10^{-3}$	$7.92 \cdot 10^{-8}$	$1.54 \cdot 10^{-2}$	$1.74 \cdot 10^{-3}$	$1.98 \cdot 10^{-2}$	$1.98 \cdot 10^{-2}$
150	$4.09 \cdot 10^{-9}$	$1.88 \cdot 10^{-3}$	$5.26 \cdot 10^{-8}$	$1.68 \cdot 10^{-2}$	$1.97 \cdot 10^{-3}$	$2.06 \cdot 10^{-2}$	$2.06 \cdot 10^{-2}$
200	$2.3 \cdot 10^{-9}$	$1.47 \cdot 10^{-3}$	$3.93 \cdot 10^{-8}$	$1.76 \cdot 10^{-2}$	$2.12 \cdot 10^{-3}$	$2.12 \cdot 10^{-2}$	$2.12 \cdot 10^{-2}$
300	$1.02 \cdot 10^{-9}$	$1.04 \cdot 10^{-3}$	$2.62 \cdot 10^{-8}$	$1.86 \cdot 10^{-2}$	$2.31 \cdot 10^{-3}$	$2.19 \cdot 10^{-2}$	$2.19 \cdot 10^{-2}$
400	$5.75 \cdot 10^{-10}$	$8.17 \cdot 10^{-4}$	$1.96 \cdot 10^{-8}$	$1.91 \cdot 10^{-2}$	$2.43 \cdot 10^{-3}$	$2.24 \cdot 10^{-2}$	$2.24 \cdot 10^{-2}$
500	$3.68 \cdot 10^{-10}$	$6.77 \cdot 10^{-4}$	$1.57 \cdot 10^{-8}$	$1.95 \cdot 10^{-2}$	$2.52 \cdot 10^{-3}$	$2.27 \cdot 10^{-2}$	$2.27 \cdot 10^{-2}$
600	$2.55 \cdot 10^{-10}$	$5.79 \cdot 10^{-4}$	$1.3 \cdot 10^{-8}$	$1.98 \cdot 10^{-2}$	$2.58 \cdot 10^{-3}$	$2.3 \cdot 10^{-2}$	$2.3 \cdot 10^{-2}$
800	$1.44 \cdot 10^{-10}$	$4.52 \cdot 10^{-4}$	$9.78 \cdot 10^{-9}$	$2.02 \cdot 10^{-2}$	$2.67 \cdot 10^{-3}$	$2.33 \cdot 10^{-2}$	$2.33 \cdot 10^{-2}$
1,000	$9.19 \cdot 10^{-11}$	$3.72 \cdot 10^{-4}$	$7.82 \cdot 10^{-9}$	$2.04 \cdot 10^{-2}$	$2.73 \cdot 10^{-3}$	$2.35 \cdot 10^{-2}$	$2.35 \cdot 10^{-2}$
1,500	$4.09 \cdot 10^{-11}$	$2.6 \cdot 10^{-4}$	$5.21 \cdot 10^{-9}$	$2.08 \cdot 10^{-2}$	$2.82 \cdot 10^{-3}$	$2.39 \cdot 10^{-2}$	$2.39 \cdot 10^{-2}$
2,000	$2.3 \cdot 10^{-11}$	$2.01 \cdot 10^{-4}$	$3.91 \cdot 10^{-9}$	$2.1 \cdot 10^{-2}$	$2.87 \cdot 10^{-3}$	$2.41 \cdot 10^{-2}$	$2.41 \cdot 10^{-2}$
3,000	$1.02 \cdot 10^{-11}$	$1.4 \cdot 10^{-4}$	$2.6 \cdot 10^{-9}$	$2.12 \cdot 10^{-2}$	$2.93 \cdot 10^{-3}$	$2.43 \cdot 10^{-2}$	$2.43 \cdot 10^{-2}$
4,000	$5.75 \cdot 10^{-12}$	$1.08 \cdot 10^{-4}$	$1.95 \cdot 10^{-9}$	$2.13 \cdot 10^{-2}$	$2.96 \cdot 10^{-3}$	$2.44 \cdot 10^{-2}$	$2.44 \cdot 10^{-2}$
5,000	$3.68 \cdot 10^{-12}$	$8.83 \cdot 10^{-5}$	$1.56 \cdot 10^{-9}$	$2.14 \cdot 10^{-2}$	$2.98 \cdot 10^{-3}$	$2.44 \cdot 10^{-2}$	$2.44 \cdot 10^{-2}$
6,000	$2.55 \cdot 10^{-12}$	$7.49 \cdot 10^{-5}$	$1.3 \cdot 10^{-9}$	$2.14 \cdot 10^{-2}$	$2.99 \cdot 10^{-3}$	$2.45 \cdot 10^{-2}$	$2.45 \cdot 10^{-2}$
8,000	$1.44 \cdot 10^{-12}$	$5.77 \cdot 10^{-5}$	$9.76 \cdot 10^{-10}$	$2.15 \cdot 10^{-2}$	$3.01 \cdot 10^{-3}$	$2.46 \cdot 10^{-2}$	$2.46 \cdot 10^{-2}$
10,000	$9.19 \cdot 10^{-13}$	$4.71 \cdot 10^{-5}$	$7.81 \cdot 10^{-10}$	$2.15 \cdot 10^{-2}$	$3.03 \cdot 10^{-3}$	$2.46 \cdot 10^{-2}$	$2.46 \cdot 10^{-2}$
15,000	$4.09 \cdot 10^{-13}$	$3.25 \cdot 10^{-5}$	$5.21 \cdot 10^{-10}$	$2.16 \cdot 10^{-2}$	$3.04 \cdot 10^{-3}$	$2.47 \cdot 10^{-2}$	$2.47 \cdot 10^{-2}$
20,000	$2.3 \cdot 10^{-13}$	$2.5 \cdot 10^{-5}$	$3.91 \cdot 10^{-10}$	$2.16 \cdot 10^{-2}$	$3.05 \cdot 10^{-3}$	$2.47 \cdot 10^{-2}$	$2.47 \cdot 10^{-2}$
30,000	$1.02 \cdot 10^{-13}$	$1.73 \cdot 10^{-5}$	$2.6 \cdot 10^{-10}$	$2.17 \cdot 10^{-2}$	$3.06 \cdot 10^{-3}$	$2.47 \cdot 10^{-2}$	$2.47 \cdot 10^{-2}$
40,000	$5.75 \cdot 10^{-14}$	$1.33 \cdot 10^{-5}$	$1.95 \cdot 10^{-10}$	$2.17 \cdot 10^{-2}$	$3.07 \cdot 10^{-3}$	$2.48 \cdot 10^{-2}$	$2.48 \cdot 10^{-2}$
50,000	$3.68 \cdot 10^{-14}$	$1.08 \cdot 10^{-5}$	$1.56 \cdot 10^{-10}$	$2.17 \cdot 10^{-2}$	$3.07 \cdot 10^{-3}$	$2.48 \cdot 10^{-2}$	$2.48 \cdot 10^{-2}$
60,000	$2.55 \cdot 10^{-14}$	$9.12 \cdot 10^{-6}$	$1.3 \cdot 10^{-10}$	$2.17 \cdot 10^{-2}$	$3.07 \cdot 10^{-3}$	$2.48 \cdot 10^{-2}$	$2.48 \cdot 10^{-2}$
80,000	$1.44 \cdot 10^{-14}$	$6.99 \cdot 10^{-6}$	$9.76 \cdot 10^{-11}$	$2.17 \cdot 10^{-2}$	$3.08 \cdot 10^{-3}$	$2.48 \cdot 10^{-2}$	$2.48 \cdot 10^{-2}$
$1 \cdot 10^5$	$9.19 \cdot 10^{-15}$	$5.69 \cdot 10^{-6}$	$7.81 \cdot 10^{-11}$	$2.17 \cdot 10^{-2}$	$3.08 \cdot 10^{-3}$	$2.48 \cdot 10^{-2}$	$2.48 \cdot 10^{-2}$

A.5 Liver

PE	SC	SI	PEA	PNF	PEF	TAWCS	TAOCS
$1 \cdot 10^{-3}$	1.34	$1.35 \cdot 10^{-2}$	3,724	0	0	3,726	3,724
$1.04 \cdot 10^{-3}$	1.33	$1.43 \cdot 10^{-2}$	3,394	0	0	3,396	3,394
$1.07 \cdot 10^{-3}$	1.32	$1.52 \cdot 10^{-2}$	3,093	0	0	3,094	3,093
$1.07 \cdot 10^{-3}$	1.32	$1.52 \cdot 10^{-2}$	3,105	0	0	3,106	3,105
$1.5 \cdot 10^{-3}$	1.23	$2.71 \cdot 10^{-2}$	1,255	0	0	1,256	1,255
$2 \cdot 10^{-3}$	1.11	$4.23 \cdot 10^{-2}$	560.9	0	0	562.1	561
$2.15 \cdot 10^{-3}$	1.07	$4.67 \cdot 10^{-2}$	459.3	0	0	460.4	459.3
$2.15 \cdot 10^{-3}$	1.07	$4.67 \cdot 10^{-2}$	465.9	0	0	467	466
$2.3 \cdot 10^{-3}$	1.03	$5.14 \cdot 10^{-2}$	380.6	0	0	381.7	380.7
$2.47 \cdot 10^{-3}$	0.99	$5.64 \cdot 10^{-2}$	310.6	0	0	311.7	310.7
$2.47 \cdot 10^{-3}$	0.99	$5.64 \cdot 10^{-2}$	316.2	0	0	317.2	316.2
$2.64 \cdot 10^{-3}$	0.95	$6.12 \cdot 10^{-2}$	261.4	0	0	262.4	261.4
$2.82 \cdot 10^{-3}$	0.91	$6.62 \cdot 10^{-2}$	215.9	0	0	216.8	215.9
$2.82 \cdot 10^{-3}$	0.91	$6.62 \cdot 10^{-2}$	218.8	0	0	219.8	218.8
$3 \cdot 10^{-3}$	0.87	$7.1 \cdot 10^{-2}$	183.5	0	0	184.4	183.5
$3.61 \cdot 10^{-3}$	0.74	$8.58 \cdot 10^{-2}$	106.9	0	0	107.7	107
$3.61 \cdot 10^{-3}$	0.74	$8.58 \cdot 10^{-2}$	110.1	0	0	111	110.2
$4 \cdot 10^{-3}$	0.68	$9.42 \cdot 10^{-2}$	81.18	0	0	81.95	81.28
$5 \cdot 10^{-3}$	0.53	0.11	41.78	0	0	42.42	41.89
$6 \cdot 10^{-3}$	0.43	0.12	24.11	0	0	24.67	24.24
$8 \cdot 10^{-3}$	0.3	0.14	10.02	0	0	10.46	10.16
$1 \cdot 10^{-2}$	0.22	0.15	5.03	0	0	5.4	5.18
$1.5 \cdot 10^{-2}$	0.13	0.17	1.41	0	0	1.71	1.58
$2 \cdot 10^{-2}$	$8.65 \cdot 10^{-2}$	0.18	0.56	0	0	0.83	0.74
$3 \cdot 10^{-2}$	$4.57 \cdot 10^{-2}$	0.18	0.15	0	0	0.38	0.33
$4 \cdot 10^{-2}$	$2.8 \cdot 10^{-2}$	0.18	$5.99 \cdot 10^{-2}$	0	0	0.27	0.24
$5 \cdot 10^{-2}$	$1.89 \cdot 10^{-2}$	0.18	$2.89 \cdot 10^{-2}$	0	0	0.23	0.21
$6 \cdot 10^{-2}$	$1.36 \cdot 10^{-2}$	0.18	$1.59 \cdot 10^{-2}$	0	0	0.2	0.19
$8 \cdot 10^{-2}$	$7.96 \cdot 10^{-3}$	0.17	$6.19 \cdot 10^{-3}$	0	0	0.18	0.17
0.1	$5.22 \cdot 10^{-3}$	0.16	$2.98 \cdot 10^{-3}$	0	0	0.17	0.16
0.15	$2.38 \cdot 10^{-3}$	0.15	$7.93 \cdot 10^{-4}$	0	0	0.15	0.15
0.2	$1.35 \cdot 10^{-3}$	0.13	$3.15 \cdot 10^{-4}$	0	0	0.14	0.13
0.3	$6.06 \cdot 10^{-4}$	0.12	$8.95 \cdot 10^{-5}$	0	0	0.12	0.12
0.4	$3.42 \cdot 10^{-4}$	0.1	$3.84 \cdot 10^{-5}$	0	0	0.11	0.1
0.5	$2.19 \cdot 10^{-4}$	$9.57 \cdot 10^{-2}$	$2.08 \cdot 10^{-5}$	0	0	$9.6 \cdot 10^{-2}$	$9.58 \cdot 10^{-2}$
0.6	$1.52 \cdot 10^{-4}$	$8.86 \cdot 10^{-2}$	$1.29 \cdot 10^{-5}$	0	0	$8.87 \cdot 10^{-2}$	$8.86 \cdot 10^{-2}$
0.8	$8.58 \cdot 10^{-5}$	$7.78 \cdot 10^{-2}$	$6.53 \cdot 10^{-6}$	0	0	$7.79 \cdot 10^{-2}$	$7.78 \cdot 10^{-2}$
1	$5.49 \cdot 10^{-5}$	$7 \cdot 10^{-2}$	$4.06 \cdot 10^{-6}$	0	0	$7.01 \cdot 10^{-2}$	$7 \cdot 10^{-2}$
1.02	$5.26 \cdot 10^{-5}$	$6.93 \cdot 10^{-2}$	$3.8 \cdot 10^{-6}$	0	0	$6.93 \cdot 10^{-2}$	$6.93 \cdot 10^{-2}$
1.25	$3.52 \cdot 10^{-5}$	$6.26 \cdot 10^{-2}$	$2.58 \cdot 10^{-6}$	$1.74 \cdot 10^{-5}$	0	$6.27 \cdot 10^{-2}$	$6.26 \cdot 10^{-2}$
1.5	$2.44 \cdot 10^{-5}$	$5.69 \cdot 10^{-2}$	$1.87 \cdot 10^{-6}$	$9.62 \cdot 10^{-5}$	0	$5.7 \cdot 10^{-2}$	$5.7 \cdot 10^{-2}$
2	$1.37 \cdot 10^{-5}$	$4.86 \cdot 10^{-2}$	$1.17 \cdot 10^{-6}$	$3.83 \cdot 10^{-4}$	0	$4.9 \cdot 10^{-2}$	$4.89 \cdot 10^{-2}$
2.04	$1.31 \cdot 10^{-5}$	$4.79 \cdot 10^{-2}$	$1.13 \cdot 10^{-6}$	$4.12 \cdot 10^{-4}$	0	$4.84 \cdot 10^{-2}$	$4.84 \cdot 10^{-2}$
3	$6.1 \cdot 10^{-6}$	$3.82 \cdot 10^{-2}$	$6.53 \cdot 10^{-7}$	$1.09 \cdot 10^{-3}$	$1.34 \cdot 10^{-5}$	$3.93 \cdot 10^{-2}$	$3.93 \cdot 10^{-2}$
4	$3.43 \cdot 10^{-6}$	$3.19 \cdot 10^{-2}$	$4.47 \cdot 10^{-7}$	$1.77 \cdot 10^{-3}$	$5.46 \cdot 10^{-5}$	$3.37 \cdot 10^{-2}$	$3.37 \cdot 10^{-2}$
5	$2.2 \cdot 10^{-6}$	$2.75 \cdot 10^{-2}$	$3.39 \cdot 10^{-7}$	$2.38 \cdot 10^{-3}$	$1.09 \cdot 10^{-4}$	$3 \cdot 10^{-2}$	$3 \cdot 10^{-2}$
6	$1.53 \cdot 10^{-6}$	$2.43 \cdot 10^{-2}$	$2.72 \cdot 10^{-7}$	$2.92 \cdot 10^{-3}$	$1.67 \cdot 10^{-4}$	$2.74 \cdot 10^{-2}$	$2.74 \cdot 10^{-2}$
7	$1.12 \cdot 10^{-6}$	$2.19 \cdot 10^{-2}$	$2.27 \cdot 10^{-7}$	$3.41 \cdot 10^{-3}$	$2.25 \cdot 10^{-4}$	$2.55 \cdot 10^{-2}$	$2.55 \cdot 10^{-2}$
8	$8.58 \cdot 10^{-7}$	$1.99 \cdot 10^{-2}$	$1.95 \cdot 10^{-7}$	$3.85 \cdot 10^{-3}$	$2.82 \cdot 10^{-4}$	$2.4 \cdot 10^{-2}$	$2.4 \cdot 10^{-2}$
9	$6.78 \cdot 10^{-7}$	$1.83 \cdot 10^{-2}$	$1.7 \cdot 10^{-7}$	$4.24 \cdot 10^{-3}$	$3.36 \cdot 10^{-4}$	$2.29 \cdot 10^{-2}$	$2.29 \cdot 10^{-2}$
10	$5.49 \cdot 10^{-7}$	$1.69 \cdot 10^{-2}$	$1.51 \cdot 10^{-7}$	$4.6 \cdot 10^{-3}$	$3.87 \cdot 10^{-4}$	$2.19 \cdot 10^{-2}$	$2.19 \cdot 10^{-2}$
11	$4.54 \cdot 10^{-7}$	$1.58 \cdot 10^{-2}$	$1.36 \cdot 10^{-7}$	$4.93 \cdot 10^{-3}$	$4.36 \cdot 10^{-4}$	$2.12 \cdot 10^{-2}$	$2.12 \cdot 10^{-2}$
12	$3.81 \cdot 10^{-7}$	$1.48 \cdot 10^{-2}$	$1.24 \cdot 10^{-7}$	$5.23 \cdot 10^{-3}$	$4.83 \cdot 10^{-4}$	$2.05 \cdot 10^{-2}$	$2.05 \cdot 10^{-2}$
13	$3.25 \cdot 10^{-7}$	$1.4 \cdot 10^{-2}$	$1.13 \cdot 10^{-7}$	$5.51 \cdot 10^{-3}$	$5.27 \cdot 10^{-4}$	$2 \cdot 10^{-2}$	$2 \cdot 10^{-2}$
14	$2.8 \cdot 10^{-7}$	$1.32 \cdot 10^{-2}$	$1.05 \cdot 10^{-7}$	$5.77 \cdot 10^{-3}$	$5.68 \cdot 10^{-4}$	$1.96 \cdot 10^{-2}$	$1.96 \cdot 10^{-2}$
15	$2.44 \cdot 10^{-7}$	$1.25 \cdot 10^{-2}$	$9.72 \cdot 10^{-8}$	$6.01 \cdot 10^{-3}$	$6.08 \cdot 10^{-4}$	$1.92 \cdot 10^{-2}$	$1.92 \cdot 10^{-2}$
16	$2.15 \cdot 10^{-7}$	$1.19 \cdot 10^{-2}$	$9.07 \cdot 10^{-8}$	$6.24 \cdot 10^{-3}$	$6.46 \cdot 10^{-4}$	$1.88 \cdot 10^{-2}$	$1.88 \cdot 10^{-2}$
18	$1.7 \cdot 10^{-7}$	$1.09 \cdot 10^{-2}$	$8 \cdot 10^{-8}$	$6.66 \cdot 10^{-3}$	$7.16 \cdot 10^{-4}$	$1.83 \cdot 10^{-2}$	$1.83 \cdot 10^{-2}$
20	$1.37 \cdot 10^{-7}$	$1.01 \cdot 10^{-2}$	$7.15 \cdot 10^{-8}$	$7.04 \cdot 10^{-3}$	$7.81 \cdot 10^{-4}$	$1.79 \cdot 10^{-2}$	$1.79 \cdot 10^{-2}$
22	$1.14 \cdot 10^{-7}$	$9.35 \cdot 10^{-3}$	$6.47 \cdot 10^{-8}$	$7.38 \cdot 10^{-3}$	$8.4 \cdot 10^{-4}$	$1.76 \cdot 10^{-2}$	$1.76 \cdot 10^{-2}$
24	$9.54 \cdot 10^{-8}$	$8.74 \cdot 10^{-3}$	$5.9 \cdot 10^{-8}$	$7.69 \cdot 10^{-3}$	$8.95 \cdot 10^{-4}$	$1.73 \cdot 10^{-2}$	$1.73 \cdot 10^{-2}$
26	$8.13 \cdot 10^{-8}$	$8.2 \cdot 10^{-3}$	$5.43 \cdot 10^{-8}$	$7.98 \cdot 10^{-3}$	$9.46 \cdot 10^{-4}$	$1.71 \cdot 10^{-2}$	$1.71 \cdot 10^{-2}$
28	$7.01 \cdot 10^{-8}$	$7.74 \cdot 10^{-3}$	$5.02 \cdot 10^{-8}$	$8.24 \cdot 10^{-3}$	$9.94 \cdot 10^{-4}$	$1.7 \cdot 10^{-2}$	$1.7 \cdot 10^{-2}$
30	$6.1 \cdot 10^{-8}$	$7.33 \cdot 10^{-3}$	$4.67 \cdot 10^{-8}$	$8.48 \cdot 10^{-3}$	$1.04 \cdot 10^{-3}$	$1.69 \cdot 10^{-2}$	$1.69 \cdot 10^{-2}$
40	$3.43 \cdot 10^{-8}$	$5.82 \cdot 10^{-3}$	$3.47 \cdot 10^{-8}$	$9.48 \cdot 10^{-3}$	$1.23 \cdot 10^{-3}$	$1.65 \cdot 10^{-2}$	$1.65 \cdot 10^{-2}$

50	$2.2 \cdot 10^{-8}$	$4.86 \cdot 10^{-3}$	$2.76 \cdot 10^{-8}$	$1.02 \cdot 10^{-2}$	$1.37 \cdot 10^{-3}$	$1.65 \cdot 10^{-2}$	$1.65 \cdot 10^{-2}$
60	$1.53 \cdot 10^{-8}$	$4.19 \cdot 10^{-3}$	$2.29 \cdot 10^{-8}$	$1.08 \cdot 10^{-2}$	$1.49 \cdot 10^{-3}$	$1.65 \cdot 10^{-2}$	$1.65 \cdot 10^{-2}$
80	$8.58 \cdot 10^{-9}$	$3.3 \cdot 10^{-3}$	$1.71 \cdot 10^{-8}$	$1.17 \cdot 10^{-2}$	$1.68 \cdot 10^{-3}$	$1.67 \cdot 10^{-2}$	$1.67 \cdot 10^{-2}$
100	$5.49 \cdot 10^{-9}$	$2.74 \cdot 10^{-3}$	$1.36 \cdot 10^{-8}$	$1.24 \cdot 10^{-2}$	$1.82 \cdot 10^{-3}$	$1.7 \cdot 10^{-2}$	$1.7 \cdot 10^{-2}$
150	$2.44 \cdot 10^{-9}$	$1.95 \cdot 10^{-3}$	$9.06 \cdot 10^{-9}$	$1.35 \cdot 10^{-2}$	$2.06 \cdot 10^{-3}$	$1.75 \cdot 10^{-2}$	$1.75 \cdot 10^{-2}$
200	$1.37 \cdot 10^{-9}$	$1.53 \cdot 10^{-3}$	$6.78 \cdot 10^{-9}$	$1.42 \cdot 10^{-2}$	$2.22 \cdot 10^{-3}$	$1.8 \cdot 10^{-2}$	$1.8 \cdot 10^{-2}$
300	$6.1 \cdot 10^{-10}$	$1.09 \cdot 10^{-3}$	$4.51 \cdot 10^{-9}$	$1.5 \cdot 10^{-2}$	$2.43 \cdot 10^{-3}$	$1.85 \cdot 10^{-2}$	$1.85 \cdot 10^{-2}$
400	$3.43 \cdot 10^{-10}$	$8.5 \cdot 10^{-4}$	$3.38 \cdot 10^{-9}$	$1.55 \cdot 10^{-2}$	$2.56 \cdot 10^{-3}$	$1.89 \cdot 10^{-2}$	$1.89 \cdot 10^{-2}$
500	$2.2 \cdot 10^{-10}$	$7.03 \cdot 10^{-4}$	$2.7 \cdot 10^{-9}$	$1.58 \cdot 10^{-2}$	$2.65 \cdot 10^{-3}$	$1.92 \cdot 10^{-2}$	$1.92 \cdot 10^{-2}$
600	$1.53 \cdot 10^{-10}$	$6.02 \cdot 10^{-4}$	$2.25 \cdot 10^{-9}$	$1.61 \cdot 10^{-2}$	$2.72 \cdot 10^{-3}$	$1.94 \cdot 10^{-2}$	$1.94 \cdot 10^{-2}$
800	$8.58 \cdot 10^{-11}$	$4.7 \cdot 10^{-4}$	$1.69 \cdot 10^{-9}$	$1.64 \cdot 10^{-2}$	$2.81 \cdot 10^{-3}$	$1.97 \cdot 10^{-2}$	$1.97 \cdot 10^{-2}$
1,000	$5.49 \cdot 10^{-11}$	$3.87 \cdot 10^{-4}$	$1.35 \cdot 10^{-9}$	$1.66 \cdot 10^{-2}$	$2.88 \cdot 10^{-3}$	$1.98 \cdot 10^{-2}$	$1.98 \cdot 10^{-2}$
1,500	$2.44 \cdot 10^{-11}$	$2.7 \cdot 10^{-4}$	$8.99 \cdot 10^{-10}$	$1.69 \cdot 10^{-2}$	$2.97 \cdot 10^{-3}$	$2.01 \cdot 10^{-2}$	$2.01 \cdot 10^{-2}$
2,000	$1.37 \cdot 10^{-11}$	$2.09 \cdot 10^{-4}$	$6.74 \cdot 10^{-10}$	$1.7 \cdot 10^{-2}$	$3.03 \cdot 10^{-3}$	$2.03 \cdot 10^{-2}$	$2.03 \cdot 10^{-2}$
3,000	$6.1 \cdot 10^{-12}$	$1.45 \cdot 10^{-4}$	$4.49 \cdot 10^{-10}$	$1.72 \cdot 10^{-2}$	$3.09 \cdot 10^{-3}$	$2.05 \cdot 10^{-2}$	$2.05 \cdot 10^{-2}$
4,000	$3.43 \cdot 10^{-12}$	$1.12 \cdot 10^{-4}$	$3.37 \cdot 10^{-10}$	$1.73 \cdot 10^{-2}$	$3.12 \cdot 10^{-3}$	$2.05 \cdot 10^{-2}$	$2.05 \cdot 10^{-2}$
5,000	$2.2 \cdot 10^{-12}$	$9.18 \cdot 10^{-5}$	$2.7 \cdot 10^{-10}$	$1.74 \cdot 10^{-2}$	$3.15 \cdot 10^{-3}$	$2.06 \cdot 10^{-2}$	$2.06 \cdot 10^{-2}$
6,000	$1.53 \cdot 10^{-12}$	$7.78 \cdot 10^{-5}$	$2.25 \cdot 10^{-10}$	$1.74 \cdot 10^{-2}$	$3.16 \cdot 10^{-3}$	$2.07 \cdot 10^{-2}$	$2.07 \cdot 10^{-2}$
8,000	$8.58 \cdot 10^{-13}$	$6 \cdot 10^{-5}$	$1.69 \cdot 10^{-10}$	$1.75 \cdot 10^{-2}$	$3.18 \cdot 10^{-3}$	$2.07 \cdot 10^{-2}$	$2.07 \cdot 10^{-2}$
10,000	$5.49 \cdot 10^{-13}$	$4.89 \cdot 10^{-5}$	$1.35 \cdot 10^{-10}$	$1.75 \cdot 10^{-2}$	$3.2 \cdot 10^{-3}$	$2.07 \cdot 10^{-2}$	$2.07 \cdot 10^{-2}$
15,000	$2.44 \cdot 10^{-13}$	$3.38 \cdot 10^{-5}$	$8.98 \cdot 10^{-11}$	$1.76 \cdot 10^{-2}$	$3.21 \cdot 10^{-3}$	$2.08 \cdot 10^{-2}$	$2.08 \cdot 10^{-2}$
20,000	$1.37 \cdot 10^{-13}$	$2.6 \cdot 10^{-5}$	$6.74 \cdot 10^{-11}$	$1.76 \cdot 10^{-2}$	$3.22 \cdot 10^{-3}$	$2.08 \cdot 10^{-2}$	$2.08 \cdot 10^{-2}$
30,000	$6.1 \cdot 10^{-14}$	$1.79 \cdot 10^{-5}$	$4.49 \cdot 10^{-11}$	$1.76 \cdot 10^{-2}$	$3.23 \cdot 10^{-3}$	$2.09 \cdot 10^{-2}$	$2.09 \cdot 10^{-2}$
40,000	$3.43 \cdot 10^{-14}$	$1.38 \cdot 10^{-5}$	$3.37 \cdot 10^{-11}$	$1.76 \cdot 10^{-2}$	$3.24 \cdot 10^{-3}$	$2.09 \cdot 10^{-2}$	$2.09 \cdot 10^{-2}$
50,000	$2.2 \cdot 10^{-14}$	$1.12 \cdot 10^{-5}$	$2.7 \cdot 10^{-11}$	$1.76 \cdot 10^{-2}$	$3.24 \cdot 10^{-3}$	$2.09 \cdot 10^{-2}$	$2.09 \cdot 10^{-2}$
60,000	$1.53 \cdot 10^{-14}$	$9.48 \cdot 10^{-6}$	$2.25 \cdot 10^{-11}$	$1.76 \cdot 10^{-2}$	$3.25 \cdot 10^{-3}$	$2.09 \cdot 10^{-2}$	$2.09 \cdot 10^{-2}$
80,000	$8.58 \cdot 10^{-15}$	$7.27 \cdot 10^{-6}$	$1.68 \cdot 10^{-11}$	$1.76 \cdot 10^{-2}$	$3.25 \cdot 10^{-3}$	$2.09 \cdot 10^{-2}$	$2.09 \cdot 10^{-2}$
$1 \cdot 10^5$	$5.49 \cdot 10^{-15}$	$5.91 \cdot 10^{-6}$	$1.35 \cdot 10^{-11}$	$1.77 \cdot 10^{-2}$	$3.25 \cdot 10^{-3}$	$2.09 \cdot 10^{-2}$	$2.09 \cdot 10^{-2}$

A.6 Lung

PE	SC	SI	PEA	PNF	PEF	TAWCS	TAOCS
$1 \cdot 10^{-3}$	1.35	$1.34 \cdot 10^{-2}$	3,802	0	0	3,804	3,802
$1.04 \cdot 10^{-3}$	1.34	$1.42 \cdot 10^{-2}$	3,465	0	0	3,467	3,465
$1.07 \cdot 10^{-3}$	1.33	$1.51 \cdot 10^{-2}$	3,158	0	0	3,160	3,158
$1.07 \cdot 10^{-3}$	1.33	$1.51 \cdot 10^{-2}$	3,170	0	0	3,171	3,170
$1.5 \cdot 10^{-3}$	1.24	$2.7 \cdot 10^{-2}$	1,283	0	0	1,284	1,283
$2 \cdot 10^{-3}$	1.12	$4.2 \cdot 10^{-2}$	573.7	0	0	574.9	573.8
$2.15 \cdot 10^{-3}$	1.08	$4.64 \cdot 10^{-2}$	469.8	0	0	470.9	469.9
$2.3 \cdot 10^{-3}$	1.04	$5.12 \cdot 10^{-2}$	387.4	0	0	388.5	387.5
$2.47 \cdot 10^{-3}$	1	$5.61 \cdot 10^{-2}$	316.1	0	0	317.2	316.2
$2.47 \cdot 10^{-3}$	1	$5.61 \cdot 10^{-2}$	321.7	0	0	322.8	321.8
$2.64 \cdot 10^{-3}$	0.96	$6.1 \cdot 10^{-2}$	265.9	0	0	266.9	266
$2.82 \cdot 10^{-3}$	0.92	$6.6 \cdot 10^{-2}$	219.6	0	0	220.6	219.7
$2.82 \cdot 10^{-3}$	0.92	$6.6 \cdot 10^{-2}$	222.5	0	0	223.5	222.6
$3 \cdot 10^{-3}$	0.88	$7.07 \cdot 10^{-2}$	186.6	0	0	187.5	186.6
$3.61 \cdot 10^{-3}$	0.76	$8.56 \cdot 10^{-2}$	108.7	0	0	109.6	108.8
$3.61 \cdot 10^{-3}$	0.76	$8.56 \cdot 10^{-2}$	111.9	0	0	112.8	112
$4 \cdot 10^{-3}$	0.68	$9.4 \cdot 10^{-2}$	82.5	0	0	83.28	82.59
$5 \cdot 10^{-3}$	0.54	0.11	42.45	0	0	43.1	42.56
$6 \cdot 10^{-3}$	0.44	0.12	24.49	0	0	25.05	24.62
$8 \cdot 10^{-3}$	0.3	0.14	10.17	0	0	10.62	10.32
$1 \cdot 10^{-2}$	0.23	0.15	5.1	0	0	5.48	5.26
$1.5 \cdot 10^{-2}$	0.13	0.17	1.43	0	0	1.73	1.6
$2 \cdot 10^{-2}$	$8.74 \cdot 10^{-2}$	0.18	0.57	0	0	0.84	0.75
$3 \cdot 10^{-2}$	$4.62 \cdot 10^{-2}$	0.18	0.15	0	0	0.38	0.34
$4 \cdot 10^{-2}$	$2.83 \cdot 10^{-2}$	0.18	$6.08 \cdot 10^{-2}$	0	0	0.27	0.24
$5 \cdot 10^{-2}$	$1.91 \cdot 10^{-2}$	0.18	$2.93 \cdot 10^{-2}$	0	0	0.23	0.21
$6 \cdot 10^{-2}$	$1.37 \cdot 10^{-2}$	0.18	$1.61 \cdot 10^{-2}$	0	0	0.21	0.19
$8 \cdot 10^{-2}$	$8.05 \cdot 10^{-3}$	0.17	$6.27 \cdot 10^{-3}$	0	0	0.18	0.17
0.1	$5.28 \cdot 10^{-3}$	0.16	$3.01 \cdot 10^{-3}$	0	0	0.17	0.16
0.15	$2.41 \cdot 10^{-3}$	0.15	$8.03 \cdot 10^{-4}$	0	0	0.15	0.15
0.2	$1.37 \cdot 10^{-3}$	0.13	$3.19 \cdot 10^{-4}$	0	0	0.14	0.13
0.3	$6.13 \cdot 10^{-4}$	0.12	$9.05 \cdot 10^{-5}$	0	0	0.12	0.12
0.4	$3.46 \cdot 10^{-4}$	0.1	$3.89 \cdot 10^{-5}$	0	0	0.11	0.1
0.5	$2.22 \cdot 10^{-4}$	$9.58 \cdot 10^{-2}$	$2.1 \cdot 10^{-5}$	0	0	$9.61 \cdot 10^{-2}$	$9.59 \cdot 10^{-2}$
0.6	$1.54 \cdot 10^{-4}$	$8.87 \cdot 10^{-2}$	$1.31 \cdot 10^{-5}$	0	0	$8.88 \cdot 10^{-2}$	$8.87 \cdot 10^{-2}$
0.8	$8.68 \cdot 10^{-5}$	$7.79 \cdot 10^{-2}$	$6.61 \cdot 10^{-6}$	0	0	$7.8 \cdot 10^{-2}$	$7.79 \cdot 10^{-2}$
1	$5.55 \cdot 10^{-5}$	$7.01 \cdot 10^{-2}$	$4.11 \cdot 10^{-6}$	0	0	$7.01 \cdot 10^{-2}$	$7.01 \cdot 10^{-2}$
1.02	$5.32 \cdot 10^{-5}$	$6.93 \cdot 10^{-2}$	$3.84 \cdot 10^{-6}$	0	0	$6.94 \cdot 10^{-2}$	$6.93 \cdot 10^{-2}$
1.25	$3.56 \cdot 10^{-5}$	$6.27 \cdot 10^{-2}$	$2.61 \cdot 10^{-6}$	$1.75 \cdot 10^{-5}$	0	$6.27 \cdot 10^{-2}$	$6.27 \cdot 10^{-2}$
1.5	$2.47 \cdot 10^{-5}$	$5.69 \cdot 10^{-2}$	$1.89 \cdot 10^{-6}$	$9.69 \cdot 10^{-5}$	0	$5.71 \cdot 10^{-2}$	$5.7 \cdot 10^{-2}$
2	$1.39 \cdot 10^{-5}$	$4.86 \cdot 10^{-2}$	$1.19 \cdot 10^{-6}$	$3.86 \cdot 10^{-4}$	0	$4.9 \cdot 10^{-2}$	$4.9 \cdot 10^{-2}$
2.04	$1.33 \cdot 10^{-5}$	$4.8 \cdot 10^{-2}$	$1.15 \cdot 10^{-6}$	$4.16 \cdot 10^{-4}$	0	$4.84 \cdot 10^{-2}$	$4.84 \cdot 10^{-2}$
3	$6.17 \cdot 10^{-6}$	$3.82 \cdot 10^{-2}$	$6.61 \cdot 10^{-7}$	$1.1 \cdot 10^{-3}$	$1.34 \cdot 10^{-5}$	$3.94 \cdot 10^{-2}$	$3.94 \cdot 10^{-2}$
4	$3.47 \cdot 10^{-6}$	$3.19 \cdot 10^{-2}$	$4.53 \cdot 10^{-7}$	$1.79 \cdot 10^{-3}$	$5.46 \cdot 10^{-5}$	$3.37 \cdot 10^{-2}$	$3.37 \cdot 10^{-2}$
5	$2.22 \cdot 10^{-6}$	$2.75 \cdot 10^{-2}$	$3.43 \cdot 10^{-7}$	$2.4 \cdot 10^{-3}$	$1.09 \cdot 10^{-4}$	$3.01 \cdot 10^{-2}$	$3.01 \cdot 10^{-2}$
6	$1.54 \cdot 10^{-6}$	$2.43 \cdot 10^{-2}$	$2.75 \cdot 10^{-7}$	$2.95 \cdot 10^{-3}$	$1.67 \cdot 10^{-4}$	$2.75 \cdot 10^{-2}$	$2.75 \cdot 10^{-2}$
7	$1.13 \cdot 10^{-6}$	$2.19 \cdot 10^{-2}$	$2.3 \cdot 10^{-7}$	$3.44 \cdot 10^{-3}$	$2.25 \cdot 10^{-4}$	$2.55 \cdot 10^{-2}$	$2.55 \cdot 10^{-2}$
8	$8.68 \cdot 10^{-7}$	$1.99 \cdot 10^{-2}$	$1.97 \cdot 10^{-7}$	$3.87 \cdot 10^{-3}$	$2.82 \cdot 10^{-4}$	$2.41 \cdot 10^{-2}$	$2.41 \cdot 10^{-2}$
9	$6.86 \cdot 10^{-7}$	$1.83 \cdot 10^{-2}$	$1.72 \cdot 10^{-7}$	$4.28 \cdot 10^{-3}$	$3.36 \cdot 10^{-4}$	$2.29 \cdot 10^{-2}$	$2.29 \cdot 10^{-2}$
10	$5.56 \cdot 10^{-7}$	$1.7 \cdot 10^{-2}$	$1.53 \cdot 10^{-7}$	$4.64 \cdot 10^{-3}$	$3.88 \cdot 10^{-4}$	$2.2 \cdot 10^{-2}$	$2.2 \cdot 10^{-2}$
11	$4.59 \cdot 10^{-7}$	$1.58 \cdot 10^{-2}$	$1.38 \cdot 10^{-7}$	$4.97 \cdot 10^{-3}$	$4.37 \cdot 10^{-4}$	$2.12 \cdot 10^{-2}$	$2.12 \cdot 10^{-2}$
12	$3.86 \cdot 10^{-7}$	$1.48 \cdot 10^{-2}$	$1.25 \cdot 10^{-7}$	$5.27 \cdot 10^{-3}$	$4.83 \cdot 10^{-4}$	$2.06 \cdot 10^{-2}$	$2.06 \cdot 10^{-2}$
13	$3.29 \cdot 10^{-7}$	$1.4 \cdot 10^{-2}$	$1.15 \cdot 10^{-7}$	$5.55 \cdot 10^{-3}$	$5.27 \cdot 10^{-4}$	$2.01 \cdot 10^{-2}$	$2.01 \cdot 10^{-2}$
14	$2.84 \cdot 10^{-7}$	$1.32 \cdot 10^{-2}$	$1.06 \cdot 10^{-7}$	$5.81 \cdot 10^{-3}$	$5.69 \cdot 10^{-4}$	$1.96 \cdot 10^{-2}$	$1.96 \cdot 10^{-2}$
15	$2.47 \cdot 10^{-7}$	$1.26 \cdot 10^{-2}$	$9.84 \cdot 10^{-8}$	$6.06 \cdot 10^{-3}$	$6.08 \cdot 10^{-4}$	$1.92 \cdot 10^{-2}$	$1.92 \cdot 10^{-2}$
16	$2.17 \cdot 10^{-7}$	$1.2 \cdot 10^{-2}$	$9.18 \cdot 10^{-8}$	$6.29 \cdot 10^{-3}$	$6.47 \cdot 10^{-4}$	$1.89 \cdot 10^{-2}$	$1.89 \cdot 10^{-2}$
18	$1.72 \cdot 10^{-7}$	$1.09 \cdot 10^{-2}$	$8.09 \cdot 10^{-8}$	$6.71 \cdot 10^{-3}$	$7.17 \cdot 10^{-4}$	$1.84 \cdot 10^{-2}$	$1.84 \cdot 10^{-2}$
20	$1.39 \cdot 10^{-7}$	$1.01 \cdot 10^{-2}$	$7.24 \cdot 10^{-8}$	$7.09 \cdot 10^{-3}$	$7.81 \cdot 10^{-4}$	$1.8 \cdot 10^{-2}$	$1.8 \cdot 10^{-2}$
22	$1.15 \cdot 10^{-7}$	$9.36 \cdot 10^{-3}$	$6.55 \cdot 10^{-8}$	$7.44 \cdot 10^{-3}$	$8.41 \cdot 10^{-4}$	$1.76 \cdot 10^{-2}$	$1.76 \cdot 10^{-2}$
24	$9.65 \cdot 10^{-8}$	$8.74 \cdot 10^{-3}$	$5.97 \cdot 10^{-8}$	$7.75 \cdot 10^{-3}$	$8.96 \cdot 10^{-4}$	$1.74 \cdot 10^{-2}$	$1.74 \cdot 10^{-2}$
26	$8.22 \cdot 10^{-8}$	$8.21 \cdot 10^{-3}$	$5.49 \cdot 10^{-8}$	$8.03 \cdot 10^{-3}$	$9.47 \cdot 10^{-4}$	$1.72 \cdot 10^{-2}$	$1.72 \cdot 10^{-2}$
28	$7.09 \cdot 10^{-8}$	$7.75 \cdot 10^{-3}$	$5.08 \cdot 10^{-8}$	$8.3 \cdot 10^{-3}$	$9.95 \cdot 10^{-4}$	$1.7 \cdot 10^{-2}$	$1.7 \cdot 10^{-2}$
30	$6.18 \cdot 10^{-8}$	$7.33 \cdot 10^{-3}$	$4.73 \cdot 10^{-8}$	$8.55 \cdot 10^{-3}$	$1.04 \cdot 10^{-3}$	$1.69 \cdot 10^{-2}$	$1.69 \cdot 10^{-2}$
40	$3.47 \cdot 10^{-8}$	$5.83 \cdot 10^{-3}$	$3.51 \cdot 10^{-8}$	$9.55 \cdot 10^{-3}$	$1.23 \cdot 10^{-3}$	$1.66 \cdot 10^{-2}$	$1.66 \cdot 10^{-2}$
50	$2.22 \cdot 10^{-8}$	$4.87 \cdot 10^{-3}$	$2.8 \cdot 10^{-8}$	$1.03 \cdot 10^{-2}$	$1.37 \cdot 10^{-3}$	$1.66 \cdot 10^{-2}$	$1.66 \cdot 10^{-2}$

60	$1.54 \cdot 10^{-8}$	$4.19 \cdot 10^{-3}$	$2.32 \cdot 10^{-8}$	$1.09 \cdot 10^{-2}$	$1.49 \cdot 10^{-3}$	$1.66 \cdot 10^{-2}$	$1.66 \cdot 10^{-2}$
80	$8.68 \cdot 10^{-9}$	$3.31 \cdot 10^{-3}$	$1.73 \cdot 10^{-8}$	$1.18 \cdot 10^{-2}$	$1.68 \cdot 10^{-3}$	$1.68 \cdot 10^{-2}$	$1.68 \cdot 10^{-2}$
100	$5.56 \cdot 10^{-9}$	$2.74 \cdot 10^{-3}$	$1.38 \cdot 10^{-8}$	$1.25 \cdot 10^{-2}$	$1.82 \cdot 10^{-3}$	$1.71 \cdot 10^{-2}$	$1.71 \cdot 10^{-2}$
150	$2.47 \cdot 10^{-9}$	$1.95 \cdot 10^{-3}$	$9.17 \cdot 10^{-9}$	$1.36 \cdot 10^{-2}$	$2.06 \cdot 10^{-3}$	$1.76 \cdot 10^{-2}$	$1.76 \cdot 10^{-2}$
200	$1.39 \cdot 10^{-9}$	$1.53 \cdot 10^{-3}$	$6.86 \cdot 10^{-9}$	$1.43 \cdot 10^{-2}$	$2.23 \cdot 10^{-3}$	$1.81 \cdot 10^{-2}$	$1.81 \cdot 10^{-2}$
300	$6.17 \cdot 10^{-10}$	$1.09 \cdot 10^{-3}$	$4.57 \cdot 10^{-9}$	$1.51 \cdot 10^{-2}$	$2.43 \cdot 10^{-3}$	$1.87 \cdot 10^{-2}$	$1.87 \cdot 10^{-2}$
400	$3.47 \cdot 10^{-10}$	$8.5 \cdot 10^{-4}$	$3.42 \cdot 10^{-9}$	$1.56 \cdot 10^{-2}$	$2.56 \cdot 10^{-3}$	$1.9 \cdot 10^{-2}$	$1.9 \cdot 10^{-2}$
500	$2.22 \cdot 10^{-10}$	$7.04 \cdot 10^{-4}$	$2.74 \cdot 10^{-9}$	$1.59 \cdot 10^{-2}$	$2.65 \cdot 10^{-3}$	$1.93 \cdot 10^{-2}$	$1.93 \cdot 10^{-2}$
600	$1.54 \cdot 10^{-10}$	$6.03 \cdot 10^{-4}$	$2.28 \cdot 10^{-9}$	$1.62 \cdot 10^{-2}$	$2.72 \cdot 10^{-3}$	$1.95 \cdot 10^{-2}$	$1.95 \cdot 10^{-2}$
800	$8.68 \cdot 10^{-11}$	$4.71 \cdot 10^{-4}$	$1.71 \cdot 10^{-9}$	$1.65 \cdot 10^{-2}$	$2.82 \cdot 10^{-3}$	$1.98 \cdot 10^{-2}$	$1.98 \cdot 10^{-2}$
1,000	$5.56 \cdot 10^{-11}$	$3.87 \cdot 10^{-4}$	$1.37 \cdot 10^{-9}$	$1.67 \cdot 10^{-2}$	$2.88 \cdot 10^{-3}$	$2 \cdot 10^{-2}$	$2 \cdot 10^{-2}$
1,500	$2.47 \cdot 10^{-11}$	$2.71 \cdot 10^{-4}$	$9.1 \cdot 10^{-10}$	$1.7 \cdot 10^{-2}$	$2.98 \cdot 10^{-3}$	$2.02 \cdot 10^{-2}$	$2.02 \cdot 10^{-2}$
2,000	$1.39 \cdot 10^{-11}$	$2.09 \cdot 10^{-4}$	$6.83 \cdot 10^{-10}$	$1.72 \cdot 10^{-2}$	$3.03 \cdot 10^{-3}$	$2.04 \cdot 10^{-2}$	$2.04 \cdot 10^{-2}$
3,000	$6.17 \cdot 10^{-12}$	$1.46 \cdot 10^{-4}$	$4.55 \cdot 10^{-10}$	$1.73 \cdot 10^{-2}$	$3.09 \cdot 10^{-3}$	$2.06 \cdot 10^{-2}$	$2.06 \cdot 10^{-2}$
4,000	$3.47 \cdot 10^{-12}$	$1.12 \cdot 10^{-4}$	$3.41 \cdot 10^{-10}$	$1.74 \cdot 10^{-2}$	$3.13 \cdot 10^{-3}$	$2.07 \cdot 10^{-2}$	$2.07 \cdot 10^{-2}$
5,000	$2.22 \cdot 10^{-12}$	$9.19 \cdot 10^{-5}$	$2.73 \cdot 10^{-10}$	$1.75 \cdot 10^{-2}$	$3.15 \cdot 10^{-3}$	$2.07 \cdot 10^{-2}$	$2.07 \cdot 10^{-2}$
6,000	$1.54 \cdot 10^{-12}$	$7.79 \cdot 10^{-5}$	$2.27 \cdot 10^{-10}$	$1.75 \cdot 10^{-2}$	$3.16 \cdot 10^{-3}$	$2.08 \cdot 10^{-2}$	$2.08 \cdot 10^{-2}$
8,000	$8.68 \cdot 10^{-13}$	$6 \cdot 10^{-5}$	$1.71 \cdot 10^{-10}$	$1.76 \cdot 10^{-2}$	$3.18 \cdot 10^{-3}$	$2.08 \cdot 10^{-2}$	$2.08 \cdot 10^{-2}$
10,000	$5.56 \cdot 10^{-13}$	$4.9 \cdot 10^{-5}$	$1.36 \cdot 10^{-10}$	$1.76 \cdot 10^{-2}$	$3.2 \cdot 10^{-3}$	$2.09 \cdot 10^{-2}$	$2.09 \cdot 10^{-2}$
15,000	$2.47 \cdot 10^{-13}$	$3.39 \cdot 10^{-5}$	$9.1 \cdot 10^{-11}$	$1.77 \cdot 10^{-2}$	$3.22 \cdot 10^{-3}$	$2.09 \cdot 10^{-2}$	$2.09 \cdot 10^{-2}$
20,000	$1.39 \cdot 10^{-13}$	$2.6 \cdot 10^{-5}$	$6.82 \cdot 10^{-11}$	$1.77 \cdot 10^{-2}$	$3.23 \cdot 10^{-3}$	$2.1 \cdot 10^{-2}$	$2.1 \cdot 10^{-2}$
30,000	$6.17 \cdot 10^{-14}$	$1.8 \cdot 10^{-5}$	$4.55 \cdot 10^{-11}$	$1.77 \cdot 10^{-2}$	$3.24 \cdot 10^{-3}$	$2.1 \cdot 10^{-2}$	$2.1 \cdot 10^{-2}$
40,000	$3.47 \cdot 10^{-14}$	$1.38 \cdot 10^{-5}$	$3.41 \cdot 10^{-11}$	$1.77 \cdot 10^{-2}$	$3.24 \cdot 10^{-3}$	$2.1 \cdot 10^{-2}$	$2.1 \cdot 10^{-2}$
50,000	$2.22 \cdot 10^{-14}$	$1.12 \cdot 10^{-5}$	$2.73 \cdot 10^{-11}$	$1.78 \cdot 10^{-2}$	$3.25 \cdot 10^{-3}$	$2.1 \cdot 10^{-2}$	$2.1 \cdot 10^{-2}$
60,000	$1.54 \cdot 10^{-14}$	$9.49 \cdot 10^{-6}$	$2.27 \cdot 10^{-11}$	$1.78 \cdot 10^{-2}$	$3.25 \cdot 10^{-3}$	$2.1 \cdot 10^{-2}$	$2.1 \cdot 10^{-2}$
80,000	$8.68 \cdot 10^{-15}$	$7.28 \cdot 10^{-6}$	$1.71 \cdot 10^{-11}$	$1.78 \cdot 10^{-2}$	$3.25 \cdot 10^{-3}$	$2.1 \cdot 10^{-2}$	$2.1 \cdot 10^{-2}$
$1 \cdot 10^5$	$5.56 \cdot 10^{-15}$	$5.92 \cdot 10^{-6}$	$1.36 \cdot 10^{-11}$	$1.78 \cdot 10^{-2}$	$3.25 \cdot 10^{-3}$	$2.1 \cdot 10^{-2}$	$2.1 \cdot 10^{-2}$

A.7 Muscle

PE	SC	SI	PEA	PNF	PEF	TAWCS	TAOCS
$1 \cdot 10^{-3}$	1.33	$1.35 \cdot 10^{-2}$	3,718	0	0	3,719	3,718
$1.04 \cdot 10^{-3}$	1.32	$1.43 \cdot 10^{-2}$	3,388	0	0	3,389	3,388
$1.07 \cdot 10^{-3}$	1.32	$1.53 \cdot 10^{-2}$	3,087	0	0	3,089	3,087
$1.07 \cdot 10^{-3}$	1.32	$1.53 \cdot 10^{-2}$	3,093	0	0	3,094	3,093
$1.5 \cdot 10^{-3}$	1.23	$2.72 \cdot 10^{-2}$	1,249	0	0	1,250	1,249
$2 \cdot 10^{-3}$	1.1	$4.23 \cdot 10^{-2}$	558.3	0	0	559.4	558.3
$2.15 \cdot 10^{-3}$	1.07	$4.67 \cdot 10^{-2}$	457	0	0	458.2	457.1
$2.15 \cdot 10^{-3}$	1.07	$4.67 \cdot 10^{-2}$	461.5	0	0	462.6	461.5
$2.3 \cdot 10^{-3}$	1.03	$5.15 \cdot 10^{-2}$	376.9	0	0	378	377
$2.47 \cdot 10^{-3}$	0.99	$5.64 \cdot 10^{-2}$	307.5	0	0	308.5	307.6
$2.47 \cdot 10^{-3}$	0.99	$5.64 \cdot 10^{-2}$	313.1	0	0	314.1	313.1
$2.64 \cdot 10^{-3}$	0.95	$6.13 \cdot 10^{-2}$	258.7	0	0	259.7	258.8
$2.82 \cdot 10^{-3}$	0.91	$6.63 \cdot 10^{-2}$	213.6	0	0	214.6	213.7
$2.82 \cdot 10^{-3}$	0.91	$6.63 \cdot 10^{-2}$	215.1	0	0	216.1	215.1
$3 \cdot 10^{-3}$	0.87	$7.11 \cdot 10^{-2}$	180.2	0	0	181.2	180.3
$3.61 \cdot 10^{-3}$	0.74	$8.59 \cdot 10^{-2}$	104.9	0	0	105.7	105
$3.61 \cdot 10^{-3}$	0.74	$8.59 \cdot 10^{-2}$	109.2	0	0	110	109.3
$4 \cdot 10^{-3}$	0.67	$9.43 \cdot 10^{-2}$	80.49	0	0	81.26	80.59
$5 \cdot 10^{-3}$	0.53	0.11	41.42	0	0	42.06	41.53
$6 \cdot 10^{-3}$	0.43	0.13	23.9	0	0	24.46	24.03
$8 \cdot 10^{-3}$	0.3	0.14	9.93	0	0	10.37	10.07
$1 \cdot 10^{-2}$	0.22	0.15	4.98	0	0	5.36	5.14
$1.5 \cdot 10^{-2}$	0.13	0.17	1.4	0	0	1.69	1.56
$2 \cdot 10^{-2}$	$8.61 \cdot 10^{-2}$	0.18	0.56	0	0	0.82	0.73
$3 \cdot 10^{-2}$	$4.55 \cdot 10^{-2}$	0.18	0.15	0	0	0.38	0.33
$4 \cdot 10^{-2}$	$2.79 \cdot 10^{-2}$	0.18	$5.94 \cdot 10^{-2}$	0	0	0.27	0.24
$5 \cdot 10^{-2}$	$1.88 \cdot 10^{-2}$	0.18	$2.87 \cdot 10^{-2}$	0	0	0.23	0.21
$6 \cdot 10^{-2}$	$1.35 \cdot 10^{-2}$	0.18	$1.58 \cdot 10^{-2}$	0	0	0.2	0.19
$8 \cdot 10^{-2}$	$7.92 \cdot 10^{-3}$	0.17	$6.14 \cdot 10^{-3}$	0	0	0.18	0.17
0.1	$5.19 \cdot 10^{-3}$	0.16	$2.95 \cdot 10^{-3}$	0	0	0.17	0.16
0.15	$2.37 \cdot 10^{-3}$	0.15	$7.87 \cdot 10^{-4}$	0	0	0.15	0.15
0.2	$1.35 \cdot 10^{-3}$	0.13	$3.13 \cdot 10^{-4}$	0	0	0.14	0.13
0.3	$6.03 \cdot 10^{-4}$	0.12	$8.88 \cdot 10^{-5}$	0	0	0.12	0.12
0.4	$3.4 \cdot 10^{-4}$	0.1	$3.81 \cdot 10^{-5}$	0	0	0.11	0.1
0.5	$2.18 \cdot 10^{-4}$	$9.58 \cdot 10^{-2}$	$2.06 \cdot 10^{-5}$	0	0	$9.6 \cdot 10^{-2}$	$9.58 \cdot 10^{-2}$
0.6	$1.52 \cdot 10^{-4}$	$8.86 \cdot 10^{-2}$	$1.28 \cdot 10^{-5}$	0	0	$8.87 \cdot 10^{-2}$	$8.86 \cdot 10^{-2}$
0.8	$8.53 \cdot 10^{-5}$	$7.78 \cdot 10^{-2}$	$6.49 \cdot 10^{-6}$	0	0	$7.79 \cdot 10^{-2}$	$7.79 \cdot 10^{-2}$
1	$5.46 \cdot 10^{-5}$	$7 \cdot 10^{-2}$	$4.03 \cdot 10^{-6}$	0	0	$7.01 \cdot 10^{-2}$	$7 \cdot 10^{-2}$
1.02	$5.23 \cdot 10^{-5}$	$6.93 \cdot 10^{-2}$	$3.77 \cdot 10^{-6}$	0	0	$6.93 \cdot 10^{-2}$	$6.93 \cdot 10^{-2}$
1.25	$3.5 \cdot 10^{-5}$	$6.26 \cdot 10^{-2}$	$2.56 \cdot 10^{-6}$	$1.74 \cdot 10^{-5}$	0	$6.27 \cdot 10^{-2}$	$6.26 \cdot 10^{-2}$
1.5	$2.43 \cdot 10^{-5}$	$5.69 \cdot 10^{-2}$	$1.85 \cdot 10^{-6}$	$9.59 \cdot 10^{-5}$	0	$5.7 \cdot 10^{-2}$	$5.7 \cdot 10^{-2}$
2	$1.37 \cdot 10^{-5}$	$4.86 \cdot 10^{-2}$	$1.16 \cdot 10^{-6}$	$3.82 \cdot 10^{-4}$	0	$4.9 \cdot 10^{-2}$	$4.89 \cdot 10^{-2}$
2.04	$1.31 \cdot 10^{-5}$	$4.8 \cdot 10^{-2}$	$1.13 \cdot 10^{-6}$	$4.11 \cdot 10^{-4}$	0	$4.84 \cdot 10^{-2}$	$4.84 \cdot 10^{-2}$
3	$6.07 \cdot 10^{-6}$	$3.82 \cdot 10^{-2}$	$6.48 \cdot 10^{-7}$	$1.09 \cdot 10^{-3}$	$1.34 \cdot 10^{-5}$	$3.93 \cdot 10^{-2}$	$3.93 \cdot 10^{-2}$
4	$3.42 \cdot 10^{-6}$	$3.19 \cdot 10^{-2}$	$4.44 \cdot 10^{-7}$	$1.77 \cdot 10^{-3}$	$5.46 \cdot 10^{-5}$	$3.37 \cdot 10^{-2}$	$3.37 \cdot 10^{-2}$
5	$2.19 \cdot 10^{-6}$	$2.75 \cdot 10^{-2}$	$3.36 \cdot 10^{-7}$	$2.37 \cdot 10^{-3}$	$1.09 \cdot 10^{-4}$	$3 \cdot 10^{-2}$	$3 \cdot 10^{-2}$
6	$1.52 \cdot 10^{-6}$	$2.43 \cdot 10^{-2}$	$2.7 \cdot 10^{-7}$	$2.92 \cdot 10^{-3}$	$1.67 \cdot 10^{-4}$	$2.74 \cdot 10^{-2}$	$2.74 \cdot 10^{-2}$
7	$1.12 \cdot 10^{-6}$	$2.19 \cdot 10^{-2}$	$2.25 \cdot 10^{-7}$	$3.4 \cdot 10^{-3}$	$2.25 \cdot 10^{-4}$	$2.55 \cdot 10^{-2}$	$2.55 \cdot 10^{-2}$
8	$8.54 \cdot 10^{-7}$	$1.99 \cdot 10^{-2}$	$1.93 \cdot 10^{-7}$	$3.84 \cdot 10^{-3}$	$2.82 \cdot 10^{-4}$	$2.4 \cdot 10^{-2}$	$2.4 \cdot 10^{-2}$
9	$6.75 \cdot 10^{-7}$	$1.83 \cdot 10^{-2}$	$1.69 \cdot 10^{-7}$	$4.23 \cdot 10^{-3}$	$3.36 \cdot 10^{-4}$	$2.29 \cdot 10^{-2}$	$2.29 \cdot 10^{-2}$
10	$5.47 \cdot 10^{-7}$	$1.7 \cdot 10^{-2}$	$1.5 \cdot 10^{-7}$	$4.59 \cdot 10^{-3}$	$3.87 \cdot 10^{-4}$	$2.19 \cdot 10^{-2}$	$2.19 \cdot 10^{-2}$
11	$4.52 \cdot 10^{-7}$	$1.58 \cdot 10^{-2}$	$1.35 \cdot 10^{-7}$	$4.92 \cdot 10^{-3}$	$4.36 \cdot 10^{-4}$	$2.12 \cdot 10^{-2}$	$2.12 \cdot 10^{-2}$
12	$3.8 \cdot 10^{-7}$	$1.48 \cdot 10^{-2}$	$1.23 \cdot 10^{-7}$	$5.22 \cdot 10^{-3}$	$4.83 \cdot 10^{-4}$	$2.05 \cdot 10^{-2}$	$2.05 \cdot 10^{-2}$
13	$3.24 \cdot 10^{-7}$	$1.4 \cdot 10^{-2}$	$1.13 \cdot 10^{-7}$	$5.5 \cdot 10^{-3}$	$5.27 \cdot 10^{-4}$	$2 \cdot 10^{-2}$	$2 \cdot 10^{-2}$
14	$2.79 \cdot 10^{-7}$	$1.32 \cdot 10^{-2}$	$1.04 \cdot 10^{-7}$	$5.76 \cdot 10^{-3}$	$5.68 \cdot 10^{-4}$	$1.95 \cdot 10^{-2}$	$1.95 \cdot 10^{-2}$
15	$2.43 \cdot 10^{-7}$	$1.25 \cdot 10^{-2}$	$9.64 \cdot 10^{-8}$	$6 \cdot 10^{-3}$	$6.08 \cdot 10^{-4}$	$1.92 \cdot 10^{-2}$	$1.92 \cdot 10^{-2}$
16	$2.14 \cdot 10^{-7}$	$1.19 \cdot 10^{-2}$	$9 \cdot 10^{-8}$	$6.23 \cdot 10^{-3}$	$6.46 \cdot 10^{-4}$	$1.88 \cdot 10^{-2}$	$1.88 \cdot 10^{-2}$
18	$1.69 \cdot 10^{-7}$	$1.09 \cdot 10^{-2}$	$7.93 \cdot 10^{-8}$	$6.65 \cdot 10^{-3}$	$7.16 \cdot 10^{-4}$	$1.83 \cdot 10^{-2}$	$1.83 \cdot 10^{-2}$
20	$1.37 \cdot 10^{-7}$	$1.01 \cdot 10^{-2}$	$7.09 \cdot 10^{-8}$	$7.02 \cdot 10^{-3}$	$7.81 \cdot 10^{-4}$	$1.79 \cdot 10^{-2}$	$1.79 \cdot 10^{-2}$
22	$1.13 \cdot 10^{-7}$	$9.35 \cdot 10^{-3}$	$6.42 \cdot 10^{-8}$	$7.36 \cdot 10^{-3}$	$8.4 \cdot 10^{-4}$	$1.76 \cdot 10^{-2}$	$1.76 \cdot 10^{-2}$
24	$9.49 \cdot 10^{-8}$	$8.74 \cdot 10^{-3}$	$5.85 \cdot 10^{-8}$	$7.67 \cdot 10^{-3}$	$8.95 \cdot 10^{-4}$	$1.73 \cdot 10^{-2}$	$1.73 \cdot 10^{-2}$
26	$8.09 \cdot 10^{-8}$	$8.2 \cdot 10^{-3}$	$5.38 \cdot 10^{-8}$	$7.95 \cdot 10^{-3}$	$9.46 \cdot 10^{-4}$	$1.71 \cdot 10^{-2}$	$1.71 \cdot 10^{-2}$
28	$6.97 \cdot 10^{-8}$	$7.74 \cdot 10^{-3}$	$4.98 \cdot 10^{-8}$	$8.22 \cdot 10^{-3}$	$9.94 \cdot 10^{-4}$	$1.7 \cdot 10^{-2}$	$1.7 \cdot 10^{-2}$
30	$6.07 \cdot 10^{-8}$	$7.33 \cdot 10^{-3}$	$4.64 \cdot 10^{-8}$	$8.46 \cdot 10^{-3}$	$1.04 \cdot 10^{-3}$	$1.68 \cdot 10^{-2}$	$1.68 \cdot 10^{-2}$
40	$3.42 \cdot 10^{-8}$	$5.82 \cdot 10^{-3}$	$3.44 \cdot 10^{-8}$	$9.45 \cdot 10^{-3}$	$1.23 \cdot 10^{-3}$	$1.65 \cdot 10^{-2}$	$1.65 \cdot 10^{-2}$

50	$2.19 \cdot 10^{-8}$	$4.86 \cdot 10^{-3}$	$2.74 \cdot 10^{-8}$	$1.02 \cdot 10^{-2}$	$1.37 \cdot 10^{-3}$	$1.64 \cdot 10^{-2}$	$1.64 \cdot 10^{-2}$
60	$1.52 \cdot 10^{-8}$	$4.19 \cdot 10^{-3}$	$2.27 \cdot 10^{-8}$	$1.08 \cdot 10^{-2}$	$1.49 \cdot 10^{-3}$	$1.65 \cdot 10^{-2}$	$1.65 \cdot 10^{-2}$
80	$8.54 \cdot 10^{-9}$	$3.3 \cdot 10^{-3}$	$1.7 \cdot 10^{-8}$	$1.17 \cdot 10^{-2}$	$1.68 \cdot 10^{-3}$	$1.67 \cdot 10^{-2}$	$1.67 \cdot 10^{-2}$
100	$5.47 \cdot 10^{-9}$	$2.74 \cdot 10^{-3}$	$1.35 \cdot 10^{-8}$	$1.24 \cdot 10^{-2}$	$1.82 \cdot 10^{-3}$	$1.69 \cdot 10^{-2}$	$1.69 \cdot 10^{-2}$
150	$2.43 \cdot 10^{-9}$	$1.95 \cdot 10^{-3}$	$8.99 \cdot 10^{-9}$	$1.35 \cdot 10^{-2}$	$2.06 \cdot 10^{-3}$	$1.75 \cdot 10^{-2}$	$1.75 \cdot 10^{-2}$
200	$1.37 \cdot 10^{-9}$	$1.53 \cdot 10^{-3}$	$6.73 \cdot 10^{-9}$	$1.42 \cdot 10^{-2}$	$2.22 \cdot 10^{-3}$	$1.79 \cdot 10^{-2}$	$1.79 \cdot 10^{-2}$
300	$6.07 \cdot 10^{-10}$	$1.09 \cdot 10^{-3}$	$4.47 \cdot 10^{-9}$	$1.5 \cdot 10^{-2}$	$2.43 \cdot 10^{-3}$	$1.85 \cdot 10^{-2}$	$1.85 \cdot 10^{-2}$
400	$3.42 \cdot 10^{-10}$	$8.5 \cdot 10^{-4}$	$3.35 \cdot 10^{-9}$	$1.55 \cdot 10^{-2}$	$2.56 \cdot 10^{-3}$	$1.89 \cdot 10^{-2}$	$1.89 \cdot 10^{-2}$
500	$2.19 \cdot 10^{-10}$	$7.03 \cdot 10^{-4}$	$2.68 \cdot 10^{-9}$	$1.58 \cdot 10^{-2}$	$2.65 \cdot 10^{-3}$	$1.91 \cdot 10^{-2}$	$1.91 \cdot 10^{-2}$
600	$1.52 \cdot 10^{-10}$	$6.02 \cdot 10^{-4}$	$2.23 \cdot 10^{-9}$	$1.6 \cdot 10^{-2}$	$2.72 \cdot 10^{-3}$	$1.93 \cdot 10^{-2}$	$1.93 \cdot 10^{-2}$
800	$8.54 \cdot 10^{-11}$	$4.7 \cdot 10^{-4}$	$1.67 \cdot 10^{-9}$	$1.63 \cdot 10^{-2}$	$2.81 \cdot 10^{-3}$	$1.96 \cdot 10^{-2}$	$1.96 \cdot 10^{-2}$
1,000	$5.47 \cdot 10^{-11}$	$3.87 \cdot 10^{-4}$	$1.34 \cdot 10^{-9}$	$1.65 \cdot 10^{-2}$	$2.88 \cdot 10^{-3}$	$1.98 \cdot 10^{-2}$	$1.98 \cdot 10^{-2}$
1,500	$2.43 \cdot 10^{-11}$	$2.7 \cdot 10^{-4}$	$8.92 \cdot 10^{-10}$	$1.68 \cdot 10^{-2}$	$2.97 \cdot 10^{-3}$	$2.01 \cdot 10^{-2}$	$2.01 \cdot 10^{-2}$
2,000	$1.37 \cdot 10^{-11}$	$2.09 \cdot 10^{-4}$	$6.69 \cdot 10^{-10}$	$1.7 \cdot 10^{-2}$	$3.03 \cdot 10^{-3}$	$2.02 \cdot 10^{-2}$	$2.02 \cdot 10^{-2}$
3,000	$6.07 \cdot 10^{-12}$	$1.45 \cdot 10^{-4}$	$4.46 \cdot 10^{-10}$	$1.72 \cdot 10^{-2}$	$3.09 \cdot 10^{-3}$	$2.04 \cdot 10^{-2}$	$2.04 \cdot 10^{-2}$
4,000	$3.42 \cdot 10^{-12}$	$1.12 \cdot 10^{-4}$	$3.34 \cdot 10^{-10}$	$1.73 \cdot 10^{-2}$	$3.13 \cdot 10^{-3}$	$2.05 \cdot 10^{-2}$	$2.05 \cdot 10^{-2}$
5,000	$2.19 \cdot 10^{-12}$	$9.18 \cdot 10^{-5}$	$2.68 \cdot 10^{-10}$	$1.73 \cdot 10^{-2}$	$3.15 \cdot 10^{-3}$	$2.06 \cdot 10^{-2}$	$2.06 \cdot 10^{-2}$
6,000	$1.52 \cdot 10^{-12}$	$7.78 \cdot 10^{-5}$	$2.23 \cdot 10^{-10}$	$1.74 \cdot 10^{-2}$	$3.16 \cdot 10^{-3}$	$2.06 \cdot 10^{-2}$	$2.06 \cdot 10^{-2}$
8,000	$8.54 \cdot 10^{-13}$	$6 \cdot 10^{-5}$	$1.67 \cdot 10^{-10}$	$1.74 \cdot 10^{-2}$	$3.18 \cdot 10^{-3}$	$2.07 \cdot 10^{-2}$	$2.07 \cdot 10^{-2}$
10,000	$5.47 \cdot 10^{-13}$	$4.89 \cdot 10^{-5}$	$1.34 \cdot 10^{-10}$	$1.75 \cdot 10^{-2}$	$3.2 \cdot 10^{-3}$	$2.07 \cdot 10^{-2}$	$2.07 \cdot 10^{-2}$
15,000	$2.43 \cdot 10^{-13}$	$3.38 \cdot 10^{-5}$	$8.91 \cdot 10^{-11}$	$1.75 \cdot 10^{-2}$	$3.22 \cdot 10^{-3}$	$2.08 \cdot 10^{-2}$	$2.08 \cdot 10^{-2}$
20,000	$1.37 \cdot 10^{-13}$	$2.6 \cdot 10^{-5}$	$6.69 \cdot 10^{-11}$	$1.75 \cdot 10^{-2}$	$3.23 \cdot 10^{-3}$	$2.08 \cdot 10^{-2}$	$2.08 \cdot 10^{-2}$
30,000	$6.07 \cdot 10^{-14}$	$1.79 \cdot 10^{-5}$	$4.46 \cdot 10^{-11}$	$1.76 \cdot 10^{-2}$	$3.24 \cdot 10^{-3}$	$2.08 \cdot 10^{-2}$	$2.08 \cdot 10^{-2}$
40,000	$3.42 \cdot 10^{-14}$	$1.38 \cdot 10^{-5}$	$3.34 \cdot 10^{-11}$	$1.76 \cdot 10^{-2}$	$3.24 \cdot 10^{-3}$	$2.08 \cdot 10^{-2}$	$2.08 \cdot 10^{-2}$
50,000	$2.19 \cdot 10^{-14}$	$1.12 \cdot 10^{-5}$	$2.67 \cdot 10^{-11}$	$1.76 \cdot 10^{-2}$	$3.25 \cdot 10^{-3}$	$2.08 \cdot 10^{-2}$	$2.08 \cdot 10^{-2}$
60,000	$1.52 \cdot 10^{-14}$	$9.48 \cdot 10^{-6}$	$2.23 \cdot 10^{-11}$	$1.76 \cdot 10^{-2}$	$3.25 \cdot 10^{-3}$	$2.09 \cdot 10^{-2}$	$2.09 \cdot 10^{-2}$
80,000	$8.54 \cdot 10^{-15}$	$7.27 \cdot 10^{-6}$	$1.67 \cdot 10^{-11}$	$1.76 \cdot 10^{-2}$	$3.25 \cdot 10^{-3}$	$2.09 \cdot 10^{-2}$	$2.09 \cdot 10^{-2}$

A.8 Trabecular Bone

PE	SC	SI	PEA	PNF	PEF	TAWCS	TAOCS
$1 \cdot 10^{-3}$	1.32	$1.44 \cdot 10^{-2}$	3,110	0	0	3,111	3,110
$1.04 \cdot 10^{-3}$	1.31	$1.53 \cdot 10^{-2}$	2,831	0	0	2,832	2,831
$1.07 \cdot 10^{-3}$	1.3	$1.62 \cdot 10^{-2}$	2,577	0	0	2,578	2,577
$1.07 \cdot 10^{-3}$	1.3	$1.62 \cdot 10^{-2}$	2,583	0	0	2,584	2,583
$1.18 \cdot 10^{-3}$	1.28	$1.92 \cdot 10^{-2}$	1,980	0	0	1,982	1,980
$1.31 \cdot 10^{-3}$	1.25	$2.26 \cdot 10^{-2}$	1,516	0	0	1,517	1,516
$1.31 \cdot 10^{-3}$	1.25	$2.26 \cdot 10^{-2}$	1,521	0	0	1,523	1,521
$1.5 \cdot 10^{-3}$	1.2	$2.84 \cdot 10^{-2}$	1,038	0	0	1,039	1,038
$2 \cdot 10^{-3}$	1.07	$4.37 \cdot 10^{-2}$	461.7	0	0	462.8	461.8
$2.15 \cdot 10^{-3}$	1.03	$4.81 \cdot 10^{-2}$	377.6	0	0	378.7	377.7
$2.15 \cdot 10^{-3}$	1.03	$4.81 \cdot 10^{-2}$	385.4	0	0	386.5	385.5
$2.3 \cdot 10^{-3}$	0.99	$5.28 \cdot 10^{-2}$	314.7	0	0	315.7	314.7
$2.47 \cdot 10^{-3}$	0.95	$5.77 \cdot 10^{-2}$	256.7	0	0	257.7	256.7
$2.47 \cdot 10^{-3}$	0.95	$5.77 \cdot 10^{-2}$	260.5	0	0	261.5	260.5
$2.64 \cdot 10^{-3}$	0.91	$6.25 \cdot 10^{-2}$	215.2	0	0	216.2	215.3
$2.82 \cdot 10^{-3}$	0.87	$6.75 \cdot 10^{-2}$	177.7	0	0	178.6	177.8
$2.82 \cdot 10^{-3}$	0.87	$6.75 \cdot 10^{-2}$	180.7	0	0	181.6	180.8
$3 \cdot 10^{-3}$	0.83	$7.21 \cdot 10^{-2}$	151.5	0	0	152.5	151.6
$3.61 \cdot 10^{-3}$	0.71	$8.65 \cdot 10^{-2}$	88.32	0	0	89.12	88.41
$3.61 \cdot 10^{-3}$	0.71	$8.65 \cdot 10^{-2}$	89.42	0	0	90.22	89.51
$4 \cdot 10^{-3}$	0.65	$9.46 \cdot 10^{-2}$	65.89	0	0	66.63	65.98
$4.04 \cdot 10^{-3}$	0.64	$9.54 \cdot 10^{-2}$	64.06	0	0	64.8	64.16
$4.04 \cdot 10^{-3}$	0.64	$9.54 \cdot 10^{-2}$	105.1	0	0	105.9	105.2
$5 \cdot 10^{-3}$	0.51	0.11	58.24	0	0	58.86	58.35
$6 \cdot 10^{-3}$	0.42	0.12	34.68	0	0	35.22	34.8
$7.11 \cdot 10^{-3}$	0.34	0.13	21.28	0	0	21.76	21.42
$7.11 \cdot 10^{-3}$	0.34	0.13	21.65	0	0	22.13	21.78
$8 \cdot 10^{-3}$	0.3	0.14	15.42	0	0	15.86	15.56
$1 \cdot 10^{-2}$	0.23	0.15	8.03	0	0	8.41	8.18
$1.5 \cdot 10^{-2}$	0.14	0.17	2.4	0	0	2.7	2.56
$2 \cdot 10^{-2}$	$9.05 \cdot 10^{-2}$	0.17	1	0	0	1.27	1.18
$3 \cdot 10^{-2}$	$4.78 \cdot 10^{-2}$	0.18	0.29	0	0	0.51	0.47
$4 \cdot 10^{-2}$	$2.94 \cdot 10^{-2}$	0.18	0.12	0	0	0.32	0.3
$5 \cdot 10^{-2}$	$1.99 \cdot 10^{-2}$	0.18	$5.78 \cdot 10^{-2}$	0	0	0.25	0.23
$6 \cdot 10^{-2}$	$1.44 \cdot 10^{-2}$	0.17	$3.24 \cdot 10^{-2}$	0	0	0.22	0.21
$8 \cdot 10^{-2}$	$8.47 \cdot 10^{-3}$	0.17	$1.3 \cdot 10^{-2}$	0	0	0.19	0.18
0.1	$5.57 \cdot 10^{-3}$	0.16	$6.38 \cdot 10^{-3}$	0	0	0.17	0.17
0.15	$2.55 \cdot 10^{-3}$	0.14	$1.76 \cdot 10^{-3}$	0	0	0.15	0.15
0.2	$1.45 \cdot 10^{-3}$	0.13	$7.12 \cdot 10^{-4}$	0	0	0.13	0.13
0.3	$6.54 \cdot 10^{-4}$	0.12	$2.07 \cdot 10^{-4}$	0	0	0.12	0.12
0.4	$3.69 \cdot 10^{-4}$	0.1	$8.99 \cdot 10^{-5}$	0	0	0.1	0.1
0.5	$2.37 \cdot 10^{-4}$	$9.45 \cdot 10^{-2}$	$4.89 \cdot 10^{-5}$	0	0	$9.48 \cdot 10^{-2}$	$9.45 \cdot 10^{-2}$
0.6	$1.65 \cdot 10^{-4}$	$8.74 \cdot 10^{-2}$	$3.06 \cdot 10^{-5}$	0	0	$8.76 \cdot 10^{-2}$	$8.74 \cdot 10^{-2}$
0.8	$9.27 \cdot 10^{-5}$	$7.68 \cdot 10^{-2}$	$1.55 \cdot 10^{-5}$	0	0	$7.69 \cdot 10^{-2}$	$7.68 \cdot 10^{-2}$
1	$5.94 \cdot 10^{-5}$	$6.91 \cdot 10^{-2}$	$9.66 \cdot 10^{-6}$	0	0	$6.91 \cdot 10^{-2}$	$6.91 \cdot 10^{-2}$
1.02	$5.68 \cdot 10^{-5}$	$6.84 \cdot 10^{-2}$	$9.1 \cdot 10^{-6}$	0	0	$6.84 \cdot 10^{-2}$	$6.84 \cdot 10^{-2}$
1.25	$3.8 \cdot 10^{-5}$	$6.18 \cdot 10^{-2}$	$6.17 \cdot 10^{-6}$	$1.77 \cdot 10^{-5}$	0	$6.18 \cdot 10^{-2}$	$6.18 \cdot 10^{-2}$
1.5	$2.64 \cdot 10^{-5}$	$5.62 \cdot 10^{-2}$	$4.46 \cdot 10^{-6}$	$9.72 \cdot 10^{-5}$	0	$5.63 \cdot 10^{-2}$	$5.63 \cdot 10^{-2}$
2	$1.49 \cdot 10^{-5}$	$4.79 \cdot 10^{-2}$	$2.78 \cdot 10^{-6}$	$3.86 \cdot 10^{-4}$	0	$4.83 \cdot 10^{-2}$	$4.83 \cdot 10^{-2}$
2.04	$1.42 \cdot 10^{-5}$	$4.73 \cdot 10^{-2}$	$2.68 \cdot 10^{-6}$	$4.16 \cdot 10^{-4}$	0	$4.78 \cdot 10^{-2}$	$4.77 \cdot 10^{-2}$
3	$6.6 \cdot 10^{-6}$	$3.77 \cdot 10^{-2}$	$1.53 \cdot 10^{-6}$	$1.1 \cdot 10^{-3}$	$1.32 \cdot 10^{-5}$	$3.88 \cdot 10^{-2}$	$3.88 \cdot 10^{-2}$
4	$3.71 \cdot 10^{-6}$	$3.14 \cdot 10^{-2}$	$1.04 \cdot 10^{-6}$	$1.78 \cdot 10^{-3}$	$5.38 \cdot 10^{-5}$	$3.33 \cdot 10^{-2}$	$3.33 \cdot 10^{-2}$
5	$2.38 \cdot 10^{-6}$	$2.72 \cdot 10^{-2}$	$7.81 \cdot 10^{-7}$	$2.39 \cdot 10^{-3}$	$1.07 \cdot 10^{-4}$	$2.97 \cdot 10^{-2}$	$2.97 \cdot 10^{-2}$
6	$1.65 \cdot 10^{-6}$	$2.4 \cdot 10^{-2}$	$6.25 \cdot 10^{-7}$	$2.94 \cdot 10^{-3}$	$1.65 \cdot 10^{-4}$	$2.71 \cdot 10^{-2}$	$2.71 \cdot 10^{-2}$
7	$1.21 \cdot 10^{-6}$	$2.16 \cdot 10^{-2}$	$5.2 \cdot 10^{-7}$	$3.42 \cdot 10^{-3}$	$2.22 \cdot 10^{-4}$	$2.52 \cdot 10^{-2}$	$2.52 \cdot 10^{-2}$
8	$9.28 \cdot 10^{-7}$	$1.96 \cdot 10^{-2}$	$4.45 \cdot 10^{-7}$	$3.86 \cdot 10^{-3}$	$2.78 \cdot 10^{-4}$	$2.38 \cdot 10^{-2}$	$2.38 \cdot 10^{-2}$
9	$7.34 \cdot 10^{-7}$	$1.81 \cdot 10^{-2}$	$3.89 \cdot 10^{-7}$	$4.26 \cdot 10^{-3}$	$3.31 \cdot 10^{-4}$	$2.26 \cdot 10^{-2}$	$2.26 \cdot 10^{-2}$
10	$5.94 \cdot 10^{-7}$	$1.67 \cdot 10^{-2}$	$3.45 \cdot 10^{-7}$	$4.62 \cdot 10^{-3}$	$3.82 \cdot 10^{-4}$	$2.17 \cdot 10^{-2}$	$2.17 \cdot 10^{-2}$
11	$4.91 \cdot 10^{-7}$	$1.56 \cdot 10^{-2}$	$3.1 \cdot 10^{-7}$	$4.95 \cdot 10^{-3}$	$4.31 \cdot 10^{-4}$	$2.1 \cdot 10^{-2}$	$2.1 \cdot 10^{-2}$
12	$4.13 \cdot 10^{-7}$	$1.46 \cdot 10^{-2}$	$2.82 \cdot 10^{-7}$	$5.25 \cdot 10^{-3}$	$4.76 \cdot 10^{-4}$	$2.04 \cdot 10^{-2}$	$2.04 \cdot 10^{-2}$
13	$3.52 \cdot 10^{-7}$	$1.38 \cdot 10^{-2}$	$2.58 \cdot 10^{-7}$	$5.53 \cdot 10^{-3}$	$5.2 \cdot 10^{-4}$	$1.98 \cdot 10^{-2}$	$1.98 \cdot 10^{-2}$
14	$3.03 \cdot 10^{-7}$	$1.3 \cdot 10^{-2}$	$2.38 \cdot 10^{-7}$	$5.79 \cdot 10^{-3}$	$5.61 \cdot 10^{-4}$	$1.94 \cdot 10^{-2}$	$1.94 \cdot 10^{-2}$
15	$2.64 \cdot 10^{-7}$	$1.24 \cdot 10^{-2}$	$2.2 \cdot 10^{-7}$	$6.04 \cdot 10^{-3}$	$6 \cdot 10^{-4}$	$1.9 \cdot 10^{-2}$	$1.9 \cdot 10^{-2}$
16	$2.32 \cdot 10^{-7}$	$1.18 \cdot 10^{-2}$	$2.06 \cdot 10^{-7}$	$6.27 \cdot 10^{-3}$	$6.37 \cdot 10^{-4}$	$1.87 \cdot 10^{-2}$	$1.87 \cdot 10^{-2}$
18	$1.83 \cdot 10^{-7}$	$1.08 \cdot 10^{-2}$	$1.81 \cdot 10^{-7}$	$6.69 \cdot 10^{-3}$	$7.07 \cdot 10^{-4}$	$1.82 \cdot 10^{-2}$	$1.82 \cdot 10^{-2}$

20	$1.49 \cdot 10^{-7}$	$9.93 \cdot 10^{-3}$	$1.62 \cdot 10^{-7}$	$7.06 \cdot 10^{-3}$	$7.7 \cdot 10^{-4}$	$1.78 \cdot 10^{-2}$	$1.78 \cdot 10^{-2}$
22	$1.23 \cdot 10^{-7}$	$9.23 \cdot 10^{-3}$	$1.46 \cdot 10^{-7}$	$7.41 \cdot 10^{-3}$	$8.29 \cdot 10^{-4}$	$1.75 \cdot 10^{-2}$	$1.75 \cdot 10^{-2}$
24	$1.03 \cdot 10^{-7}$	$8.62 \cdot 10^{-3}$	$1.33 \cdot 10^{-7}$	$7.72 \cdot 10^{-3}$	$8.83 \cdot 10^{-4}$	$1.72 \cdot 10^{-2}$	$1.72 \cdot 10^{-2}$
26	$8.79 \cdot 10^{-8}$	$8.1 \cdot 10^{-3}$	$1.23 \cdot 10^{-7}$	$8 \cdot 10^{-3}$	$9.34 \cdot 10^{-4}$	$1.7 \cdot 10^{-2}$	$1.7 \cdot 10^{-2}$
28	$7.58 \cdot 10^{-8}$	$7.64 \cdot 10^{-3}$	$1.13 \cdot 10^{-7}$	$8.27 \cdot 10^{-3}$	$9.81 \cdot 10^{-4}$	$1.69 \cdot 10^{-2}$	$1.69 \cdot 10^{-2}$
30	$6.6 \cdot 10^{-8}$	$7.23 \cdot 10^{-3}$	$1.05 \cdot 10^{-7}$	$8.51 \cdot 10^{-3}$	$1.03 \cdot 10^{-3}$	$1.68 \cdot 10^{-2}$	$1.68 \cdot 10^{-2}$
40	$3.71 \cdot 10^{-8}$	$5.75 \cdot 10^{-3}$	$7.82 \cdot 10^{-8}$	$9.51 \cdot 10^{-3}$	$1.21 \cdot 10^{-3}$	$1.65 \cdot 10^{-2}$	$1.65 \cdot 10^{-2}$
50	$2.38 \cdot 10^{-8}$	$4.8 \cdot 10^{-3}$	$6.21 \cdot 10^{-8}$	$1.03 \cdot 10^{-2}$	$1.36 \cdot 10^{-3}$	$1.64 \cdot 10^{-2}$	$1.64 \cdot 10^{-2}$
60	$1.65 \cdot 10^{-8}$	$4.13 \cdot 10^{-3}$	$5.15 \cdot 10^{-8}$	$1.09 \cdot 10^{-2}$	$1.47 \cdot 10^{-3}$	$1.65 \cdot 10^{-2}$	$1.65 \cdot 10^{-2}$
80	$9.28 \cdot 10^{-9}$	$3.26 \cdot 10^{-3}$	$3.84 \cdot 10^{-8}$	$1.18 \cdot 10^{-2}$	$1.66 \cdot 10^{-3}$	$1.67 \cdot 10^{-2}$	$1.67 \cdot 10^{-2}$
100	$5.94 \cdot 10^{-9}$	$2.71 \cdot 10^{-3}$	$3.06 \cdot 10^{-8}$	$1.24 \cdot 10^{-2}$	$1.79 \cdot 10^{-3}$	$1.69 \cdot 10^{-2}$	$1.69 \cdot 10^{-2}$
150	$2.64 \cdot 10^{-9}$	$1.93 \cdot 10^{-3}$	$2.03 \cdot 10^{-8}$	$1.35 \cdot 10^{-2}$	$2.03 \cdot 10^{-3}$	$1.75 \cdot 10^{-2}$	$1.75 \cdot 10^{-2}$
200	$1.49 \cdot 10^{-9}$	$1.51 \cdot 10^{-3}$	$1.52 \cdot 10^{-8}$	$1.42 \cdot 10^{-2}$	$2.19 \cdot 10^{-3}$	$1.79 \cdot 10^{-2}$	$1.79 \cdot 10^{-2}$
300	$6.6 \cdot 10^{-10}$	$1.07 \cdot 10^{-3}$	$1.01 \cdot 10^{-8}$	$1.5 \cdot 10^{-2}$	$2.4 \cdot 10^{-3}$	$1.85 \cdot 10^{-2}$	$1.85 \cdot 10^{-2}$
400	$3.71 \cdot 10^{-10}$	$8.38 \cdot 10^{-4}$	$7.58 \cdot 10^{-9}$	$1.55 \cdot 10^{-2}$	$2.53 \cdot 10^{-3}$	$1.89 \cdot 10^{-2}$	$1.89 \cdot 10^{-2}$
500	$2.38 \cdot 10^{-10}$	$6.94 \cdot 10^{-4}$	$6.06 \cdot 10^{-9}$	$1.58 \cdot 10^{-2}$	$2.62 \cdot 10^{-3}$	$1.92 \cdot 10^{-2}$	$1.92 \cdot 10^{-2}$
600	$1.65 \cdot 10^{-10}$	$5.94 \cdot 10^{-4}$	$5.05 \cdot 10^{-9}$	$1.61 \cdot 10^{-2}$	$2.68 \cdot 10^{-3}$	$1.94 \cdot 10^{-2}$	$1.94 \cdot 10^{-2}$
800	$9.28 \cdot 10^{-11}$	$4.64 \cdot 10^{-4}$	$3.78 \cdot 10^{-9}$	$1.64 \cdot 10^{-2}$	$2.78 \cdot 10^{-3}$	$1.96 \cdot 10^{-2}$	$1.96 \cdot 10^{-2}$
1,000	$5.94 \cdot 10^{-11}$	$3.82 \cdot 10^{-4}$	$3.03 \cdot 10^{-9}$	$1.66 \cdot 10^{-2}$	$2.84 \cdot 10^{-3}$	$1.98 \cdot 10^{-2}$	$1.98 \cdot 10^{-2}$
1,500	$2.64 \cdot 10^{-11}$	$2.67 \cdot 10^{-4}$	$2.02 \cdot 10^{-9}$	$1.69 \cdot 10^{-2}$	$2.94 \cdot 10^{-3}$	$2.01 \cdot 10^{-2}$	$2.01 \cdot 10^{-2}$
2,000	$1.49 \cdot 10^{-11}$	$2.06 \cdot 10^{-4}$	$1.51 \cdot 10^{-9}$	$1.71 \cdot 10^{-2}$	$2.99 \cdot 10^{-3}$	$2.03 \cdot 10^{-2}$	$2.03 \cdot 10^{-2}$
3,000	$6.6 \cdot 10^{-12}$	$1.44 \cdot 10^{-4}$	$1.01 \cdot 10^{-9}$	$1.73 \cdot 10^{-2}$	$3.05 \cdot 10^{-3}$	$2.04 \cdot 10^{-2}$	$2.04 \cdot 10^{-2}$
4,000	$3.71 \cdot 10^{-12}$	$1.11 \cdot 10^{-4}$	$7.56 \cdot 10^{-10}$	$1.73 \cdot 10^{-2}$	$3.09 \cdot 10^{-3}$	$2.05 \cdot 10^{-2}$	$2.05 \cdot 10^{-2}$
5,000	$2.38 \cdot 10^{-12}$	$9.06 \cdot 10^{-5}$	$6.05 \cdot 10^{-10}$	$1.74 \cdot 10^{-2}$	$3.11 \cdot 10^{-3}$	$2.06 \cdot 10^{-2}$	$2.06 \cdot 10^{-2}$
6,000	$1.65 \cdot 10^{-12}$	$7.68 \cdot 10^{-5}$	$5.04 \cdot 10^{-10}$	$1.75 \cdot 10^{-2}$	$3.13 \cdot 10^{-3}$	$2.07 \cdot 10^{-2}$	$2.07 \cdot 10^{-2}$
8,000	$9.28 \cdot 10^{-13}$	$5.92 \cdot 10^{-5}$	$3.78 \cdot 10^{-10}$	$1.75 \cdot 10^{-2}$	$3.15 \cdot 10^{-3}$	$2.07 \cdot 10^{-2}$	$2.07 \cdot 10^{-2}$
10,000	$5.94 \cdot 10^{-13}$	$4.83 \cdot 10^{-5}$	$3.02 \cdot 10^{-10}$	$1.75 \cdot 10^{-2}$	$3.16 \cdot 10^{-3}$	$2.08 \cdot 10^{-2}$	$2.08 \cdot 10^{-2}$
15,000	$2.64 \cdot 10^{-13}$	$3.34 \cdot 10^{-5}$	$2.02 \cdot 10^{-10}$	$1.76 \cdot 10^{-2}$	$3.18 \cdot 10^{-3}$	$2.08 \cdot 10^{-2}$	$2.08 \cdot 10^{-2}$
20,000	$1.49 \cdot 10^{-13}$	$2.57 \cdot 10^{-5}$	$1.51 \cdot 10^{-10}$	$1.76 \cdot 10^{-2}$	$3.19 \cdot 10^{-3}$	$2.08 \cdot 10^{-2}$	$2.08 \cdot 10^{-2}$
30,000	$6.6 \cdot 10^{-14}$	$1.77 \cdot 10^{-5}$	$1.01 \cdot 10^{-10}$	$1.76 \cdot 10^{-2}$	$3.2 \cdot 10^{-3}$	$2.09 \cdot 10^{-2}$	$2.09 \cdot 10^{-2}$
40,000	$3.71 \cdot 10^{-14}$	$1.36 \cdot 10^{-5}$	$7.56 \cdot 10^{-11}$	$1.77 \cdot 10^{-2}$	$3.21 \cdot 10^{-3}$	$2.09 \cdot 10^{-2}$	$2.09 \cdot 10^{-2}$
50,000	$2.38 \cdot 10^{-14}$	$1.11 \cdot 10^{-5}$	$6.05 \cdot 10^{-11}$	$1.77 \cdot 10^{-2}$	$3.21 \cdot 10^{-3}$	$2.09 \cdot 10^{-2}$	$2.09 \cdot 10^{-2}$
60,000	$1.65 \cdot 10^{-14}$	$9.35 \cdot 10^{-6}$	$5.04 \cdot 10^{-11}$	$1.77 \cdot 10^{-2}$	$3.21 \cdot 10^{-3}$	$2.09 \cdot 10^{-2}$	$2.09 \cdot 10^{-2}$
80,000	$9.28 \cdot 10^{-15}$	$7.17 \cdot 10^{-6}$	$3.78 \cdot 10^{-11}$	$1.77 \cdot 10^{-2}$	$3.22 \cdot 10^{-3}$	$2.09 \cdot 10^{-2}$	$2.09 \cdot 10^{-2}$
$1 \cdot 10^5$	$5.94 \cdot 10^{-15}$	$5.83 \cdot 10^{-6}$	$3.02 \cdot 10^{-11}$	$1.77 \cdot 10^{-2}$	$3.22 \cdot 10^{-3}$	$2.09 \cdot 10^{-2}$	$2.09 \cdot 10^{-2}$

A.9 Water

PE	SC	SI	PEA	PNF	PEF	TAWCS	TAOCS
$1 \cdot 10^{-3}$	1.37	$1.32 \cdot 10^{-2}$	4,076	0	0	4,077	4,076
$1.5 \cdot 10^{-3}$	1.27	$2.67 \cdot 10^{-2}$	1,374	0	0	1,376	1,374
$2 \cdot 10^{-3}$	1.15	$4.18 \cdot 10^{-2}$	616.2	0	0	617.3	616.2
$3 \cdot 10^{-3}$	0.91	$7.08 \cdot 10^{-2}$	191.9	0	0	192.8	191.9
$4 \cdot 10^{-3}$	0.71	$9.43 \cdot 10^{-2}$	81.97	0	0	82.77	82.07
$5 \cdot 10^{-3}$	0.56	0.11	41.92	0	0	42.59	42.03
$6 \cdot 10^{-3}$	0.45	0.13	24.07	0	0	24.64	24.19
$8 \cdot 10^{-3}$	0.31	0.14	9.92	0	0	10.37	10.06
$1 \cdot 10^{-2}$	0.23	0.16	4.94	0	0	5.33	5.1
$1.5 \cdot 10^{-2}$	0.13	0.17	1.37	0	0	1.67	1.54
$2 \cdot 10^{-2}$	$8.86 \cdot 10^{-2}$	0.18	0.54	0	0	0.81	0.72
$3 \cdot 10^{-2}$	$4.69 \cdot 10^{-2}$	0.18	0.15	0	0	0.38	0.33
$4 \cdot 10^{-2}$	$2.87 \cdot 10^{-2}$	0.18	$5.68 \cdot 10^{-2}$	0	0	0.27	0.24
$5 \cdot 10^{-2}$	$1.94 \cdot 10^{-2}$	0.18	$2.73 \cdot 10^{-2}$	0	0	0.23	0.21
$6 \cdot 10^{-2}$	$1.39 \cdot 10^{-2}$	0.18	$1.49 \cdot 10^{-2}$	0	0	0.21	0.19
$8 \cdot 10^{-2}$	$8.17 \cdot 10^{-3}$	0.17	$5.77 \cdot 10^{-3}$	0	0	0.18	0.18
0.1	$5.35 \cdot 10^{-3}$	0.16	$2.76 \cdot 10^{-3}$	0	0	0.17	0.17
0.15	$2.44 \cdot 10^{-3}$	0.15	$7.31 \cdot 10^{-4}$	0	0	0.15	0.15
0.2	$1.39 \cdot 10^{-3}$	0.14	$2.89 \cdot 10^{-4}$	0	0	0.14	0.14
0.3	$6.22 \cdot 10^{-4}$	0.12	$8.16 \cdot 10^{-5}$	0	0	0.12	0.12
0.4	$3.51 \cdot 10^{-4}$	0.11	$3.49 \cdot 10^{-5}$	0	0	0.11	0.11
0.5	$2.25 \cdot 10^{-4}$	$9.66 \cdot 10^{-2}$	$1.88 \cdot 10^{-5}$	0	0	$9.69 \cdot 10^{-2}$	$9.67 \cdot 10^{-2}$
0.6	$1.56 \cdot 10^{-4}$	$8.94 \cdot 10^{-2}$	$1.17 \cdot 10^{-5}$	0	0	$8.96 \cdot 10^{-2}$	$8.94 \cdot 10^{-2}$
0.8	$8.79 \cdot 10^{-5}$	$7.86 \cdot 10^{-2}$	$5.92 \cdot 10^{-6}$	0	0	$7.87 \cdot 10^{-2}$	$7.86 \cdot 10^{-2}$
1	$5.63 \cdot 10^{-5}$	$7.07 \cdot 10^{-2}$	$3.68 \cdot 10^{-6}$	0	0	$7.07 \cdot 10^{-2}$	$7.07 \cdot 10^{-2}$
1.02	$5.39 \cdot 10^{-5}$	$6.99 \cdot 10^{-2}$	$3.43 \cdot 10^{-6}$	0	0	$7 \cdot 10^{-2}$	$6.99 \cdot 10^{-2}$
1.25	$3.6 \cdot 10^{-5}$	$6.32 \cdot 10^{-2}$	$2.33 \cdot 10^{-6}$	$1.78 \cdot 10^{-5}$	0	$6.32 \cdot 10^{-2}$	$6.32 \cdot 10^{-2}$
1.5	$2.5 \cdot 10^{-5}$	$5.74 \cdot 10^{-2}$	$1.69 \cdot 10^{-6}$	$9.82 \cdot 10^{-5}$	0	$5.75 \cdot 10^{-2}$	$5.75 \cdot 10^{-2}$
2	$1.41 \cdot 10^{-5}$	$4.9 \cdot 10^{-2}$	$1.06 \cdot 10^{-6}$	$3.91 \cdot 10^{-4}$	0	$4.94 \cdot 10^{-2}$	$4.94 \cdot 10^{-2}$
2.04	$1.35 \cdot 10^{-5}$	$4.84 \cdot 10^{-2}$	$1.03 \cdot 10^{-6}$	$4.21 \cdot 10^{-4}$	0	$4.88 \cdot 10^{-2}$	$4.88 \cdot 10^{-2}$
3	$6.26 \cdot 10^{-6}$	$3.86 \cdot 10^{-2}$	$5.94 \cdot 10^{-7}$	$1.12 \cdot 10^{-3}$	$1.35 \cdot 10^{-5}$	$3.97 \cdot 10^{-2}$	$3.97 \cdot 10^{-2}$
4	$3.52 \cdot 10^{-6}$	$3.22 \cdot 10^{-2}$	$4.08 \cdot 10^{-7}$	$1.81 \cdot 10^{-3}$	$5.51 \cdot 10^{-5}$	$3.4 \cdot 10^{-2}$	$3.4 \cdot 10^{-2}$
5	$2.25 \cdot 10^{-6}$	$2.78 \cdot 10^{-2}$	$3.09 \cdot 10^{-7}$	$2.43 \cdot 10^{-3}$	$1.1 \cdot 10^{-4}$	$3.03 \cdot 10^{-2}$	$3.03 \cdot 10^{-2}$
6	$1.56 \cdot 10^{-6}$	$2.45 \cdot 10^{-2}$	$2.48 \cdot 10^{-7}$	$2.99 \cdot 10^{-3}$	$1.69 \cdot 10^{-4}$	$2.77 \cdot 10^{-2}$	$2.77 \cdot 10^{-2}$
7	$1.15 \cdot 10^{-6}$	$2.21 \cdot 10^{-2}$	$2.08 \cdot 10^{-7}$	$3.48 \cdot 10^{-3}$	$2.27 \cdot 10^{-4}$	$2.58 \cdot 10^{-2}$	$2.58 \cdot 10^{-2}$
8	$8.8 \cdot 10^{-7}$	$2.01 \cdot 10^{-2}$	$1.78 \cdot 10^{-7}$	$3.93 \cdot 10^{-3}$	$2.84 \cdot 10^{-4}$	$2.43 \cdot 10^{-2}$	$2.43 \cdot 10^{-2}$
9	$6.95 \cdot 10^{-7}$	$1.85 \cdot 10^{-2}$	$1.56 \cdot 10^{-7}$	$4.33 \cdot 10^{-3}$	$3.39 \cdot 10^{-4}$	$2.31 \cdot 10^{-2}$	$2.31 \cdot 10^{-2}$
10	$5.63 \cdot 10^{-7}$	$1.71 \cdot 10^{-2}$	$1.39 \cdot 10^{-7}$	$4.7 \cdot 10^{-3}$	$3.91 \cdot 10^{-4}$	$2.22 \cdot 10^{-2}$	$2.22 \cdot 10^{-2}$
11	$4.65 \cdot 10^{-7}$	$1.6 \cdot 10^{-2}$	$1.25 \cdot 10^{-7}$	$5.03 \cdot 10^{-3}$	$4.4 \cdot 10^{-4}$	$2.14 \cdot 10^{-2}$	$2.14 \cdot 10^{-2}$
12	$3.91 \cdot 10^{-7}$	$1.5 \cdot 10^{-2}$	$1.13 \cdot 10^{-7}$	$5.34 \cdot 10^{-3}$	$4.87 \cdot 10^{-4}$	$2.08 \cdot 10^{-2}$	$2.08 \cdot 10^{-2}$
13	$3.33 \cdot 10^{-7}$	$1.41 \cdot 10^{-2}$	$1.04 \cdot 10^{-7}$	$5.63 \cdot 10^{-3}$	$5.32 \cdot 10^{-4}$	$2.03 \cdot 10^{-2}$	$2.03 \cdot 10^{-2}$
14	$2.87 \cdot 10^{-7}$	$1.33 \cdot 10^{-2}$	$9.59 \cdot 10^{-8}$	$5.89 \cdot 10^{-3}$	$5.74 \cdot 10^{-4}$	$1.98 \cdot 10^{-2}$	$1.98 \cdot 10^{-2}$
15	$2.5 \cdot 10^{-7}$	$1.27 \cdot 10^{-2}$	$8.91 \cdot 10^{-8}$	$6.14 \cdot 10^{-3}$	$6.14 \cdot 10^{-4}$	$1.94 \cdot 10^{-2}$	$1.94 \cdot 10^{-2}$
16	$2.2 \cdot 10^{-7}$	$1.21 \cdot 10^{-2}$	$8.31 \cdot 10^{-8}$	$6.38 \cdot 10^{-3}$	$6.52 \cdot 10^{-4}$	$1.91 \cdot 10^{-2}$	$1.91 \cdot 10^{-2}$
18	$1.74 \cdot 10^{-7}$	$1.1 \cdot 10^{-2}$	$7.33 \cdot 10^{-8}$	$6.8 \cdot 10^{-3}$	$7.23 \cdot 10^{-4}$	$1.85 \cdot 10^{-2}$	$1.85 \cdot 10^{-2}$
20	$1.41 \cdot 10^{-7}$	$1.02 \cdot 10^{-2}$	$6.56 \cdot 10^{-8}$	$7.19 \cdot 10^{-3}$	$7.88 \cdot 10^{-4}$	$1.81 \cdot 10^{-2}$	$1.81 \cdot 10^{-2}$
22	$1.16 \cdot 10^{-7}$	$9.44 \cdot 10^{-3}$	$5.93 \cdot 10^{-8}$	$7.54 \cdot 10^{-3}$	$8.48 \cdot 10^{-4}$	$1.78 \cdot 10^{-2}$	$1.78 \cdot 10^{-2}$
24	$9.78 \cdot 10^{-8}$	$8.82 \cdot 10^{-3}$	$5.41 \cdot 10^{-8}$	$7.85 \cdot 10^{-3}$	$9.03 \cdot 10^{-4}$	$1.76 \cdot 10^{-2}$	$1.76 \cdot 10^{-2}$
26	$8.33 \cdot 10^{-8}$	$8.28 \cdot 10^{-3}$	$4.98 \cdot 10^{-8}$	$8.14 \cdot 10^{-3}$	$9.55 \cdot 10^{-4}$	$1.74 \cdot 10^{-2}$	$1.74 \cdot 10^{-2}$
28	$7.18 \cdot 10^{-8}$	$7.81 \cdot 10^{-3}$	$4.61 \cdot 10^{-8}$	$8.41 \cdot 10^{-3}$	$1 \cdot 10^{-3}$	$1.72 \cdot 10^{-2}$	$1.72 \cdot 10^{-2}$
30	$6.26 \cdot 10^{-8}$	$7.4 \cdot 10^{-3}$	$4.29 \cdot 10^{-8}$	$8.66 \cdot 10^{-3}$	$1.05 \cdot 10^{-3}$	$1.71 \cdot 10^{-2}$	$1.71 \cdot 10^{-2}$
40	$3.52 \cdot 10^{-8}$	$5.88 \cdot 10^{-3}$	$3.19 \cdot 10^{-8}$	$9.67 \cdot 10^{-3}$	$1.24 \cdot 10^{-3}$	$1.68 \cdot 10^{-2}$	$1.68 \cdot 10^{-2}$
50	$2.25 \cdot 10^{-8}$	$4.91 \cdot 10^{-3}$	$2.53 \cdot 10^{-8}$	$1.05 \cdot 10^{-2}$	$1.39 \cdot 10^{-3}$	$1.67 \cdot 10^{-2}$	$1.67 \cdot 10^{-2}$
60	$1.56 \cdot 10^{-8}$	$4.23 \cdot 10^{-3}$	$2.1 \cdot 10^{-8}$	$1.11 \cdot 10^{-2}$	$1.51 \cdot 10^{-3}$	$1.68 \cdot 10^{-2}$	$1.68 \cdot 10^{-2}$
80	$8.8 \cdot 10^{-9}$	$3.33 \cdot 10^{-3}$	$1.57 \cdot 10^{-8}$	$1.2 \cdot 10^{-2}$	$1.69 \cdot 10^{-3}$	$1.7 \cdot 10^{-2}$	$1.7 \cdot 10^{-2}$
100	$5.63 \cdot 10^{-9}$	$2.77 \cdot 10^{-3}$	$1.25 \cdot 10^{-8}$	$1.27 \cdot 10^{-2}$	$1.83 \cdot 10^{-3}$	$1.73 \cdot 10^{-2}$	$1.73 \cdot 10^{-2}$
150	$2.5 \cdot 10^{-9}$	$1.97 \cdot 10^{-3}$	$8.32 \cdot 10^{-9}$	$1.38 \cdot 10^{-2}$	$2.08 \cdot 10^{-3}$	$1.79 \cdot 10^{-2}$	$1.79 \cdot 10^{-2}$
200	$1.41 \cdot 10^{-9}$	$1.55 \cdot 10^{-3}$	$6.23 \cdot 10^{-9}$	$1.45 \cdot 10^{-2}$	$2.24 \cdot 10^{-3}$	$1.83 \cdot 10^{-2}$	$1.83 \cdot 10^{-2}$
300	$6.26 \cdot 10^{-10}$	$1.1 \cdot 10^{-3}$	$4.14 \cdot 10^{-9}$	$1.53 \cdot 10^{-2}$	$2.45 \cdot 10^{-3}$	$1.89 \cdot 10^{-2}$	$1.89 \cdot 10^{-2}$
400	$3.52 \cdot 10^{-10}$	$8.57 \cdot 10^{-4}$	$3.11 \cdot 10^{-9}$	$1.58 \cdot 10^{-2}$	$2.58 \cdot 10^{-3}$	$1.93 \cdot 10^{-2}$	$1.93 \cdot 10^{-2}$
500	$2.25 \cdot 10^{-10}$	$7.1 \cdot 10^{-4}$	$2.48 \cdot 10^{-9}$	$1.62 \cdot 10^{-2}$	$2.68 \cdot 10^{-3}$	$1.95 \cdot 10^{-2}$	$1.95 \cdot 10^{-2}$
600	$1.56 \cdot 10^{-10}$	$6.08 \cdot 10^{-4}$	$2.07 \cdot 10^{-9}$	$1.64 \cdot 10^{-2}$	$2.74 \cdot 10^{-3}$	$1.97 \cdot 10^{-2}$	$1.97 \cdot 10^{-2}$
800	$8.8 \cdot 10^{-11}$	$4.75 \cdot 10^{-4}$	$1.55 \cdot 10^{-9}$	$1.67 \cdot 10^{-2}$	$2.84 \cdot 10^{-3}$	$2 \cdot 10^{-2}$	$2 \cdot 10^{-2}$
1,000	$5.63 \cdot 10^{-11}$	$3.91 \cdot 10^{-4}$	$1.24 \cdot 10^{-9}$	$1.69 \cdot 10^{-2}$	$2.9 \cdot 10^{-3}$	$2.02 \cdot 10^{-2}$	$2.02 \cdot 10^{-2}$
1,500	$2.5 \cdot 10^{-11}$	$2.73 \cdot 10^{-4}$	$8.26 \cdot 10^{-10}$	$1.72 \cdot 10^{-2}$	$3 \cdot 10^{-3}$	$2.05 \cdot 10^{-2}$	$2.05 \cdot 10^{-2}$

2,000	$1.41 \cdot 10^{-11}$	$2.11 \cdot 10^{-4}$	$6.19 \cdot 10^{-10}$	$1.74 \cdot 10^{-2}$	$3.05 \cdot 10^{-3}$	$2.06 \cdot 10^{-2}$	$2.06 \cdot 10^{-2}$
3,000	$6.26 \cdot 10^{-12}$	$1.47 \cdot 10^{-4}$	$4.13 \cdot 10^{-10}$	$1.76 \cdot 10^{-2}$	$3.11 \cdot 10^{-3}$	$2.08 \cdot 10^{-2}$	$2.08 \cdot 10^{-2}$
4,000	$3.52 \cdot 10^{-12}$	$1.13 \cdot 10^{-4}$	$3.1 \cdot 10^{-10}$	$1.77 \cdot 10^{-2}$	$3.15 \cdot 10^{-3}$	$2.09 \cdot 10^{-2}$	$2.09 \cdot 10^{-2}$
5,000	$2.25 \cdot 10^{-12}$	$9.26 \cdot 10^{-5}$	$2.48 \cdot 10^{-10}$	$1.77 \cdot 10^{-2}$	$3.17 \cdot 10^{-3}$	$2.1 \cdot 10^{-2}$	$2.1 \cdot 10^{-2}$
6,000	$1.56 \cdot 10^{-12}$	$7.86 \cdot 10^{-5}$	$2.06 \cdot 10^{-10}$	$1.78 \cdot 10^{-2}$	$3.19 \cdot 10^{-3}$	$2.1 \cdot 10^{-2}$	$2.1 \cdot 10^{-2}$
8,000	$8.8 \cdot 10^{-13}$	$6.05 \cdot 10^{-5}$	$1.55 \cdot 10^{-10}$	$1.78 \cdot 10^{-2}$	$3.21 \cdot 10^{-3}$	$2.11 \cdot 10^{-2}$	$2.11 \cdot 10^{-2}$
10,000	$5.63 \cdot 10^{-13}$	$4.94 \cdot 10^{-5}$	$1.24 \cdot 10^{-10}$	$1.78 \cdot 10^{-2}$	$3.22 \cdot 10^{-3}$	$2.11 \cdot 10^{-2}$	$2.11 \cdot 10^{-2}$
15,000	$2.5 \cdot 10^{-13}$	$3.41 \cdot 10^{-5}$	$8.25 \cdot 10^{-11}$	$1.79 \cdot 10^{-2}$	$3.24 \cdot 10^{-3}$	$2.12 \cdot 10^{-2}$	$2.12 \cdot 10^{-2}$
20,000	$1.41 \cdot 10^{-13}$	$2.63 \cdot 10^{-5}$	$6.19 \cdot 10^{-11}$	$1.79 \cdot 10^{-2}$	$3.25 \cdot 10^{-3}$	$2.12 \cdot 10^{-2}$	$2.12 \cdot 10^{-2}$
30,000	$6.26 \cdot 10^{-14}$	$1.81 \cdot 10^{-5}$	$4.13 \cdot 10^{-11}$	$1.8 \cdot 10^{-2}$	$3.26 \cdot 10^{-3}$	$2.12 \cdot 10^{-2}$	$2.12 \cdot 10^{-2}$
40,000	$3.52 \cdot 10^{-14}$	$1.39 \cdot 10^{-5}$	$3.1 \cdot 10^{-11}$	$1.8 \cdot 10^{-2}$	$3.27 \cdot 10^{-3}$	$2.12 \cdot 10^{-2}$	$2.12 \cdot 10^{-2}$
50,000	$2.25 \cdot 10^{-14}$	$1.13 \cdot 10^{-5}$	$2.48 \cdot 10^{-11}$	$1.8 \cdot 10^{-2}$	$3.27 \cdot 10^{-3}$	$2.13 \cdot 10^{-2}$	$2.13 \cdot 10^{-2}$
60,000	$1.56 \cdot 10^{-14}$	$9.57 \cdot 10^{-6}$	$2.06 \cdot 10^{-11}$	$1.8 \cdot 10^{-2}$	$3.27 \cdot 10^{-3}$	$2.13 \cdot 10^{-2}$	$2.13 \cdot 10^{-2}$
80,000	$8.8 \cdot 10^{-15}$	$7.34 \cdot 10^{-6}$	$1.55 \cdot 10^{-11}$	$1.8 \cdot 10^{-2}$	$3.28 \cdot 10^{-3}$	$2.13 \cdot 10^{-2}$	$2.13 \cdot 10^{-2}$
$1 \cdot 10^5$	$5.63 \cdot 10^{-15}$	$5.97 \cdot 10^{-6}$	$1.24 \cdot 10^{-11}$	$1.8 \cdot 10^{-2}$	$3.28 \cdot 10^{-3}$	$2.13 \cdot 10^{-2}$	$2.13 \cdot 10^{-2}$